

DISTRIBUTION AGREEMENT

In presenting this thesis or dissertation as a partial fulfillment of the requirements for an advanced degree from Emory University, I hereby grant to Emory University and its agents the non-exclusive license to archive, make accessible, and display my thesis or dissertation in whole or in part in all forms of media, now or hereafter known, including display on the world wide web. I understand that I may select some access restrictions as part of the online submission of this thesis or dissertation. I retain all ownership rights to the copyright of the thesis or dissertation. I also retain the right to use in future works (such as articles or books) all or part of this thesis or dissertation.

Kathryn Anna Knoop

Date

DEVELOPMENT OF M CELLS AND SMALL LYMPHOID TISSUES IN THE INTESTINE

By

Kathryn A. Knoop

Doctor of Philosophy
Graduate Division of Biological and Biomedical Sciences
Immunology and Molecular Pathogenesis

Ifor R. Williams, M.D., Ph.D.
Advisor

Max D. Cooper, M.D.
Committee Member

Brian D. Evavold, Ph.D.
Committee Member

Joshy T. Jacob, Ph.D.
Committee Member

Robert S. Mittler, Ph.D.
Committee Member

Andrew S. Neish, M.D.
Committee Member

Development of M Cells and
Small Lymphoid Tissues in the Intestine

By

Kathryn Anna Knoop

B.S., Drake University, Des Moines, IA, 50311

Adviser: Ifor R. Williams, M.D., Ph.D.

An abstract of a dissertation submitted to the Faculty of the
Graduate School of Emory University in partial fulfillment of the
requirements for the degree of Doctor of Philosophy

Graduate Division of Biological and Biomedical Sciences
Program in Immunology and Molecular Pathogenesis
2011

ABSTRACT

Mucosal surfaces are constantly bombarded with commensal bacteria and foreign antigen. To prevent constant inflammation, tolerance is induced to many of the foreign antigens encountered in Peyer's patches (PP) and isolated lymphoid follicles (ILF). Microfold cells (M cells), found as part of the follicle-associated epithelium (FAE) overlaying the PPs and ILFs, are specialized epithelial cells that constantly transcytosing antigen. The factors driving M cell development were previously unknown; the commonly held model being factors from the B cells and developing follicle foster the growth of M cells, as most M cells develop over follicles. RANKL, a member of the TNF superfamily, has been shown to be critical in development of lymphoid aggregates including lymph nodes and isolated lymphoid follicles. Direct interaction of RANKL⁺ stromal cells in the subepithelial dome and RANK⁺ epithelial cells on the FAE appears to be essential to M cell differentiation.

In the absence of RANKL, M cells are reduced 98% and have a disrupted pattern across the follicle; these changes contribute to a reduction in germinal centers in PP and fecal IgA. Recombinant RANKL can rescue M cell development in RANKL^{-/-} mice and promote the development of villous M cells on all of the small intestinal villi, drastically increasing the ability of the small intestine to take up antigens. The development of villous M cells can also be induced by the enteric flora, specifically the enteric flora found in mice lacking IgA. These villous M cells were dependent on systemic RANKL, supporting a model in which the commensal microflora and RANKL coordinately regulate the extent of vM cell differentiation in the small intestine.

Next, a model of acute B cell depletion was used to better understand the role of B cells in M cell development. After two weeks of continuous B cell depletion, M cell development on the PP dome is virtually unchanged. Furthermore, B cell deficient mice maintain a wild type M cell density on the PP domes, though the absolute number of M cells is decreased as the follicle and FAE shrinks. Finally, in the absence of RANKL development small lymphoid tissue aggregates in the small intestine, cryptopatches and ILFs, is disrupted. Cryptopatches are reduced four-fold, and ILFs are completely absent. This lack of ILF development is due to the lack of CXCL13 in these aggregates and a failure to attract B cells to the follicle. Interestingly a dependence on RANKL for cryptopatch and ILF development is not seen in the large intestine, where CXCL13 expression is controlled by some other mechanism, perhaps the increased density of enteric flora.

In conclusion, the data presented here suggests a new model of M cell development in which the major signal is derived from RANKL and secondary contributions may come from the enteric flora. Additionally, RANKL is critical in the development of ILFs in the small intestine. These novel functions of RANKL suggest this single cytokine is imperative in two events in the development of the mucosal immune system. By controlling both antigen sampling within the PP and ILFs, and the development of ILFs, RANKL is an important factor in orchestrating peripheral tolerance. Alongside RANKL, the enteric flora exerts collaborative and partially redundant signals to induce and maintain M cells in the FAE and ILFs.

Development of M Cells and
Small Lymphoid Tissues in the Intestine

By

Kathryn Anna Knoop

B.S., Drake University, Des Moines, IA, 50311

Adviser: Ifor R. Williams, M.D., Ph.D.

A dissertation submitted to the Faculty of the Graduate
School of Emory University in partial fulfillment of the
requirements for the degree of Doctor of Philosophy

Graduate Division of Biological and Biomedical Sciences
Program in Immunology and Molecular Pathogenesis
2011

ADKNOWLEDGMENTS

Five years ago, I visited Emory unaware of where my graduate education was going to take me. Now I look back upon my years full of amazement at my luck to have experienced so much. This is, of course, all thanks to my mentor Ifor Williams, to whom I owe my success in graduate school. Always the mentor, he would credit my accomplishments to my hard-working nature, but it is his patient teaching that fostered my continued interest and ability in research science. Ifor's immediate acceptance of me not as a student, but as a colleague is what challenged me to become worthy of that title. Through his example I've learned how to live a balanced life with a passion in science. I look forward to visiting with him as a friend and associate at future scientific meetings throughout our careers.

Most of the reason I love what I do is because of the people I've gotten to work with over the years. So, I would also like to thank my fellow lab mates: Betsy Butler, Nachiket Kumar, and Daniel Rios. This work could not have been done without their advice and technical support, and all the entertaining down time. I would also like to thank my classmate Erin West who has made my time at Emory so much more rewarding both academically and socially.

Finally, much gratitude goes out to my husband Travis for his love, support, and pride in me and my work. Though his natural desire to solve problems was tried at times as he realized the complicated details of my research, his continued willingness to learn, listen, and offer his own unique perspective to my nuanced research is so much more than I could ask.

TABLE OF CONTENTS

PAGE

ABSTRACT

ACKNOWLEDGEMENTS

LIST OF FIGURES

LIST OF TABLES

INTRODUCTION

1

RESULTS

CHAPTER 1: RANKL is necessary and sufficient to initiate development of antigen-sampling M cells in the intestinal epithelium

15

CHAPTER 2: Differentiation of Peyer's patch M cells does not require signals from B cells

59

CHAPTER 3: Escape of the enteric microflora from the normal homeostatic control of secretory IgA results in expanded development of small intestinal villous M cells

94

CHAPTER 4: Other examples of an association of stromal RANKL and GP2⁺ M cells in organized intestinal lymphoid tissues

122

CHAPTER 5: Distinct developmental requirements for isolated lymphoid follicle formation in the small and large intestine: RANKL is essential only in the small intestine

133

DISCUSSION	162
LITERATURE CITED IN INTRODUCTION AND DISCUSSION	169
LIST OF PUBLICATIONS AND PRESENTATIONS	181

LIST OF FIGURES		<u>PAGE</u>
(Listed in order of appearance in each chapter)		
1-1	Peyer's patches of RANKL null mice contain very few M cells.	48
1-2	Administration of rRANKL to RANKL null mice restores PP M cells.	50
1-3	Administration of rRANKL induces development of villous M cells on all small intestinal villi.	52
1-4	RANKL-induced villous M cells are functional for bead and bacteria uptake from the intestinal lumen.	53
1-5	Treatment of wild type mice with neutralizing anti-RANKL leads to loss of PP M cells.	55
1-6	Intestinal epithelial cells express RANK.	57
1-7	RANKL ^{-/-} mice have fewer germinal centers in their PP follicles and lower levels of fecal IgA.	55
1-SF1	PPs from RANKL null mice have very few cells reactive with the NKM 16-2-4 monoclonal antibody specific for M cells.	58
2-1	Mice maintain functional M cells after B cell depletion.	86
2-2	J _H ^{-/-} mice lack B cells, yet still have M cells, while RANKL ^{-/-} mice lack M cells in the presence of B cells.	88
2-3	M cell density is similar in wild type, B cell depleted, and J _H ^{-/-} mice.	90
2-4	RANKL necessary for M cell differentiation is supplied by a non-hematopoietic source.	91
2-5	M cell development in J _H ^{-/-} mice can be blocked with neutralizing RANKL antibody.	92
2-SF1	The human CD20 Transgene does not affect gut humoral responses.	93
3-1	Villous M cells develop in large numbers in the distal ileum of J _H ^{-/-} mice.	116

3-2	Mice lacking IgA have an increased villous M cell density.	118
3-3	Elimination of enteric flora reduces villous M cell development.	119
3-4	Villous M cells appear in $J_H^{-/-}$ mice during weaning.	120
3-5	Villous M cells in $J_H^{-/-}$ mice require RANKL.	121
4-1	Large intestinal GALT contain $GP2^+$ M cells above $RANKL^+$ stroma.	130
4-2	Colonic ILFs in $RANKL^{-/-}$ mice lack M cells.	131
4-3	PPs express RANKL on stromal cells in the subepithelial dome.	132
5-1	Cryptopatches are less frequent and smaller in the small intestine of $RANKL^{-/-}$ mice compared to wild type controls.	156
5-2	Cryptopatches in the small intestine of $RANKL^{-/-}$ mice do not contain any B cells.	157
5-3	In utero $LT\beta R$ -Ig treatment does not restore isolated lymphoid follicle development in the small intestine of $RANKL^{-/-}$ mice.	158
5-4	Colonic lymphoid aggregates in $RANKL^{-/-}$ mice include B cell follicles.	159
5-5	$RANKL^{-/-}$ cryptopatches have a normal density and distribution of $CD11c^+$ cells.	160
5-6	CXCL13-expressing cells are absent from small intestinal lymphoid aggregates in $RANKL^{-/-}$ mice.	161
5-7	Stromal cells in small intestinal but not colonic cryptopatches from $RANKL^{-/-}$ mice do not express several $LT\beta R$ -dependent antigens.	162

LIST OF TABLES
(listed in order of appearance in each chapter)

PAGE

Table 2-1 Extent of M cell depletion seen in three mutant mouse models

85

Development of M Cells and
Small Lymphoid Tissues in the Intestine

By

Kathryn Anna Knoop

B.S., Drake University, Des Moines, IA, 50311

Adviser: Ifor R. Williams, M.D., Ph.D.

A dissertation submitted to the Faculty of the Graduate
School of Emory University in partial fulfillment of the
requirements for the degree of Doctor of Philosophy

Graduate Division of Biological and Biomedical Sciences
Program in Immunology and Molecular Pathogenesis
2011

Introduction

The dynamic relationship between the enteric flora and the intestine are controlled by two related processes: antigen sampling and the induction of tolerance. Microfold cells (M cells) are epithelial cells that constantly transcytose particulate antigens from the lumen. M cells are most commonly found as part of the follicle-associated epithelium (FAE) over Peyer's patches (PP) and isolated lymphoid Follicles (ILFs) in the small intestine, and the cecal patch, colonic patch, and colonic ILFs in the large intestine. These gut-associated lymphoid tissues (GALT) are the main inductive sites where immune responses are initiated that lead to the production of the IgA that is continually secreted into the lumen controlling the enteric flora. The full development of GALT requires internal signals from regulated cytokines and chemokines, and external signals from the enteric flora. The data presented describes previously undefined inducers of M cell development: a critical cytokine being the receptor activator of NF- κ B ligand (RANKL) and the enteric flora. We also show RANKL to be critical in the development of ILFs in the small intestine. These novel functions of RANKL suggest there is a common pathway between the development of small GALT structures and the M cells that overlay them.

The specific aims of this dissertation were 1) to characterize the role of RANKL in intestinal M cell development, 2) to determine if there is any synergy between B cells and RANKL in PP M cell development, 3) to investigate if the enteric flora can influence the development of M cells, and 4) to describe the role of RANKL in small lymphoid tissues in the intestine.

The nature of the mucosal immune response

The mucosal immune response is coordinated differently from the rest of the systemic immune response (1). Systemic responses initiated in lymph nodes are mostly inflammatory in an attempt to remove all pathogens and kill all infected cells. The development of memory responses for stronger and faster secondary responses is a hallmark of a strong systemic immune response. The intestinal tract is full of antigen introduced from the lumen of the gut into either PP or ILFs (2), the inductive lymphoid tissues of the intestine, akin to lymph nodes. Strong inflammatory responses to antigens from food or commensal bacteria would certainly cause harsh disease, so most antigens seen in the gut require tolerogenic responses: the induction of IgA for secretion into the lumen (3) and T regulatory cells to prevent inflammatory future T cell responses (4). Though relatively low levels of IgA are found in the serum, IgA is the most abundantly produced antibody isotype, comprising 70% of all antibodies produced (5, 6). Most of this protective IgA is secreted into the lumen of the intestine via the polymeric immunoglobulin receptor on epithelial cells (7) and neutralizes bacterial antigens and toxins before they can damage tissue (8). While IgA prevents future bacterial attacks occurring from the lumen, mucosal induced T cell responses prevent systemic inflammatory responses from occurring against common oral antigens (9). Utilizing the mucosal immune response and the commonly observed phenomenon of oral tolerance, when animals orally fed antigens become tolerant to the same antigen if subsequently given systemically (10), has been viewed as a hopeful vaccine strategy in a number of models from inducing protective immune responses to pathogens to suppressing systemic responses to autoantigens or allergens (11).

Organized Lymphoid Tissue in the Intestine

The small intestine contains three types of organized lymphoid tissue: PP, ILFs, and CPs. Similar structures are found in the large intestine, which contain both ILFs and CPs, and also colonic patches, which are similar to PP (12). PP and colonic patches contain multiple follicles and form during embryonic development requiring lymphotoxin (LT) signaling similar to lymph node development (13, 14); by disrupting LT signaling during the embryonic stage, development of these patches can be completely blocked and will not be rescued during adulthood (13, 15) (16). Most lab strains of mice develop between eight to twelve PP spread down the length of the small intestine; PPs are not found in specific locations along the gut, though generally there is one in the first 2 cm and last 2 cm of the small intestine. In the large intestine, the cecal patch develops on the tip of the cecum (17), and the colonic patch generally develops within the first 2 cm of the colon (12). Most of these patches contain five to nine B cell follicles capable of generating IgA-producing B cells. Covering each follicle is a single layer of follicle-associated epithelium (FAE) which separates the follicles from the lumen (18). Antigen from the lumen is introduced into the follicles through antigen-sampling M cells, which are part of the FAE. Without M cells, both oral tolerance and IgA responses could be drastically reduced.

ILFs also serve as sites of IgA production and secretion (2). Unlike PPs, they develop postnatally throughout adulthood in response to internal and external stimuli. Though most specific pathogen free mice develop a very limited number of ILFs, they can be found in increased numbers in mice lacking PPs (19) acting as a compensatory

mechanism for the production of IgA, though ILFs alone cannot compensate for the lack of PP in the induction of T cell dependent oral tolerance(20). Interestingly mice lacking activation-induced cytidine deaminase (AID) still have PP, but have a significant increase in ILF development due to the expanded number of anaerobic bacteria found in these mice (21), showing the ability of the ILFs to attempt to regulate the microflora back to homeostasis. ILFs contain single follicles of B cells, are also covered by M cell-containing FAE, and function similar to PP in response to luminal antigen. As M cells are not normally part of the villous epithelium, the introduction of antigens through M cells to the local area where an immature ILF may be developing is probably not the mechanism which induces the development of ILFs in response to commensal load. Instead bacterial stimulation of NOD1 in the epithelium can start a signal cascade leading to ILF development (22), revealing the crosstalk between the epithelium and lymphoid tissue.

A third type of organized lymphoid tissue included in the gut-associated lymphoid tissue (GALT) is the cryptopatch (CP), a small aggregate of cells in the lamina propria of the small intestine comprised of 1000+ lymphoid tissue inducer cells (LTic) and lymphoid tissue organizer cells (LTo), developing in the lamina propria around the crypts of the small intestine. The smallest of all the GALT, CPs are reminiscent of the early stages of organized mucosal lymphoid tissue (23). CP begin to develop around postnatal day 14 in wild type mice, and are maintained at a stable level of around 1500 CP during adulthood (24, 25). Currently evidence shows that de novo development of CP does not continually occur throughout adulthood (26): as needed, CP may grow to fill a villi and develop further into an ILF (27). CP are present in germ-free mice and ILF can develop

from this population only with commensal signals (15, 24). Recently it has been hypothesized that CP and ILF are not distinct organs, but rather two extremes on a continuum of solitary intestinal lymphoid tissue (SILT), with CP developing into ILF in response to signals originating from the commensal enteric flora (28).

M cells and antigen uptake

Both PP and ILF are covered by follicle-associated epithelium (FAE) and constantly bombarded with antigenic protein, though very little of this antigen material represents “danger” for the organism. Constant sampling of the luminal contents is a function of M cells, which are specialized epithelial cells found in the FAE. M cells differ from surrounding enterocytes by their ability to transcytose particulate antigen, and by their short and stubby microvilli on the apical side compared to the longer microvilli of the enterocyte (29, 30). An invaginated pocket on the basolateral side of the cell is often occupied by lymphocytes or dendritic cells, shortening the distance endocytic vesicles must traverse through the cell and allowing immune cells to rapidly phagocytose the antigens transcytosed by M cells (31). Functionally very different from enterocytes (32), M cells are the gatekeepers of the mucosal immune response, acting as the functional equivalent of an afferent lymphatic vessel.

M cells are generally studied through the use of various microscopy techniques, first being identified as an epithelial cell distinct from enterocytes through transmission electron microscopy in the early 1970’s (29, 33). Though it was known the FAE had some mechanism of transport into the lymphoid epithelium, the recognition that a single specialized cell type provided this function was a landmark discovery (34). Hundreds of

subsequent studies have examined the use of targeting M cells in vaccine development for the intentional initiation of mucosal specific immune responses (35). Few M cell-specific markers exist; the most commonly used reagent for staining mouse M cells is a lectin from *Ulex europaeus* known as UEA-I. UEA-I, binding an α 1,2 fucose linkage found on the surface of M cells and in mucus, is not specific for M cells, as it also stains goblet cells and Paneth cells, mucous containing epithelial cells. PPs are generally mucous free, and rarely are goblet cells found on the FAE. Recently two monoclonal antibodies to mouse M cells have been described; the first, NKM 16-2-4, binding an α 1,2 fucose group, similar to the UEA-I target (36). The other is an antibody against the glycoprotein 2 (GP2) receptor found specifically on M cells (37). GP2 binds fimbrial proteins found on both commensal and pathogenic enterobacteria and facilitates their uptake through M cells. Other proteins from pathogenic viruses, bacteria, and even prions have also been shown to bind to M cells, although the specific targets on the M cell are not always. For example, sigma 1 protein of reovirus binds sialic acids in the glycocalyx of M cells (38). Species of *Yersinia* adhere to β 1 integrin on M cells (39). M cells can bind the cellular prion protein, PrPC facilitating prion uptake (40, 41). Such proteins have been suggested as reagents to target M cells either for identification or vaccine purposes (42). Bacterial products can also be recognized by pattern recognition receptors such as TLRs found on M cells (43); attachment to M cells through any means generally results in activation of transcytosis (44). Besides receptor-mediated endocytosis, M cells also utilize endocytosis of clathrin-coated vesicles, actin-dependent phagocytosis, and fluid-phase pinocytosis or macropinocytosis, accommodating a variety of soluble or particulate antigens from nanometers to microns in diameter (45). M cells do not process or present

antigen in the manner professional antigen-processing cells do; rather the payload is dropped off to dendritic cells or lymphocytes waiting in the basolateral pocket of the M cell. These cells are then free to initiate responses against the antigens, if the right signals are present (46).

M cells: a differentiated epithelial cell or a variant of enterocytes?

A key question is whether M cells represent a fully differentiated epithelial cell type, or if they are a transient phase of enterocyte development. Enterocytes develop from Lgr5^{hi} stem cells located in the crypts surrounding villi. These long-lived stem cells are nestled between Paneth cells, and producing either new stem cells or transit amplifying cells which begin to differentiate into one of the epithelial cell types as they migrate up or down the villi (47). If these cells migrate down toward the bottom of the crypts, they become Paneth cells which secrete defensins and other antimicrobial products. The rest of the cells migrate up toward the tip of the villi or PP dome during a three or four day process, destined to become a member of the absorptive epithelium or the secretory lineage, which includes goblet cells and enteroendocrine cells. The signaling mechanisms that lead to the differentiation of a transit amplifying cell into either an enterocyte, goblet cell, enteroendocrine cell, or a Paneth cell have been extensively analyzed (48). Questions still exist regarding where M cells fall in the classification of intestinal epithelial cells, including how they develop and what factors may influence their differentiation.

PPs are surrounded by specialized follicle-associated crypts that produce mostly enterocytes or M cells, and only rarely goblet or enteroendocrine cells. Cells are either sloughed off along the way or undergo apoptosis at the top of the dome, taking about four

days to reach the apex. Approximately 5-10% of the PP epithelial cells are M cells in mice and humans, though this percentage can be more in other animals: rabbit PP FAE contains about 50% M cells (18). M cells develop from specialized epithelial crypts adjacent to PP, and migrate upwards in a line, creating radial strips amongst the enterocytes (49). These columns also contain enterocytes in between individual M cells, and it is unclear what factors induce M cell differentiation and when this signaling needs to occur.

It has been suggested M cells transdifferentiate from enterocytes and only transiently possess the ability to take up antigen before transitioning back to enterocytes as they reach the apex of the PP dome (50). This idea has been propagated by the popular in vitro systems replicating the M cell phenomenon using Caco-2 cells, a human epithelial cell line (51). When Raji B cells are added to Caco-2 cells, the Caco-2 cells differentiate into cells that are better able to transcytose nanoparticles (52, 53). Whether the end product of this system truly replicates M cells is a concern as studies have failed to elucidate the exact mechanism behind the differentiation of the M like cells. Most in vivo studies suggest M cells represent a fully differentiated type of enterocyte, which have stopped dividing, and cannot transcytose antigen outside of the FAE microenvironment (54).

Another lingering idea about M cell development from the Caco-2 model is the hypothesis that B cells are an important factor in M cell development. B cell deficient mice have reduced number of M cells (55). M cells were still found on the PP of these mice, but injection of lymphocytes beneath the epithelium that appeared to induce M cell differentiation (51). However it has become apparent separating direct induction of M

cells and full development of the entire FAE is convoluted at best; absence of B cells correlated with a decrease in the size of the FAE (56). The requirement of B cells for the maintenance of M cells and homeostasis of the FAE rather than the development of M cells has been suggested (57), though attempting to demonstrate this using mice with genetic B cell deficiency does not separate M cell maintenance from the initial development of the FAE. If B cells directly induce M cell development, the specific signaling mechanism is still unknown as well. B cells do not need to be activated by T cells or secrete immunoglobulin to induce M cell differentiation (55), and no mechanism has emerged from studies using the Caco-2/Raji model. Furthermore, this phenomenon has yet to become universally applicable with other intestinal cell cultures. When a mouse intestinal epithelial cell line (MIE) is cultured with murine B cells alone, no transformation into antigen-transporting M cell-like cells is seen (58). Only when activated T and B cells are cocultured with epithelial cells do the MIE cells increase their ability to transcytose nanoparticles.

Villous M cells

If little is known about classical FAE M cells, even less is known about the M cells occurring on the villi of the small intestine, villous M cells. These M cells are UEA-I+, NKM 16-2-4+, able to transcytose antigen, and only found rarely naturally in wild type mice, though may develop in increased numbers in mice lacking PP, such as in utero LT- β R-Ig-treated, LT α -/-, or TNF- α /LT α -/- (36, 59, 60). If ILF become increased in mice when normal PP induced immune responses are not enough, perhaps villous M cells represent a similar induced mechanism, substituting for classical FAE M cells when they

are missing, or assisting during an infection. Villous M cells are distinct from M cells that are part of the ILF FAE, and overlay villi that do not have an organized lymphoid structure inside. Presumably villous M cells would hand off transported antigens to resident CD103⁺ dendritic cells which readily migrate to the mesenteric lymph node and are able to initiate adaptive responses (61). Alternatively gut resident CX3CR1⁺ macrophages can pick up antigen taken up by villous M cells and interact with intestinal T cells to maintain oral tolerance (62).

M cells also represent a potential weak link in an otherwise tight epithelial barrier (63). Indeed pathogens can hijack M cells as a means to enter the small intestine tissue, leading to infection (64), which may suggest why only a small number of villous M cells develop naturally, minimizing the number of ‘holes’ in the epithelium. If any pathogens did commandeer M cells for their own entry purposes, a number of mechanisms are in place to contain these rogue pathogens. First, a population of CX₃CR1⁺ APCs resides in villi and is ready to phagocytose any potential threat. These cells maintain close contact to the epithelium, which express the ligand for CX₃CR1, fractalkine/CX₃CL1 (65), and can expand in response to commensal bacteria load (66). Second, if pathogens do get past the lamina propria, they become detained in the mesenteric lymph node (67). Thus it may be in the best interest of the organism to risk the potential danger of M cells for the preferred result of better immune surveillance, when it is only the extremely rare pathogen that can bypass the variety of containment mechanism the mucosal system possesses.

Targeting classical and villous M cells for tolerance or administration of oral vaccinations

M cells have been touted as specific targets for oral vaccines to better induce desired immune responses. Indeed targeting orally delivered antigens along with a strong mucosal adjuvant to M cells has shown strong results in the establishment of mucosal and systemic immunity as a strategy of vaccination (36). Entrance through an M cell does not dictate a specific immune response in a natural setting, and the same is true for vaccines. Depending on the antigen and how it is presented, a variety of immune responses can be induced and for this reason, M cell targeting has been implicated as a potential strategy in a number of models. A protective vaccine for HIV is, perhaps, the holy grail of vaccines currently. It is an attractive idea to elicit a protective mucosal immune response where the initial danger of infection occurs (68). Other more common infections also require protective mucosal responses, like bacterial infections resulting in acute gastroenteritis, or viruses which enter through the oral route. Whole *Campylobacter* targeted to M cells results in protective immunity without any added adjuvant, the danger signals internal to the bacteria presumably being enough to trigger the response (69). Nanoparticles containing hepatitis B antigens targeted to M cells initiated secretory IgA and a systemic inflammatory response, exemplifying how the use of an appropriate adjuvant can break oral tolerance (70). Vaccine trials targeting M cells have been taken into higher mammals, establishing these strategies can work in primates (71). Targeting oral vaccines to dendritic cells has been shown to increase protective immunity against *Bacillus anthracis* (72); the ability of one vaccine to target M cells, followed by dendritic cells could only synergize these effects resulting in a drastic increase in efficacy. Now that

tools exist to get through the clutter of the luminal load of the small intestine, a plethora of options exist to build better oral vaccines, combining M cell targeting with adjuvants, immune cell targeting, nanoparticles, encapsulated microparticles, DNA vaccines, bacterial vectors, or other vaccine technology.

Due to the naturally tolerogenic PP environment, targeting M cells may result in better tolerance induction as well (73). Allergic hypersensitivities occur when aberrant inflammation leading to allergen-specific IgE production is induced against inhaled or ingested allergens affecting 12% and 4% of Americans, respectively (74). Targeting low doses of OVA to M cells resulted in continued unresponsiveness to peripheral OVA challenges (75). In the same vein, targeted birch pollen to PP M cells induced T_H1 and IgG2 responses in the lungs after challenge(76), (77). It would be interesting to discern if this technique could desensitize animals with models of allergy and switch T_H2 and IgE responses to more appropriate responses. These studies also show the potential of immune responses originating in the gut to protect other mucosal tissues such as the lung, though this theory could also be applied to the desensitization of food allergies.

Though only discussed as part of the intestinal FAE, M cells are also identified on FAE of almost every other mucosal associated lymphoid tissue. In the eye, M cells have been found in the tear duct-associated lymphoid tissue (78) and the conjunctiva-associated lymphoid tissue (79). In the upper airway, M cells can be found in both the nasal-associated lymphoid tissue (80) and salivary duct-associated lymphoid tissue (81). In the lung bronchial-associated lymphoid tissue contains M cells (82). Most of these lymphoid tissues are difficult to study and only develop when induced to by bacterial stimulation, so little data is available as to whether or not these M cells are similar to

intestinal M cells other than the ability to transcytose antigen (49). With the popularity of intranasal immunization, the NALT has been studied, though without the success seen in the PP. Targeting NALT M cells in intranasal vaccines currently appears to not be a strong enough inducer of protective immunity, and can block uptake (83, 84).

RANKL

Receptor activator of NF- κ B ligand (RANKL) is a member of the TNF superfamily and also referred to as TNF-related activation-induced cytokine (TRANCE) and TNFSF11 (85). Like TNF- α , RANKL is a type 2 transmembrane protein, initially synthesized as a transmembrane protein, but able to be released from the cell surface following cleavage by one of several metalloproteases (86, 87). It binds to the receptor activator of NF- κ B (RANK) and signals through a downstream pathway that involves TRAF6 and the activation of NF- κ B (88, 89). The RANKL-RANK interaction has been best described in the skeletal system where RANKL is needed for osteoclast development and bone remodeling (90, 91). Deficiencies in RANK or RANKL lead to abnormal skeletal development because of a lack of osteoclast development and bone remodeling (91). The RANKL-RANK pathway also is essential for lymph node development, AIRE expression on the medullary thymic epithelial cells, mammary gland lactation, and provision of survival signals to dendritic cells (91-96).

RANKL-deficient mice lack lymph nodes, but still develop PPs (90, 91). Recent data from our lab showed that RANKL was also important in the gut-associated lymphoid tissue. RANKL staining was found on the stromal cells throughout CP, but in PP and ILF, RANKL staining is confined to the subepithelial dome, or the area right

beneath the FAE (97), suggesting RANKL could play multiple roles in the development and function of these lymphoid tissues.

Chapter 1

RANKL is necessary and sufficient to initiate development of antigen-sampling M cells in the intestinal epithelium

Kathryn A. Knoop¹, Nachiket Kumar¹, Betsy R. Butler¹, Senthil Sakthivel¹, Rebekah T. Taylor¹, Tomonori Nochi³, Hisaya Akiba², Hideo Yagita², Hiroshi Kiyono³, and Ifor R. Williams¹

¹Department of Pathology and Laboratory Medicine, Emory University School of Medicine, Atlanta, GA

²Division of Mucosal Immunology, Department of Microbiology and Immunology, University of Tokyo, Tokyo, Japan

³Department of Immunology, Juntendo University School of Medicine, Tokyo, Japan

Published in The Journal of Immunology, vol. 183 (9) pp. 5738-47. 2009.

Copyright 2009. The American Association of Immunologists, Inc.

All experiments in this study were performed by Kathryn A. Knoop, with assistance from Betsy R. Butler and Tomonori Nochi.

This manuscript was written by Kathryn A. Knoop and Ifor R. Williams.

Abstract

Microfold cells (M cells) are specialized epithelial cells found in Peyer's patches (PP) and other organized mucosal lymphoid tissues that take up particulate antigens and deliver them to antigen-presenting cells. The TNF superfamily member RANKL is selectively expressed by subepithelial stromal cells in PP domes. RANKL null mice had less than 2% of wild type levels of M cells and markedly diminished uptake of particulate antigens. These deficits were corrected by systemic administration of exogenous RANKL. Treatment with RANKL also induced the differentiation of villous M cells on all small intestinal villi. Antibody-mediated neutralization of RANKL in adult wild type mice eliminated most PP M cells. Availability of RANKL is the critical factor controlling the differentiation of M cells from RANK-expressing intestinal epithelial precursor cells.

Introduction

The organized lymphoid tissues of the intestine are inductive sites for both the generation of secretory IgA and the generation of T cell tolerance to antigens present in the intestinal lumen, including those derived from food and the commensal flora (1, 2). The follicle-associated epithelium (FAE) that covers the lymphoid follicles of both Peyer's patches (PP) and isolated lymphoid follicles (ILF) contains specialized epithelial cells known as microfold cells (M cells) that provide a portal for efficient sampling of particulate antigens from the lumen (3, 4). Antigens acquired through this major pathway for antigen sampling in the intestine are delivered into intraepithelial pockets within the M cells that lymphocytes and APC access from the subepithelial dome region. The M cell-mediated antigen-sampling pathway has a central role in the development of immune responses to both pathogenic bacteria and commensal bacteria. Production of protective fecal IgA in mice after oral infection with invasive *Salmonella* species requires the presence of PP with M cells (5, 6). In addition, some commensal bacteria internalized through M cells are passed into dendritic cells that travel with their cargo to the draining mesenteric lymph node, leading to both IgA antibody production and establishment of T cell tolerance (7). M cells also promote the development of T cell tolerance to antigens acquired through the gastrointestinal tract. Targeting OVA to mouse M cells via the reovirus sigma 1 protein resulted in enhanced development of oral tolerance in CD4⁺ T cells (8). While most M cells in the small intestine of wild type mice are localized to the FAE of PP and ILF, occasional villi contain clusters of cells known as villous M cells that exhibit all the major defining characteristics of PP M cells including reactivity with

the UEA-I lectin recognizing α 1-2 fucose, stubby microvilli, and the capacity to ingest and transcytose particles the size of bacteria (9). The relative density of villous M cells separates villi into those with diffuse and dense patterns of villous M cells.

While the basic functional and ultrastructural features of M cells were initially described over 30 years ago (10), many basic questions about M cell differentiation and function remain unsolved. It has been proposed that specific factors released from the lymphoid microenvironment immediately beneath the FAE have the potential to elicit M cell differentiation in the FAE and promote the function of M cells, but specific signaling mediators with such activity have not been identified to date (11, 12). Debate continues on whether M cells are a distinct lineage arising from crypt stem cells like other differentiated intestinal epithelial cells or whether M cells can instead arise from normal FAE enterocytes with the plasticity to transition into M cells upon encountering the right set of stimuli (13-15).

RANKL (receptor activator of NF- κ B ligand) is a member of the TNF superfamily (16) that is also referred to as TNF-related activation-induced cytokine (TRANCE) and TNFSF11. Like TNF- α , RANKL is initially synthesized as a transmembrane protein that can be released from the cell surface following cleavage by one of several metalloproteases (17, 18). RANKL signals through its receptor RANK (receptor activator of NF- κ B) and a downstream pathway that involves TRAF6 and the activation of NF- κ B (19, 20). Osteoprotegerin (OPG) is a soluble decoy receptor for RANKL that allows for tight regulation of the circulating levels of RANKL (21). A major breakthrough in establishing a biological role for RANKL-RANK interactions was the discovery that RANKL signaling through RANK is required for normal osteoclast

function (22, 23). Mice deficient in either RANKL or RANK have osteopetrosis and severe skeletal abnormalities because they lack the number of osteoclasts needed to remodel bone normally. RANKL-RANK signaling is also involved in several other critical biological processes including development of lymph nodes, development of medullary thymic epithelial cells (mTEC), mammary gland lactation, and provision of survival signals to dendritic cells (22-27). The absence of all lymph nodes in RANKL-deficient mice demonstrates that RANKL is an essential mediator in lymphoid organogenesis (22, 28). RANKL induces lymphotoxin (LT) $\alpha_1\beta_2$ expression by lymphoid tissue inducer cells in the lymph node anlage (29). RANKL is not required for PP development, but the reduced size of PP reported in two independent lines of RANKL-deficient mice indicates that RANKL signaling is contributing to normal PP function (22, 23). More specific studies of PP and mucosal immune function were not reported as part of the initial characterization of these mice.

We previously showed that RANKL is selectively expressed by stromal cells in the subepithelial dome region beneath the FAE of both PP and ILF (30). Stromal cells with phenotypic characteristics similar to neonatal lymph node organizer cells including RANKL expression were recently identified in multiple secondary lymphoid tissues including mucosal-associated lymphoid tissues and lymph nodes (31). The polarized pattern of RANKL expression by stromal cells beneath the FAE of PP and ILF suggested a possible function for RANKL in regulating the induction of mucosal immune responses to particulate luminal antigens taken up through the FAE. In this study, we evaluated the function of PP in RANKL null mice and found that absence of RANKL is associated with loss of the vast majority of UEA-I⁺ M cells in the FAE. The depletion of M cells

correlated with a profound functional defect in uptake from the intestinal lumen of fluorescent beads used as model particulate antigens. Systemic administration of exogenous soluble RANKL restored functional UEA-I⁺ M cells to the PP of RANKL null mice and simultaneously led to widespread induction of functional M cells on the epithelium covering small intestinal villi in both RANKL null mice and wild type mice. These findings demonstrate that the RANKL-RANK pathway plays a pivotal nonredundant role in establishing the M cell-mediated pathway of antigen acquisition and handling.

Materials and Methods

Mice

Mice carrying a RANKL null mutation on a C57BL/6 background (28) obtained from Dr. Yongwon Choi at the University of Pennsylvania were used to establish a breeding colony in a conventional mouse facility at Emory University. Because RANKL null mice lack teeth, weanling null mice born in this colony are routinely given powdered mouse chow. Mice heterozygous for the RANKL null mutation were also backcrossed to BALB/c mice (Taconic) for a total of 4 generations. Male C57BL/6 RANKL^{+/-} mice and female BALB/c RANKL^{+/-} mice were intercrossed to produce RANKL null mice and littermate controls on a background roughly equivalent to (C57BL/6 X BALB/c)F₁ mice. RANKL null mice on this “F1 equivalent” genetic background are closer in weight to their heterozygous and wild type littermates and less likely to die prematurely compared to RANKL null mice on the two inbred backgrounds. Experiments using RANKL null mice were done with either the C57BL/6 background mice or the mice with a mixed C57BL/6 and BALB/c background. BALB/c mice (Taconic) were used for experiments examining the effects of anti-RANKL mAb on PP M cells. Two models of B cell deficient mice were used: μ MT mice obtained from Dr. Sam Speck at Emory University and J_H^{-/-} mice (Taconic). CCR6 deficient mice were from a colony of homozygous Ccr6^{tm1(EGFP)Irw} mice maintained on a C57BL/6 background (32). All animal studies were reviewed and approved by the Emory University Institutional Animal Care and Use Committee.

Recombinant mouse RANKL

A bacterial expression construct encoding a glutathione S-transferase (GST) fusion protein containing amino acids 137-316 of mouse RANKL was assembled in the pGEX-5X-1 vector (GE Healthcare) using a modification of a previously described method (33). The primers 5'-CACCCCCGGGTCAGCGCTTCTCAGGAGCT-3' and 5'-CTCGAGTCAGTCTATGTCCTGAAC-3' were used to PCR amplify a cDNA clone for mouse RANKL (Open Biosystems). After the PCR product was cloned into the pENTR-D-TOPO cloning vector (Invitrogen) and sequenced, the SmaI-XhoI fragment was subcloned into pGEX-5X-1. The construct was transformed into the BL21 *E. coli* strain (Stratagene) for fusion protein expression. The cultures were induced with 20 μ M IPTG for 16 hours at 20°C and the GST-RANKL purified from bacterial lysate by affinity chromatography on a GSTrap FF column (GE Healthcare) followed by dialysis against multiple changes of PBS. Recombinant GST used as a control was prepared by the same method using empty pGEX-5X-1. Biological activity of the GST-RANKL fusion protein was confirmed by its ability to induce differentiation of the RAW264.7 macrophage line (American Type Culture Collection) into multinucleate osteoclasts positive for tartrate resistant acid phosphatase. The GST-RANKL fusion protein was administered to RANKL null mice by daily i.p. or s.c. injections of 50 to 250 μ g per day for up to 7 days. Recombinant GST prepared from empty pGEX-5X-1 vector was used as a control for GST-RANKL.

Bacterial strains

A wild type strain of *Salmonella enterica* serovar Typhimurium (SL3201) transformed with the DsRed-Express plasmid (Clontech) encoding a cytoplasmic red fluorescent protein was kindly provided by Dr. Andrew Neish at Emory University. A *Yersinia enterocolitica* isolate (ATCC 29913) was purchased from the ATCC (Manassas, VA) and labeled with Alexa546-succidymyl ester (Molecular Probes) for 1 hour at room temperature following the manufacturer's suggestions. The bacteria were grown overnight in LB broth and washed in PBS prior to injection into loops of small intestine.

In vivo assessment of M cell uptake of fluorescent beads and bacteria

The uptake of 200 nm diameter fluorescent polystyrene latex nanoparticles (Fluoresbrite YG; Polysciences) and fluorescent bacteria by M cells in the FAE of individual PP or by villous M cells induced by exogenous RANKL treatment was assessed by either oral gavage or by using a modification of previously described isolated small intestinal loop models (34, 35). In oral gavage experiments examining uptake of the by RANKL-induced villous M cells, aliquots of 1×10^{11} 200 nm diameter nanoparticles in a volume of 100 μ l were fed to the mice. To prepare isolated small intestinal loops, mice were anesthetized using an isoflurane vaporizer. After opening the peritoneum through a longitudinal midline incision, 2 or 3 segments of small intestine measuring 2-5 cm in length and containing either a single PP (to assess PP M cell uptake) or no PP (to assess villous M cell uptake) were tied off with nylon filament. For bead uptake studies, the loops were injected with 200-400 μ l of a suspension of 200 nm nanoparticles diluted in PBS to a concentration of 1×10^{12} beads/ml and returned to the peritoneal cavity. The

mice were euthanized 90 to 120 minutes after the loops were injected, and the individual PP were excised, washed in 0.5% Tween 20-PBS, fixed in 4% paraformaldehyde in PBS for 15 minutes, and embedded in OCT. Frozen sections cut from these PP were examined by microscopy after counterstaining with DAPI, leaving out a cold acetone fixation step because acetone dissolved the polystyrene Fluoresbrite beads, preventing their visualization. For bacterial uptake studies, loops containing no PP were injected with 300 to 500 μ l of bacterial suspension at a concentration of 5×10^9 organisms/ml. After 120 minutes the mice were euthanized and the intestine tissue within the loop was embedded in OCT as a Swiss roll. Frozen sections from this tissue were fixed with -20°C acetone since this fixation did not interfere with detection of the fluorescent bacteria.

Antibodies and lectins

Monoclonal and polyclonal antibodies were purchased from eBioscience, unless otherwise stated. The mAbs used for immunofluorescence staining of frozen sections were anti-RANKL (IK22-5), anti-RANK (R12-31), PE-conjugated anti-B220 (RA3-6B2), biotinylated GL7 (for detection of activated germinal center B cells), APC-conjugated anti-Thy-1.2 (53-2.1; BD Biosciences), and anti-CD68 (FA-11; AbD Serotec). The rat mAb NKM 16-2-4 specific for mouse M cells was purified from hybridoma supernatant and labeled with FITC (36). A purified rat IgG2a isotype control mAb (BD Biosciences) was used as a control for staining of frozen tissue sections with the rat IgG2a anti-RANKL and anti-RANK mAbs. Biotinylated polyclonal goat anti-rat IgG (BD Biosciences) was used as a secondary reagent for detection of most unconjugated rat primary antibodies. Alexa546-conjugated goat anti-rat IgG (Invitrogen)

was used for the detection of the anti-CD68 mAb. Rhodamine-UEA-I was purchased from Vector Labs. The anti-RANKL antibody (IK22-5) used for in vivo RANKL neutralization experiments was prepared as described previously (37). Mice were treated with 250 µg of antibody i.p. every 2 days.

Immunofluorescence staining of frozen sections

Frozen sections of PP and adjacent intestinal tissue were cut on a cryostat and prepared for antibody staining experiments as previously described (30). The sections were washed in PBS and blocked in TNB buffer (PerkinElmer Life Sciences). Antibodies diluted in TNB buffer were applied for one hour at room temperature or overnight at 4°C. Biotinylated primary mAbs were detected using streptavidin-conjugated peroxidase followed by FITC-tyramide from a tyramide signal amplification kit (PerkinElmer Life Sciences). Unconjugated primary rat mAbs were detected by a combination of biotinylated polyclonal goat-anti-rat IgG (BD Biosciences) followed by streptavidin-peroxidase and FITC-tyramide. DAPI (Sigma-Aldrich) at 10 ng/ml was used as a nuclear counterstain. The slides were mounted in ProLong antifade reagent (Invitrogen). Images were acquired using a Nikon 80i fluorescence microscope and edited when necessary with Photoshop (Adobe Systems).

Electron microscopy

Mice were perfusion fixed using 2.5% glutaraldehyde solution in 0.1M cacodylate buffer. For transmission electron microscopy, individual PP were isolated, bisected through the center of the domes, and embedded in Epon resin. Thin sections from the PP domes of control and RANKL null mice were examined using a JEOL JEM-1210 microscope. For

scanning electron microscopy, small intestinal villi were subjected to critical point drying, sputter coated with gold, and examined on a Topcon DS-130F field emission scanning electron microscope.

Whole mount staining of small intestine tissue for detection of UEA-I⁺ M cells

For detection of M cells in PP, individual PP were excised and vortex mixed in 0.5% Tween20-PBS followed by a shaking incubation with 100 µg/ml DNase for 20 minutes at 37°C to promote dissociation of mucus from the epithelial layer. The PP were blocked with TNB buffer for 15 minutes at 4°C, and stained with rhodamine-UEA-I in TNB for 40 minutes at 4° C. Each stained PP was mounted under a 20 mm X 20 mm coverslip in 100 µl PBS. A count of UEA-I⁺ M cells was done for the PP follicle with the most M cells. This method resulted in some degree of underestimation of the full extent of M cell depletion in RANKL null mice because often only one of several PP follicles had any M cells in the mutant mice, while all the follicles in wild type PP typically had a comparable number of M cells. To examine small intestine tissue for the presence of villous M cells, thin strips of tissue were cut and stained with rhodamine UEA-I as described above for PP. Villi with M cells on their surface were classified as showing a dense or diffuse pattern of villous M cells using criteria based on the initial description of these patterns by Jang et al. (9). Specifically, villi with one or more clusters of M cells in which 75% or more of the area within the cluster was occupied with M cells were considered to have a dense distribution of villous M cells. Villi with at least one characteristic UEA-I⁺ M cell on the surface, but not meeting the dense distribution criteria, were considered to have a diffuse distribution.

Quantitative analysis of fluorescent bead and bacteria uptake by M cells

Analysis of the degree of bead uptake from loops containing PP was done by threshold analysis using ImageJ v1.36b software (<http://rsb.info.nih.gov/ij/>). Images of the fluorescent beads found within sections of individual PP follicles were saved as 8-bit grayscale images and then converted to binary images showing the beads by thresholding at a grayscale cutoff point of 75 out of 255. The percentage of the pixels with a signal intensity that exceeded this cutoff was calculated for the area occupied by each PP follicle. Analysis of the bead uptake from loops lacking PP was done by a similar approach. Images of sections showing just the fluorescent beads within epithelial cells and the villi were thresholded at a grayscale cutoff point of 55 out of 255. Images of the DAPI-stained nuclei in the same field acquired in a separate channel were thresholded at a cutoff point of 70. The extent of bead uptake was expressed as the ratio of pixels with fluorescent beads to pixels with DAPI after normalization to a mean value of 1.0 for loops from mice not treated with RANKL. Analysis of fluorescent bacteria uptake from loops lacking PP was done by counting of the number of organisms present in sections of villi showing the villus from its base to the tip. The data were reported as the percentage of villi that included at least one organism and the average number of organisms per villus. The latter statistic was normalized to a value of 1.0 for loops from mice not treated with RANKL.

ELISA for measurement of fecal IgA

Fecal pellet samples were collected and extracted by making a 1:10 suspension (w/v) with PBS. After the suspension was vortexed and spun for 10 min at 12,000g, the

supernatant was stored at -70°C . Polyclonal goat anti-mouse IgA antibody (Southern Biotechnology) was used as a capture antibody. The bound mouse IgA was detected with peroxidase-labeled goat anti-mouse IgA antibody (Southern Biotechnology) using TMB (BD Biosciences) as the peroxidase substrate. A mouse IgA, κ isotype control mAb (BD Biosciences) was used to establish a standard curve.

Statistical analysis

Differences between the mean values for groups were analyzed by either two-tailed ANOVA with Tukey correction (for multiple groups), two-tailed Student's t test, or two-tailed Mann-Whitney test as calculated using Prism (GraphPad Software). Differences in the frequency of bacterial uptake into villi were analyzed by Fisher's exact test and also calculated with Prism. A p value of less than 0.01 was considered significant.

Results

UEA-I⁺ M cells are dramatically decreased in the FAE of PP from RANKL null mice

M cells in mouse PP can be detected using the UEA-I lectin specific for $\alpha(1,2)$ -fucose linkages. In wild type mice, whole mount microscopy of PP follicles revealed an average of over 100 radially arranged UEA-I⁺ M cells that extended from the edges of the follicles towards the central subepithelial dome area. In contrast, UEA-I⁺ M cells were either completely absent or very sparsely represented in individual follicles from the PP RANKL null mice (Fig. 1A). The few remaining UEA-I⁺ cells in RANKL null mice were mostly located at the periphery of the follicle and did not have the usual polygonal shape of normal M cells, features suggesting these remaining M cells were abnormal. The loss of M cells in PP from RANKL null mice was confirmed by staining PP sections with NKM 16-2-4 (Fig. S1), a recently described rat mAb that is more selective than UEA-I for the specific $\alpha(1,2)$ -fucose moiety characteristically displayed by mouse M cells (36). Cells with the defining ultrastructural features of M cells by transmission electron microscopy (i.e. presence of intraepithelial pockets and blunting of the apical microvilli in comparison to normal enterocytes) were readily apparent in the FAE from control mice, but absent from the FAE of RANKL null mice (Fig. 1B). While the number of UEA-I⁺ M cells was significantly decreased in all PP examined from RANKL null mice, a proximal to distal gradient in the number of UEA-I⁺ cells per dome was observed in RANKL null mice that was not seen in wild type mice (Fig. 1C). UEA-I⁺ M cells were almost completely absent in the most proximal PP from RANKL null mice, and progressively increased in more distal PP. In RANKL null mice, the highest number of

residual UEA-I⁺ cells was consistently detected in the most distal ileal PP. Taking into account the decreases in RANKL null mice in the number of PP, the number of follicles in each PP, and the number of M cells per follicle, loss of RANKL is associated with a 73-fold overall depletion of UEA-I⁺ M cells. This extent of loss of M cells is roughly 10-fold greater than the losses we observed in both μ MT B cell deficient mice and CCR6 deficient mice (data not shown), strains of mutant mice previously shown to have a significant reduction in the number of M cells (38, 39).

UEA-I⁺ M cells can be restored in RANKL null mice by treatment with exogenous RANKL

To determine if the deficiency of M cells in the FAE of RANKL null PP could be restored by replacement of RANKL, RANKL null mice were injected i.p. for 7 consecutive days with 250 μ g per day of either recombinant GST-RANKL fusion protein or recombinant GST as a control. On day 7, the PP follicles of RANKL null mice treated with GST-RANKL had a near normal number of UEA-I⁺ M cells distributed in the typical radial pattern, while GST-treated mice remained profoundly M cell deficient (Fig. 2A). Daily treatment of RANKL null mice with rGST-RANKL for shorter intervals demonstrated that day 5 was the first time point at which the number of UEA-I⁺ M cells was significantly increased over untreated RANKL null mice (Fig. 2B).

RANKL null mice have a defect in the uptake of 200 nm fluorescent beads into PP follicles that is corrected by administration of RANKL

While UEA-I is a useful immunohistochemical marker of mouse M cells, this method of identification does not detect M cells based on their specialized ability to take up particulate antigens from the lumen and transport them to meet APC in the intraepithelial pockets. Measuring uptake of fluorescent nanoparticles injected into loops of small intestine is a method that directly assesses M cell function in the FAE of PP (34, 35). Frozen sections of PP in isolated loops of small intestine from RANKL null mice and RANKL null mice treated with GST-RANKL or GST (as a control) were compared at 90 minutes after injection of fluorescent 200 nm nanoparticles into the loops. In the GST-RANKL-treated mice more UEA-I⁺ M cells were present and some of these cells contained multiple fluorescent beads (Fig. 2C). Beads that had already passed through the epithelial layer to reach the PP follicle were observed in APC in the vicinity of the subepithelial dome or deeper in the B cell follicle. Image analysis was used to quantify the magnitude of bead uptake in the GST-RANKL reconstituted mice and controls (Fig. 2D). Untreated RANKL null mice or those treated with GST had over 10-fold less uptake of beads than control wild type mice. GST-RANKL treatment for 7 days restored bead uptake to near wild type levels.

Systemic administration of RANKL also leads to widespread induction of villous M cells

In the course of treating RANKL null mice with GST-RANKL and evaluating the reconstitution of M cells in PP, we noticed that the number of UEA-I⁺ cells present on small intestinal villi was also increased. This effect of RANKL treatment was further evaluated in BALB/c mice, in which less than 10% of small intestinal villi have any villous M cells at baseline, with most of these rare villous M cells arranged in a diffuse

pattern (Fig. 3A). Treatment with systemic GST-RANKL i.p. for 4 consecutive days induced substantial increase in the number of UEA-I⁺ cells with the features of M cells on the surface of the villi (Fig. 3B). Induction of an increased number of villous M cells began by 24 hours after the first injection of GST-RANKL; 4 days after the start of RANKL treatment all small intestinal villi had at least some UEA-I⁺ cells present, with 70% of villi showing a diffuse pattern and the remaining 30% exhibiting a dense pattern (Fig. 3C). In villi showing a diffuse pattern of villous M cells, UEA-I⁺ cells represented approximately 3% of the total number of cells with DAPI⁺ nuclei. Scanning electron microscopy of villi from RANKL-treated mice revealed slightly sunken cells with the characteristic stubby microvilli characteristic of M cells (Fig. 3D).

RANKL-induced villous M cells are functional M cells capable of taking up 200 nm beads and enteric bacteria

To determine whether the villous M cells induced by systemic RANKL treatment were capable of increased transport of particulate antigens across the epithelium, mice were treated with s.c. injections of RANKL for 4 consecutive days and gavaged with 200 nm diameter fluorescent nanoparticles at the same time as the last 2 RANKL injections. PP from these mice were excised 24 hours after the second dose of beads and frozen sections cut to identify beads that had been taken up into the PP by M cells. Bead uptake was readily apparent in M cells and within the villi of the RANKL-treated mice, but barely evident in the control untreated mice (Fig. 4A). Uptake of fluorescent beads was increased by an average of 74-fold over the baseline of untreated mice as a result of RANKL-induction of villous M cells (Fig. 4B). To test whether the RANKL-induced

villous M cells were also capable of enhanced uptake of enteric bacteria, isolated segments of small intestine lacking any PP from mice treated with RANKL for 4 days were injected with fluorescently labeled live enteric bacteria. Sections of the intestinal wall taken 2 hours after the introduction of the bacteria revealed substantially enhanced uptake of both *Salmonella enterica* serovar Typhimurium (35-fold) and *Yersinia enterocolitica* (46-fold) as a consequence of villous M cell induction by RANKL (Fig. 4C and 4D).

Neutralizing antibody to RANKL reproduces the M cell deficiency observed in RANKL null mice

Some of the developmental defects in RANKL null mice, such as the total absence of lymph nodes, cannot be corrected by simply injecting the mice with the absent cytokine as adults. This raises the issue of whether the M cell deficit observed in PP from RANKL null mice might be a byproduct of early developmental alterations in the PP of these mice. To address this issue, wild type BALB/c mice were treated i.p. with a neutralizing anti-RANKL antibody to determine if acute blockade of RANK/RANKL signaling would lead to loss of PP M cells. Mice were treated i.p. with 250 μ g of the IK22-5 rat anti-mouse RANKL mAb every 2 days, a dose previously shown to block the activity of RANKL in vivo (37). The number of M cells in the PP follicles was evaluated after various lengths of treatment by both UEA-I staining and by uptake of fluorescent 200 nm beads from isolated small intestinal loops. After 8 days of antibody treatment, the number of M cells present in the PP and the degree of uptake of fluorescent beads by PP in isolated loops were both dramatically decreased (Fig. 5A-C). Analysis of the

kinetics of the anti-RANKL effects showed that the number of UEA-I⁺ M cells dropped precipitously between 2 and 4 days, and declined further between 4 and 8 days (Fig. 5D).

Epithelial cells in the small intestine express RANK

RANK is expressed by multiple cell types including osteoclasts, dendritic cells, mammary epithelial cells, and thymic epithelial cells. Since our experiments with RANKL null mice and neutralizing anti-RANKL antibody showed that RANKL is essential for normal M cell development within the FAE, we used immunohistochemical staining with anti-RANK antibodies to determine what cells in the vicinity of PP expressed the RANK. Staining for RANK was observed on epithelial cells in the FAE and was also detected on villous and crypt epithelial cells (Fig. 6). Serial sections of the same PP showed that RANKL expression was restricted to stromal cells concentrated beneath the FAE as previously shown (30). These results suggest that RANKL exerts its effects on M cell differentiation through short-range delivery from the stromal cells to the FAE on the other side of the basement membrane.

RANKL null mice exhibit decreased PP germinal center formation and fecal IgA production

PP were previously reported to be smaller than normal in two independently derived strains of RANKL null mice (22, 28), but other aspects of PP function were not examined in the initial reports. We asked whether the loss of M cell function in RANKL null mice was associated with impaired B cell responses to antigens internalized from the intestinal lumen. We compared the frequency and extent of germinal center development

in PP from RANKL null mice and littermate controls using an antibody (GL7) that preferentially binds activated germinal center B cells. Compared to PP from controls, PP from RANKL null mice at 10 to 12 weeks of age exhibited a smaller percentage of germinal centers containing GL7⁺ cells in the B cell zones and a relative expansion of the T cell zones (Fig. 7A). This finding suggested that the production of secretory IgA might also be impaired in RANKL null mice. Fecal IgA concentrations in mice from 4 to 12 weeks of age were consistently decreased in RANKL null mice compared to littermate controls (Fig. 7B).

Discussion

Antigen-sampling M cells have been described in both mammalian and avian species as part of the FAE covering the organized lymphoid structures of the respiratory and digestive tract (3, 40, 41). However, the specific signals and signaling pathways that trigger the differentiation of these M cells from precursor cells located in the stem cell zone of the crypts or from the enterocytes on the surface of the FAE remain to be identified (12). Some clues have emerged from analysis of strains of mutant mice created by gene-targeting that retain PP but exhibit decreased numbers of M cells in these PP. Specifically, B cell deficient mice such as μ MT mice exhibit significantly reduced numbers of M cells in PP (38). Additional support for a role of B cells in promoting M cell development has come from in vitro studies in which co-culture of freshly isolated B lymphocyte or B lymphocyte lines with model intestinal epithelial cell lines cultured on semipermeable supports promoted the development of M cell-like features by the epithelial cells, including transcytosis of particulate antigens (11, 42). However, neither in vivo analysis of PP from B cell deficient mice or experiments based on the in vitro M cell differentiation system have elucidated a specific mechanism by which B cells promote differentiation of M cells in the FAE.

RANKL emerged as a cytokine with a potential role in the differentiation of the FAE and M cells as a result of experiments demonstrating RANKL expression on stromal cells located immediately beneath the FAE in ILF and PP (30). To determine if PP were functionally compromised in the absence of RANKL, we characterized the PP of RANKL null mice. Staining of PP from RANKL null mice with the UEA-I lectin

reactive with murine M cells revealed a profound depletion in UEA-I⁺ cells compared to wild type mice. Taking into account all of the factors that contribute to the total number of M cells within small intestinal PP (i.e. number of PP, number of follicles per PP, number of M cells per follicle), we find that RANKL null mice have less than 2% of the number of UEA-I⁺ M cells found in wild type mice. While the UEA-I lectin is the immunohistochemical reagent we relied on the most to establish that RANKL null mice are deficient in M cells, we have used several independent means of confirming this deficiency in M cells including functional measurements of M cell activity using uptake of fluorescent nanoparticles and bacteria, transmission electron microscopy, and immunostaining with the NKM 16-2-4 monoclonal antibody specific for mouse M cells.

RANKL acting through its specific receptor (RANK) plays an important developmental role in multiple tissues. The most striking and best-studied of the deficits in RANKL null mice are the absence of any lymph nodes and the failure of osteoclast development, leading to osteopetrosis and a malformed skeleton. One potential explanation of the loss of M cells we observed in PP from RANKL null mice is an early developmental defect in PP development that permanently compromises the capacity of the FAE to generate conventional M cells. Two types of experiments were done to test this possibility. First, we examined whether the M cell defect was reversible if a source of exogenous recombinant RANKL was provided. Daily injections of GST-RANKL given for 5 or more days provided a nearly complete reconstitution of the number of M cells per PP follicle. Second, we used neutralizing mAb to RANKL to test whether acute depletion of RANKL in adult wild type mice would also cause loss of M cells. After 4 days of anti-RANKL treatment to inhibit normal RANKL-RANK interactions, the

number of UEA-I⁺ M cells in each PP follicle plunged to levels approaching those in the RANKL null mice. Thus, production of RANKL must be sustained in the adult PP to permit the continued production and/or survival of M cells.

RANK is expressed on multiple cell types including osteoclasts and their precursors, dendritic cells, endothelial cells, mTEC, and mammary epithelial cells. The simplest model to explain the observed effects of RANKL on M cell differentiation is to propose that RANKL derived from the subepithelial dome stromal cells in the PP acts in a paracrine fashion on the adjacent epithelial cells of the FAE. Because RANKL is a type II membrane protein that is synthesized in a transmembrane form, cleavage by metalloproteases is needed to generate a soluble form of the cytokine (17, 18). We favor the hypothesis that RANKL is acting directly through RANK on enterocytes because immunohistochemical staining of small intestinal tissue including a PP showed that the bulk of the RANK staining is localized to the epithelium, with roughly equivalent levels of RANK on the FAE and villous epithelium. Gene expression profiling studies comparing flow sorted PP M cells and villous enterocytes revealed that both of these intestinal epithelial cell types express mRNA for RANK (36) (gene expression data for RANK archived in NCBI Gene Expression Omnibus under accession number GSE7838).

The capacity of soluble recombinant RANKL injected systemically to induce the appearance of M cells on all small intestinal villi provides further insights into the mechanism of action of RANKL. RANK-expressing epithelial precursor cells located in both dome-associated crypts next to PP follicles and in standard small intestinal crypts have the potential to differentiate into M cells if exposed to sufficient stimulation with RANKL. RANKL-induced villous M cells have most of the same features as PP M cells,

including reactivity with UEA-I, stubby surface microvilli observed by scanning electron microscopy, and most importantly the capacity for constitutive uptake of particulate antigens. Under normal conditions, M cell development is primarily restricted (other than a small number of scattered villous M cells) to the organized lymphoid tissues of the small intestine (i.e. PP and ILF) because constitutive expression of RANKL is restricted to subepithelial stromal cells at these sites. When the spatial restriction of RANKL availability in the small intestine is bypassed by systemic injection, RANKL is able to trigger M cell differentiation in a fraction of epithelial precursors in both dome-associated crypts adjacent to organized lymphoid tissues and normal crypts.

While our results identify RANKL as a key cytokine signal involved in inducing the differentiation of M cells from precursors in the FAE, we consistently observed a trace number of residual UEA-I⁺ M cells in a few of the PP follicles in RANKL null mice. Our results fit best with a model that postulates that there are additional signals besides RANKL that contribute to the development of M cells. We found that the most distal PP in RANKL null mice was invariably the PP with the largest number of residual M cells per follicle, suggesting that an increased density of luminal commensal bacteria can accentuate the extent of M cell differentiation locally in situations in which loss of an M cell-inducing factor results in a global decrease in M cell differentiation. One of the other signals capable of promoting M cell development may be contributed by local B cells in the PP, since absence of mature B cells also leads to depletion of PP M cells (38), although the degree of M cell deficit is far less pronounced. Exogenous administration of GST-RANKL to B cell deficient $J_H^{-/-}$ mice does not increase the number of PP M cells (unpublished observations), indicating that the contribution of B cells to the development

of M cells does not involve simply providing RANKL. Given that TNF family members are known to have overlapping and partially redundant functions in other developmental contexts (e.g. the known contributions of $LT\alpha_1\beta_2$, RANKL, and TNF- α to the normal formation and organization of secondary lymphoid structures) (43), other TNF family members may contribute to the induction of M cell differentiation and account for the low level of residual M cell formation in the absence of RANKL. Cooperation of RANKL with the TNF family member CD40L has recently been established for the induction of mTEC differentiation (24, 25). RANKL is the most critical TNF family member in inducing normal mTEC differentiation during embryonic development of the thymus, with CD40L playing a complementary role in the postnatal thymus (24). Interesting parallels exist between the role of RANKL in inducing differentiation of UEA-I⁺ M cells in the FAE of PP and its role in inducing the differentiation of UEA-I⁺ mTEC in the thymus. The RANKL-induced mTECs are critical for establishment of central T cell tolerance, while RANKL-induced M cells contribute to the establishment of peripheral T cell tolerance to bacterial antigens at mucosal surfaces normally colonized by commensal bacteria.

The identification of RANKL as a key switch factor that can elicit M cell development by intestinal epithelial precursors has the potential to yield valuable translational applications in the areas of mucosal vaccine development and oral tolerance induction. Specifically targeting orally administered antigens to M cells using either monoclonal antibodies to M cell surface receptors, lectins, or bacterial adhesins specific for M cells remains an active area in the development of vaccines for oral delivery (44). Combining antibody-mediated M cell targeting of antigen with a strong mucosal adjuvant

(e.g. cholera toxin) already shows promise as a strategy for the establishment of both mucosal and systemic immunity to vaccine antigens (45). The efficacy of such approaches may be boosted if preceded by systemic or ideally local delivery of exogenous RANKL aimed at increasing the frequency of human M cells in the PP FAE and particularly in the villous epithelium to supraphysiologic levels, thereby increasing the efficiency of delivery of M cell-targeted vaccines administered at mucosal surfaces.

Acknowledgements

We thank Dr. Max Cooper for valuable suggestions and Dr. Tim Denning for comments on the manuscript. We also thank Dr. Yongwon Choi for providing us with RANKL knockout mice, Katy Gray in Dr. Sam Speck's laboratory for help obtaining breeder pairs of μ MT mice, and Jeannette Taylor from the Robert P. Apkarian Integrated Electron Microscopy Core for expert technical assistance with electron microscopy. This work was supported by grants from the NIH (DK64730 to I.R.W. and DK64399 supporting the Imaging Core Facility of the Emory Digestive Diseases Research Development Center) and a Senior Research Award from the Crohn's & Colitis Foundation of America (to I.R.W.).

References

1. Fagarasan, S. & Honjo, T. Regulation of IgA synthesis at mucosal surfaces. *Curr. Opin. Immunol.* **16**, 277-283 (2004).
2. Iweala, O.I. & Nagler, C.R. Immune privilege in the gut: the establishment and maintenance of non-responsiveness to dietary antigens and commensal flora. *Immunol. Rev.* **213**, 82-100 (2006).
3. Kraehenbuhl, J.P. & Neutra, M.R. Epithelial M cells: differentiation and function. *Annu. Rev. Cell Dev. Biol.* **16**, 301-332 (2000).
4. Pabst, O., Bernhardt, G. & Forster, R. The impact of cell-bound antigen transport on mucosal tolerance induction. *J. Leukocyte Biol.* **82**, 795-800 (2007).
5. Martinoli, C., Chiavelli, A. & Rescigno, M. Entry route of *Salmonella typhimurium* directs the type of induced immune response. *Immunity* **27**, 975-984 (2007).
6. Hashizume, T. *et al.* Peyer's patches are required for intestinal immunoglobulin A responses to *Salmonella*. *Infect. Immun.* **76**, 927-934 (2008).
7. Macpherson, A.J. & Uhr, T. Compartmentalization of the mucosal immune responses to commensal intestinal bacteria. *Ann. N. Y. Acad. Sci.* **1029**, 36-43 (2004).
8. Suzuki, H. *et al.* Ovalbumin-protein sigma 1 M-cell targeting facilitates oral tolerance with reduction of antigen-specific CD4+ T cells. *Gastroenterology* **135**, 917-925 (2008).
9. Jang, M.H. *et al.* Intestinal villous M cells: an antigen entry site in the mucosal epithelium. *Proc. Natl. Acad. Sci. USA* **101**, 6110-6115 (2004).
10. Owen, R.L. & Jones, A.L. Epithelial cell specialization within human Peyer's patches: an ultrastructural study of intestinal lymphoid follicles. *Gastroenterology* **66**, 189-203 (1974).

11. Kerneis, S., Bogdanova, A., Kraehenbuhl, J.P. & Pringault, E. Conversion by Peyer's patch lymphocytes of human enterocytes into M cells that transport bacteria. *Science* **277**, 949-952 (1997).
12. Mach, J., Hsieh, T., Hsieh, D., Grubbs, N. & Chervonsky, A. Development of intestinal M cells. *Immunol. Rev.* **206**, 177-189 (2005).
13. Kerneis, S. & Pringault, E. Plasticity of the gastrointestinal epithelium: the M cell paradigm and opportunism of pathogenic microorganisms. *Semin. Immunol.* **11**, 205-215 (1999).
14. Gebert, A., Fassbender, S., Werner, K. & Weissferdt, A. The development of M cells in Peyer's patches is restricted to specialized dome-associated crypts. *Am. J. Pathol.* **154**, 1573-1582 (1999).
15. Lelouard, H., Sahuquet, A., Reggio, H. & Montcourrier, P. Rabbit M cells and dome enterocytes are distinct cell lineages. *J. Cell. Sci.* **114**, 2077-2083 (2001).
16. Bachmann, M.F. *et al.* TRANCE, a tumor necrosis factor family member critical for CD40 ligand-independent T helper cell activation. *J. Exp. Med.* **189**, 1025-1031 (1999).
17. Lum, L. *et al.* Evidence for a role of a tumor necrosis factor- α (TNF- α)-converting enzyme-like protease in shedding of TRANCE, a TNF family member involved in osteoclastogenesis and dendritic cell survival. *J. Biol. Chem.* **274**, 13613-13618 (1999).
18. Hikita, A. *et al.* Negative regulation of osteoclastogenesis by ectodomain shedding of receptor activator of NF- κ B ligand. *J. Biol. Chem.* **281**, 36846-36855 (2006).
19. Wong, B.R. *et al.* The TRAF family of signal transducers mediates NF- κ B activation by the TRANCE receptor. *J. Biol. Chem.* **273**, 28355-28359 (1998).
20. Galibert, L., Tometsko, M.E., Anderson, D.M., Cosman, D. & Dougall, W.C. The involvement of multiple tumor necrosis factor receptor (TNFR)-associated factors in the signaling mechanisms of receptor activator of NF- κ B, a member of the TNFR superfamily. *J. Biol. Chem.* **273**, 34120-34127 (1998).

21. Simonet, W.S. *et al.* Osteoprotegerin: a novel secreted protein involved in the regulation of bone density. *Cell* **89**, 309-319 (1997).
22. Kong, Y.Y. *et al.* OPGL is a key regulator of osteoclastogenesis, lymphocyte development and lymph-node organogenesis. *Nature* **397**, 315-323 (1999).
23. Kim, N., Odgren, P.R., Kim, D.K., Marks, S.C., Jr. & Choi, Y. Diverse roles of the tumor necrosis factor family member TRANCE in skeletal physiology revealed by TRANCE deficiency and partial rescue by a lymphocyte-expressed TRANCE transgene. *Proc. Natl. Acad. Sci. U.S.A.* **97**, 10905-10910 (2000).
24. Akiyama, T. *et al.* The tumor necrosis factor family receptors RANK and CD40 cooperatively establish the thymic medullary microenvironment and self-tolerance. *Immunity* **29**, 423-437 (2008).
25. Hikosaka, Y. *et al.* The cytokine RANKL produced by positively selected thymocytes fosters medullary thymic epithelial cells that express autoimmune regulator. *Immunity* **29**, 438-450 (2008).
26. Wong, B.R. *et al.* TRANCE (tumor necrosis factor [TNF]-related activation-induced cytokine), a new TNF family member predominantly expressed in T cells, is a dendritic cell-specific survival factor. *J. Exp. Med.* **186**, 2075-2080 (1997).
27. Fata, J.E. *et al.* The osteoclast differentiation factor osteoprotegerin-ligand is essential for mammary gland development. *Cell* **103**, 41-50 (2000).
28. Yoshida, H. *et al.* Different cytokines induce surface lymphotoxin- $\alpha\beta$ on IL-7 receptor- α cells that differentially engender lymph nodes and Peyer's patches. *Immunity* **17**, 823-833 (2002).
29. Taylor, R.T. *et al.* Lymphotoxin-independent expression of TNF-related activation-induced cytokine by stromal cells in cryptopatches, isolated lymphoid follicles, and Peyer's patches. *J. Immunol.* **178**, 5659-5667 (2007).

30. Katakai, T. *et al.* Organizer-like reticular stromal cell layer common to adult secondary lymphoid organs. *J. Immunol.* **181**, 6189-6200 (2008).
31. Terahara, K. *et al.* Comprehensive gene expression profiling of Peyer's patch M cells, villous M-like cells, and intestinal epithelial cells. *J. Immunol.* **180**, 7840-7846 (2008).
32. Golovkina, T.V., Shlomchik, M., Hannum, L. & Chervonsky, A. Organogenic role of B lymphocytes in mucosal immunity. *Science* **286**, 1965-1968 (1999).
33. Lugerling, A. *et al.* Absence of CCR6 inhibits CD4⁺ regulatory T-cell development and M-cell formation inside Peyer's patches. *Am. J. Pathol.* **166**, 1647-1654 (2005).
34. Pappo, J. & Ermak, T.H. Uptake and translocation of fluorescent latex particles by rabbit Peyer's patch follicle epithelium: a quantitative model for M cell uptake. *Clin. Exp. Immunol.* **76**, 144-148 (1989).
35. Chabot, S., Wagner, J.S., Farrant, S. & Neutra, M.R. TLRs regulate the gatekeeping functions of the intestinal follicle-associated epithelium. *J. Immunol.* **176**, 4275-4283 (2006).
36. Shepherd, N.A., Crocker, P.R., Smith, A.P. & Levison, D.A. Exogenous pigment in Peyer's patches. *Hum. Pathol.* **18**, 50-54 (1987).
37. Urbanski, S.J., Arsenault, A.L., Green, F.H. & Haber, G. Pigment resembling atmospheric dust in Peyer's patches. *Mod. Pathol.* **2**, 222-226 (1989).
38. Powell, J.J. *et al.* Characterisation of inorganic microparticles in pigment cells of human gut associated lymphoid tissue. *Gut* **38**, 390-395 (1996).
39. Thoree, V. *et al.* Phenotype of exogenous microparticle-containing pigment cells of the human Peyer's patch in inflamed and normal ileum. *Inflamm. Res.* **57**, 374-378 (2008).
40. Kamijo, S. *et al.* Amelioration of bone loss in collagen-induced arthritis by neutralizing anti-RANKL monoclonal antibody. *Biochem. Biophys. Res. Commun.* **347**, 124-132 (2006).

41. Neutra, M.R., Mantis, N.J. & Kraehenbuhl, J.P. Collaboration of epithelial cells with organized mucosal lymphoid tissues. *Nat. Immunol.* **2**, 1004-1009 (2001).
42. Kunisawa, J., Nochi, T. & Kiyono, H. Immunological commonalities and distinctions between airway and digestive immunity. *Trends Immunol.* **29**, 505-513 (2008).
43. des Rieux, A. *et al.* An improved in vitro model of human intestinal follicle-associated epithelium to study nanoparticle transport by M cells. *Eur. J. Pharm. Sci.* **30**, 380-391 (2007).
44. Powell, J.J., Thoree, V. & Pele, L.C. Dietary microparticles and their impact on tolerance and immune responsiveness of the gastrointestinal tract. *Br. J. Nutr.* **98 Suppl 1**, S59-63 (2007).
45. Pfeffer, K. Biological functions of tumor necrosis factor cytokines and their receptors. *Cytokine Growth Factor Rev.* **14**, 185-191 (2003).
46. Foxwell, A.R., Cripps, A.W. & Kyd, J.M. Optimization of oral immunization through receptor-mediated targeting of M cells. *Hum. Vaccin.* **3**, 220-223 (2007).
47. Nochi, T. *et al.* A novel M cell-specific carbohydrate-targeted mucosal vaccine effectively induces antigen-specific immune responses. *J. Exp. Med.* **204**, 2789-2796 (2007).
48. Kim, D. *et al.* Regulation of peripheral lymph node genesis by the tumor necrosis factor family member TRANCE. *J. Exp. Med.* **192**, 1467-1478 (2000).
49. Kucharzik, T., Hudson, J.T., 3rd, Waikel, R.L., Martin, W.D. & Williams, I.R. CCR6 expression distinguishes mouse myeloid and lymphoid dendritic cell subsets: demonstration using a CCR6 EGFP knock-in mouse. *Eur. J. Immunol.* **32**, 104-112 (2002).
50. Kubota, K., Sakikawa, C., Katsumata, M., Nakamura, T. & Wakabayashi, K. Platelet-derived growth factor BB secreted from osteoclasts acts as an osteoblastogenesis inhibitory factor. *J. Bone Miner. Res.* **17**, 257-265 (2002).

Figure Legends

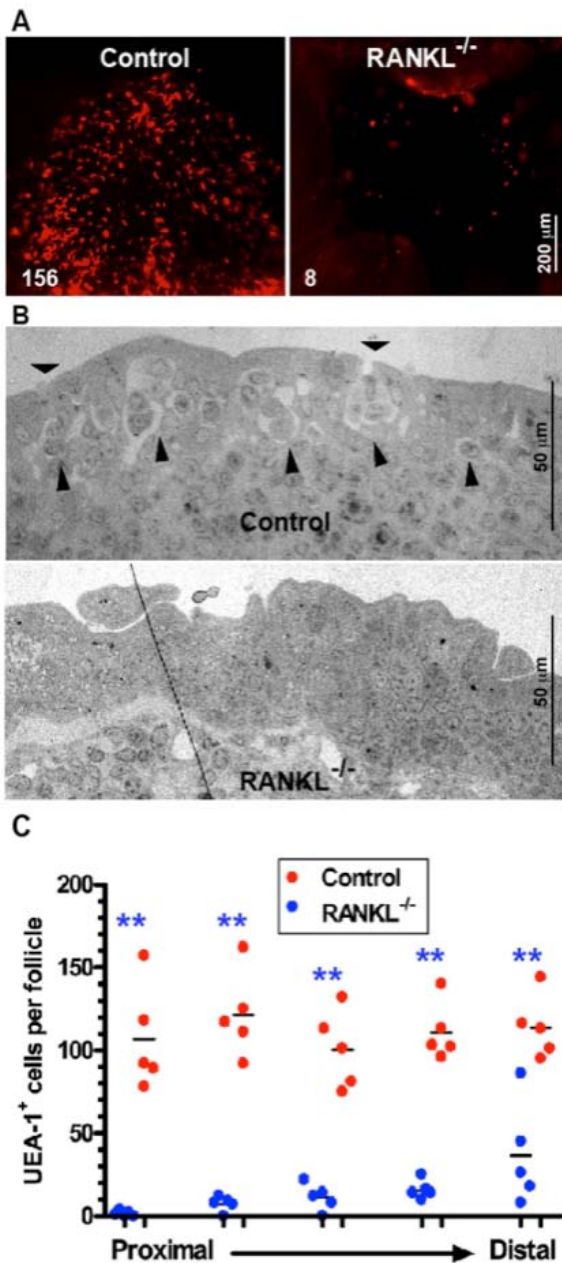


Figure 1. PP of RANKL null mice contain very few M cells. A, UEA-I staining reveals far fewer M cells in a representative follicle from a RANKL null PP compared to a wild type control PP. The number of M cells counted in the follicle is indicated in the lower left hand corner. The follicles shown are from the middle portion of the small intestine. Scale bar, 200 μm . B, FAE of RANKL null mice showed a lack of characteristic M cell

features by transmission electron microscopy. The long arrowheads indicate intraepithelial pockets within the M cells. The short arrowheads point to the shorter microvilli found on the apical surface of M cells. Scale bars, 50 μm . C, Scatter plot summarizing frequency of UEA-I⁺ M cells in individual PP follicles from RANKL null and control mice (n=5 mice for both groups). All PP examined were assigned to 1 of 5 groups based on proximal to distal position. **, $p \leq 0.001$ compared to control mice by ANOVA.

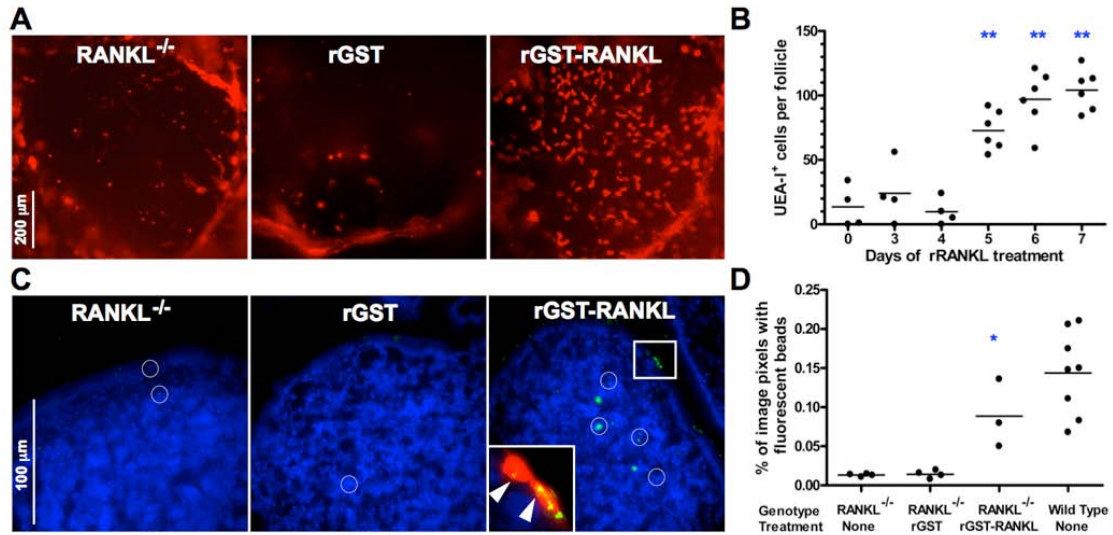


Figure 2. Administration of rRANKL to RANKL null mice restores PP M cells. A, RANKL null mice were treated i.p. for 7 days with 250 μg/day of GST-RANKL or GST as a control. UEA-I staining of representative follicles from the distal small intestine shows restoration of the normal number and pattern of UEA-I⁺ M cells by GST-RANKL, but not by GST. Scale bar, 200 μm. B, Reconstitution of UEA-I⁺ M cells requires 5 days of treatment with GST-RANKL. The results are based on 3 to 6 mice at each time point and include data from all PP except the most distal PP. ** indicates $p \leq 0.001$ compared to untreated mice by ANOVA. C, Uptake of 200 nm diameter fluorescent beads from isolated small intestinal loops into PP of RANKL null mice 90 minutes after bead injection is restored to near wild type levels by prior treatment with GST-RANKL for 5 days. Merged images of bead fluorescence and DAPI fluorescence from frozen sections of PP are shown with the white circles indicating the location of individual beads or clusters of beads. The inset shows a magnified image of the boxed area additionally merged with the rhodamine-UEA-I signal to show that the clusters of fluorescent beads (indicated by arrowheads) within 2 adjacent UEA-I⁺ M cells on the surface of the FAE. Scale bar, 100 μm. D, Summary scatter plot showing that GST-RANKL treatment

reconstitutes uptake of fluorescent beads as assessed by image analysis of the percentage of pixels containing green fluorescent beads within the area of the PP follicles. *, $p < 0.01$ compared to untreated mice by ANOVA.

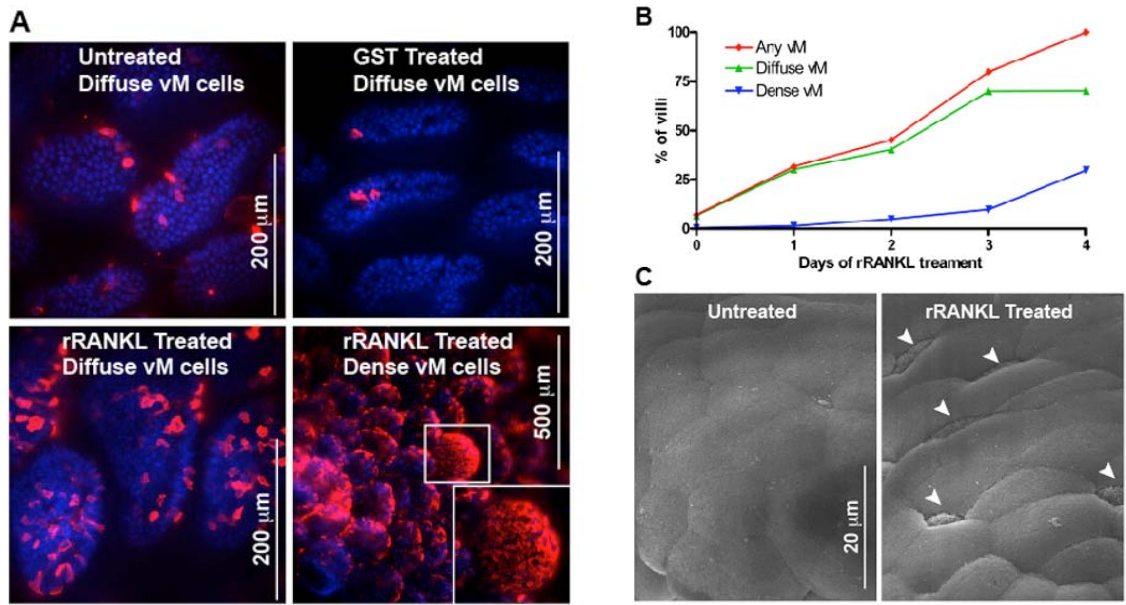


Figure 3. Administration of rRANKL induces development of villous M cells on all small intestinal villi. A, Whole mount staining of villous M cells in untreated BALB/c mice, BALB/c mice treated for 4 days with GST (an initial injection of 50 μ g i.p. followed by 100 μ g s.c. of GST every 24 hours), or BALB/c mice treated for 4 days with GST-RANKL (an initial injection of 50 μ g i.p. followed by 100 μ g of GST-RANKL every 24 hours) with rhodamine-UEA-I and DAPI. Villous M cells in diffuse patterns are found on occasional villi. GST-RANKL treatment leads to an increased fraction of villi with M cells and an increase in the number of M cells per villus. Both diffuse and dense patterns of villous M cell distribution were observed. Scale bar, 200 μ m and 500 μ m. B, Summary graph showing kinetics of induction of villous M cells in the diffuse and dense patterns of distribution following GST-RANKL administration. C, Scanning electron microscopy reveals the presence of cells with a depressed surface and attenuated and blunted microvilli characteristic of M cells.

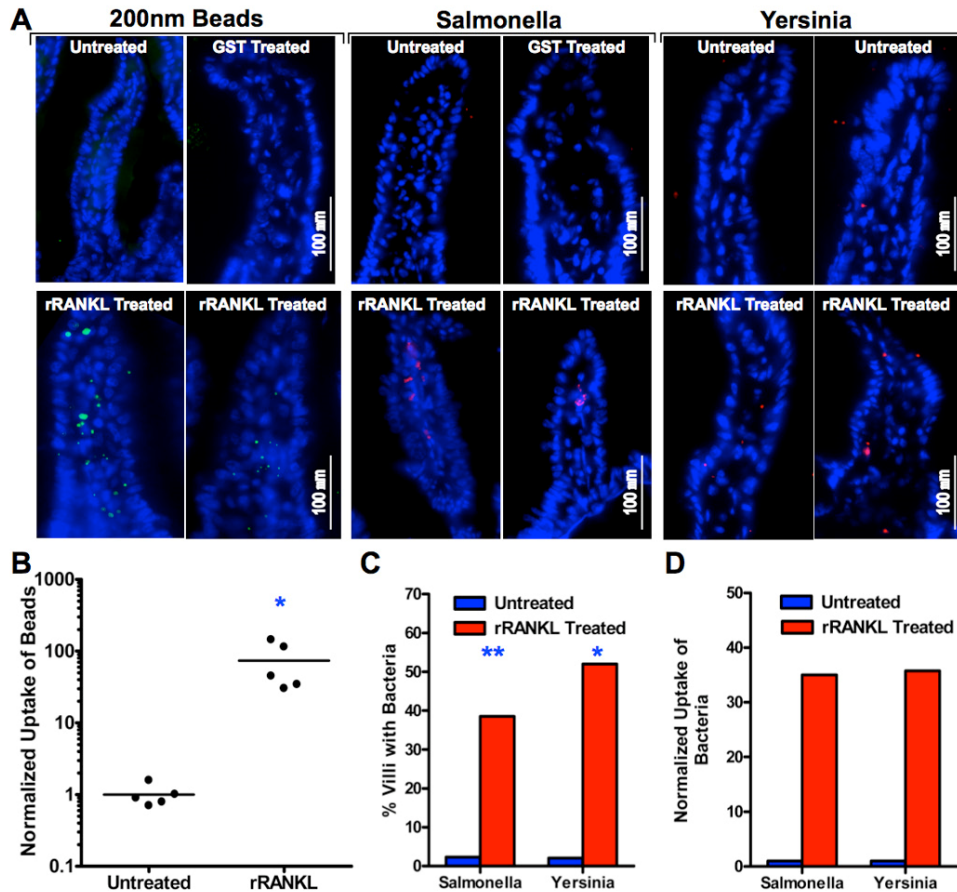


Figure 4. RANKL-induced villous M cells are functional for bead and bacteria uptake from the intestinal lumen. A, Wild type (C57BL/6 x BALB/c)_{F1} mice were treated with 100 μg of GST-RANKL, or GST s.c. once a day for 4 consecutive days. On the last two days of injections, the mice and untreated controls also received 1×10^{11} 200 nm fluorescent beads by gavage. One day after the last dose of GST-RANKL or GST, segments of small intestine were harvested and sectioned to check for the presence of green fluorescent beads. Alternatively, isolated small intestinal loops were prepared in anesthetized mice treated for 4 days with RANKL, or GST and untreated controls and these loops were injected with *Salmonella enterica* serovar Typhimurium expressing DsRed-Express or *Yersinia enterocolitica* labeled with Alexa546. After 2 hour incubation, the tissue was harvested for frozen sections. The merged images show

representative villi with DAPI positive nuclei and either green fluorescent beads or red fluorescent bacteria within the villi. B, Uptake of beads was quantitated by image analysis and normalized so that the average uptake in untreated controls was 1.0. *, $p < 0.01$ by Mann-Whitney test. C, The percentage of villi containing at least one bacterial organism was substantially increased in RANKL-treated mice. **, $p \leq 0.001$; *, $p < 0.01$ (both by Fisher's exact test). D, Uptake of bacteria was quantitated by counting individual bacteria within villi. The mean number of bacteria found per villus was normalized to a value of 1.0 for the untreated controls.

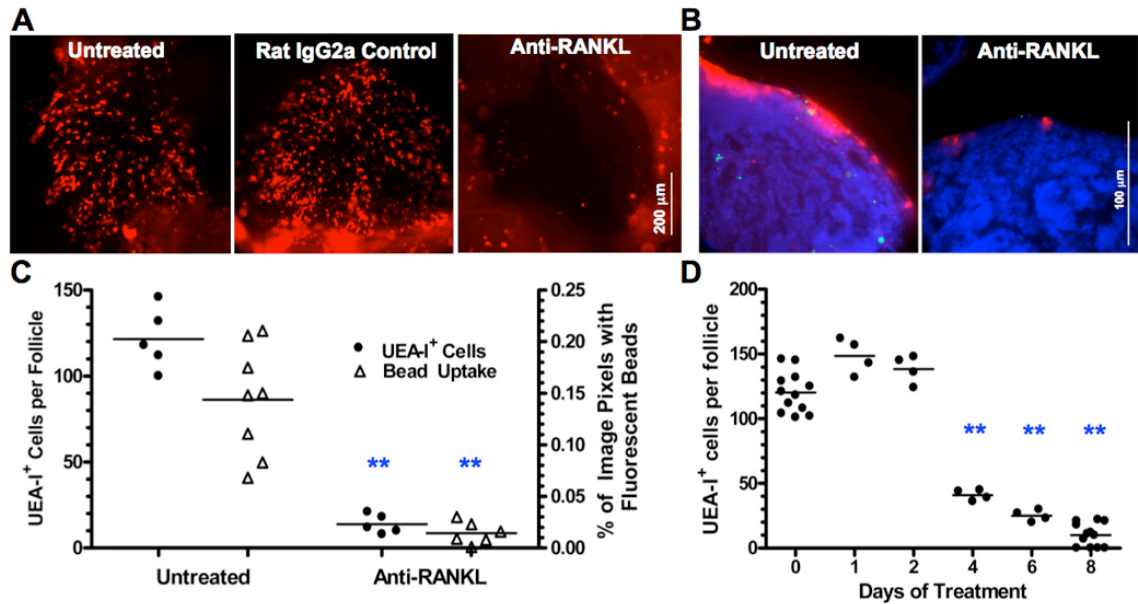


Figure 5. Treatment of wild type mice with neutralizing anti-RANKL leads to loss of PP M cells. A,B, BALB/c mice were treated i.p. with 250 μg of IKK22-5 mAb, or functional isotype control rat IgG2a antibody on days 0, 2, 4, and 6. On day 8, isolated bowel loops containing PP were injected with fluorescent beads and the mice euthanized after 90 minutes. Anti-RANKL treatment led to loss of UEA-I⁺ M cells detected by whole mount staining (A) and a decrease in the uptake of fluorescent beads detected on frozen sections of PP from the bead-injected loops (B). Scale bar, 200 μm in A and 100 μm in B. C, Summary of data from all PP analyzed in A and B for UEA-I⁺ cells and fluorescent bead uptake. D, Anti-RANKL-induced loss of UEA-I⁺ M cells detected by whole mount staining begins by 4 days after start of antibody treatment. ** in C and D indicates $p < 0.001$ compared to untreated mice by t-test (C) or ANOVA (D)

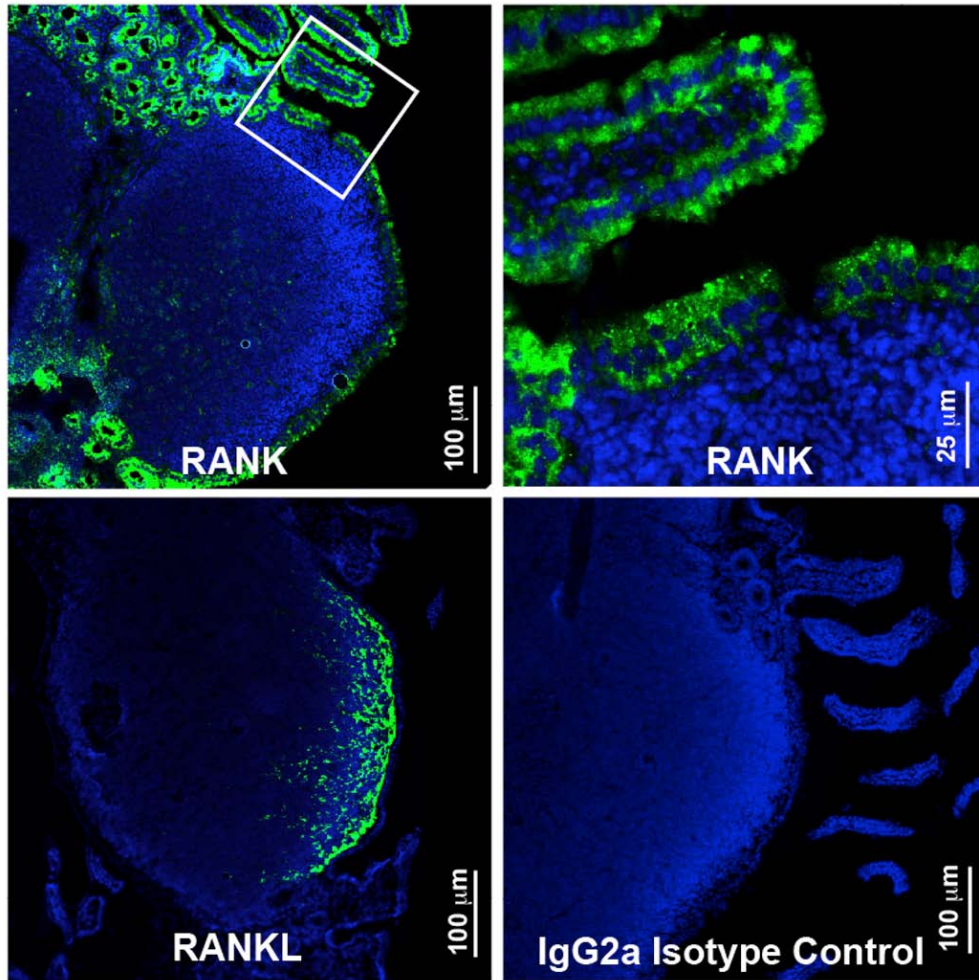


Figure 6. Intestinal epithelial cells express RANK. Frozen sections of a PP from a wild type BALB/c mouse were stained with rat mAbs to mouse RANK (A, B), mouse RANKL (C), or an isotype control rat IgG2a antibody (D), followed by a biotinylated secondary antibody, streptavidin-peroxidase, and FITC-tyramide plus DAPI as a counterstain. A. RANK expression is localized to epithelial cells in the FAE and on the adjacent villi. Scale bar, 200 μm . B. Higher magnification of RANK staining show RANK is present throughout the cell, including the apical and basolateral membranes. Scale bar, 100 μm . C. Reticular stromal cells concentrated immediately beneath the epithelial layer are the only cells on which RANKL is detected. Scale bar, 200 μm .

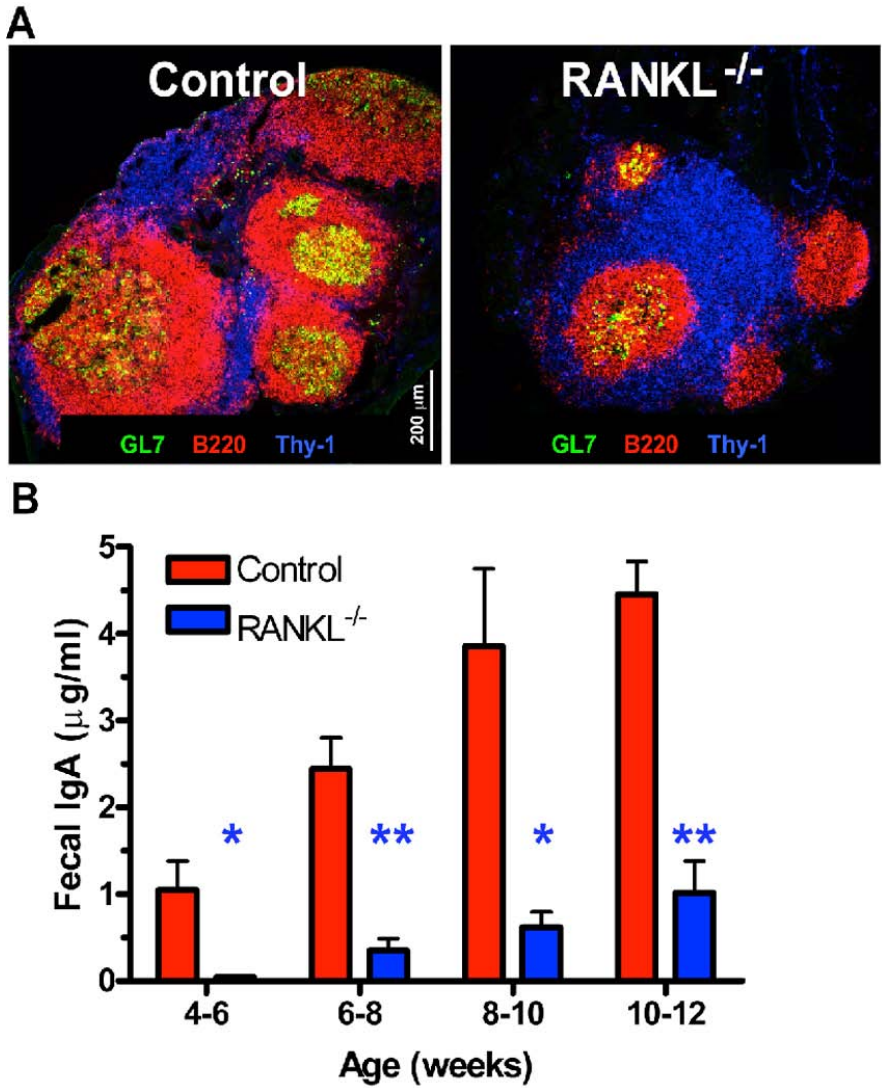
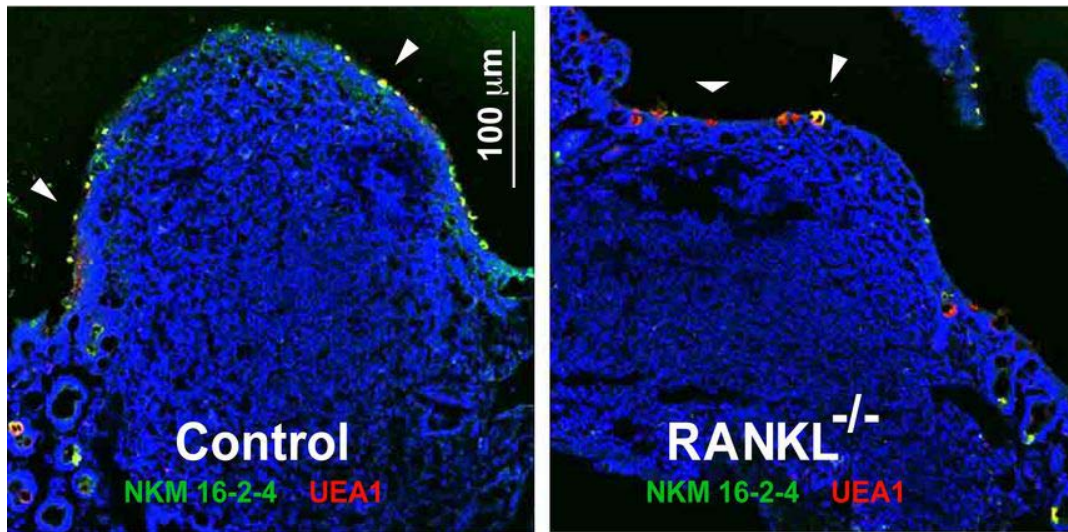


Figure 7. RANKL^{-/-} mice have fewer germinal centers in their PP follicles and lower levels of fecal IgA. A, RANKL^{-/-} PP have fewer and less developed germinal centers identified by GL7⁺ cells than control PP. B, Fecal IgA concentrations (mean ± S.D.) measured by ELISA were consistently decreased in RANKL^{-/-} mice compared to littermate controls based on analysis of samples from 5 to 16 mice of each genotype in each age range tested. *, p < 0.01; **, p < 0.001 (compared to control mice by t-test).



Supplemental Figure 1. PP from RANKL null mice have very few cells reactive with the NKM 16-2-4 monoclonal antibody specific for M cells. A,B, sections of PP from the middle portion of the small intestine from wild type mice (A) and RANKL null mice (B) were stained with FITC-NKM 16-2-4 and rhodamine-UEA-I. The small arrowhead indicates a cell positive from UEA-I, but negative from NKM 16-2-4. Scale bar, 100 μ m.

Chapter 2

Differentiation of Peyer's patch M cells does not require signals from B cells

Kathryn A. Knoop¹, Betsy R. Butler¹, Nachiket Kumar¹, Hideo Yagita², and Ifor R. Williams¹

¹Department of Pathology and Laboratory Medicine, Emory University School of Medicine, Atlanta, GA 30322

²Department of Internal Medicine, Washington University School of Medicine, Tokyo, Japan

Manuscript in progress

All experiments in this study were performed by Kathryn A. Knoop, with assistance from Betsy R. Butler.

This manuscript was written by Kathryn A. Knoop.

Abstract

Microfold (M) cells are antigen-sampling cells in the epithelium covering Peyer's patches (PP) and other mucosal lymphoid tissues, imperative for immune surveillance in the gut. The exact cues for M cell differentiation have long been sought after. The previously demonstrated reduction in the number of PP M cells in B cell deficient mice led to a model proposing that B cells provide critical signals supporting M cell differentiation. We show with a model of acute antibody-mediated B cell depletion, the number of PP M cells per dome was essentially unchanged. Comparing the number of M cells per dome to the dome surface area shows while B cell deficient mice do have fewer M cells and smaller domes, the density of M cells on the PP dome is the same for BALB/c, B cell depleted, or B cell deficient mice. The only mouse model that shows a significant decrease in the M cell density is the RANKL^{-/-} mouse. We conclude that B cells from PPs are not required normal differentiation of PP M cells. Rather, the modest decrease in the number of PP M cells observed in B cell deficient mice appears to be a consequence of abnormal embryonic PP and FAE development rather than just absence of B cells.

Introduction

In the small intestine, the ability to constantly sample luminal antigens is essential in preserving homeostasis and maintaining tolerance to antigens derived from food and commensal bacteria while still maintaining the ability to launch an effective response against pathogens (1). Acting as the main sampling mechanism in the gut, M cells are specialized epithelial cells able to transcytose particulate antigen (2). M cells differ from enterocytes on both the apical and basolateral sides of the cells. M cells lack the longer brush border seen in enterocytes cells and instead are lined with short microvilli containing unique glycoproteins (3, 4). M cells have an invagination on the basolateral side of the cell is often occupied by lymphocytes or dendritic cells, referred to as the intraepithelial pocket. (5, 6). The majority of M cells are found part of the follicle-associated epithelium (FAE) overlaying Peyer's patches (PP) or isolated lymphoid follicles (ILFs) (4, 7). All of the small intestinal epithelium, including the FAE is a single-cell layer of epithelium that undergoes replacement every 3 days (8). Proliferating stem cells in the crypts give rise to a variety of cells, including enterocytes, M cells, Paneth cells, goblet cells, and enteroendocrine cells, based on different signals the cells receive (9, 10). Because M cells are primarily found over lymphoid tissue, and only rarely are found on villi, it has been hypothesized that lymphocytes (vs. lymphoid tissue) somehow trigger the development of M cells. Idea of B cells vs. stromal molecule. RANKL data suggests stroma plays a major role, but some RANKL could still be coming from hematopoietic cells (cite manuscripts showing B cell subsets with RANKL and activated T cells making RANKL).

B cells have long been considered an important factor in M cell development since the finding that B cell deficient mice have a reduced number of M cells (11). Due to the proximity of M cells to B cells as M cells are mostly found overlaying PP follicles, it was hypothesized lymphocytes could regulate M cell development. Further adding credit to this theory was the development of in vitro systems replicating the M cell phenomenon using lymphocytes and epithelial cells (12). The addition of Raji B cells to Caco-2 cells has been shown to induce the ability of Caco-2 cells to transcytose nanoparticles (13). This system has been used to show B cells can modulate gene expression in M cells (14). The exact signal B cells use to promote M cell has yet to be found; M cells do not require activated B cells or secreted immunoglobulin for differentiation (11). Disruption of the lymphotoxin system, known to be important in the development of proper architecture of lymphoid tissues (15), via inhibition of $LT\beta R$ can reduce M cell development (16). However lymphotoxin from B cells is not required for M cell development (16, 17).

The extent B cells play in M cell differentiation in vivo, however, seems to be minimal; M cells develop in all B cell deficient mice and $Rag1^{-/-}$ (16). The chemokine/receptor partnership CCR6, on lymphocytes, and CCL20, expressed by FAE, is required for the homing of B cells to PPs (18). $CCR6^{-/-}$ mice have smaller PP domes, less FAE, but still maintain M cells (18). While B cells are not required for the in vivo development of M cells, B cells, however, are imperative for proper development of the FAE (16); absence of B cells correlated with a decrease in the size of the FAE. The requirement of B cells for the maintenance of M cells and homeostasis of the FAE rather than the development of M cells has been suggested (19), though attempting to

demonstrate this using mice with genetic B cell deficiency does not separate M cell maintenance from the initial development of the FAE. The impaired development of PPs and FAE in mice with genetic deficiencies of B cells may confound results when studying M cell development and homeostasis of the epithelium.

In this study, we use a model of acute B cell depletion to reassess the role of B cells in the development of M cells by allowing the FAE to properly develop prior to B cell depletion. We show depletion of B cells from PPs is not correlated with a decrease in M cells. Comparing the number of M cells per PP dome and the size of the PP dome, we also show the density of M cells on PP domes is constant in wild type, B cell depleted, or B cell deficient mice. We have previously shown RANKL is expressed on stromal cells in the subepithelial dome underlying the follicle associated epithelium of Peyer's patches and is necessary for the development of PP M cells, demonstrating that the RANKL-RANK pathway plays a pivotal nonredundant role in establishing the M cell-mediated pathway of antigen acquisition and handling. The M cell density on PPs in RANKL^{-/-} mice is one tenth the density found in wild type or B cell deficient mice. We find that RANKL, present on non-hematopoietic cells and not B cells is a specific trigger for the development of M cells.

Methods and Materials

Mice

Mice carrying a human CD20 (hCD20) transgene on a BALB/c background were obtained from Dr. Mark Schlomchik at Harvard University (Boston, MA). $J_H^{-/-}$ mice were purchased from Taconic Farms (Hudson, NY). BALB/c mice used in experiments were purchased from Jackson Labs (Bar Harbor, ME). Mice carrying a RANKL null mutation on a C57BL/6 background (31) obtained from Dr. Yongwon Choi at the University of Pennsylvania (Philadelphia, PA) were also backcrossed to BALB/c mice as previously described to produce RANKL null mice and littermate controls on a background roughly equivalent to (C57BL/6 X BALB/c) F1 mice (20). All mice used in the experiments were at least 8 weeks old. All animal studies were reviewed and approved by the Emory University Institutional Animal Care and Use Committee.

Bone Marrow Chimeras

For WT into RANKL^{-/-} bone marrow chimera mice, BM was eluted from the tibia and femur of donor mice. A single-cell suspension was prepared in complete media. RANKL^{-/-} recipient mice were given 600 rads of gamma-irradiation from a cesium source. C57BL/6 recipient mice were given a total of 1000 rad. Donor BM cells were resuspended in PBS and 2×10^7 cells were injected i.v. into recipient mice. For RANKL^{-/-} into CD45.1 chimera mice, fetal liver cells from were isolated from embryonic day 14 mice. A single-cell suspension was prepared in complete media. CD45.1 recipient mice

were given a total of 1000 rad. Mice were given drinking water supplemented with neomycin sulfate (2 mg/ml) for 2 wk after transfer.

Rituximab B cell Depletion of hCD20 Transgenic Mice

To acutely deplete B cells in adult mice, mice with a hCD20 transgene were injected IP with 2mg of Rituxan® (Rituximab, Biogen Idec, Weston MA, and Genentech, San Francisco CA), an anti-CD20 depleting antibody, every 4 days for 16 days. Depletion was measured in both the spleens and Peyer's patch through flow cytometry, comparing the total number of CD19⁺ B220⁺ B cells in a rituximab-treated hCD20 transgenic mouse to a rituximab-treated control mouse.

Antibodies and Lectins

Monoclonal antibodies were purchased from eBioscience (San Diego, CA) unless otherwise stated. The mAbs used for immunofluorescence detection of mouse cells on frozen sections included PE- and FITC-anti-Thy 1.2 (53-2.1), PE-CD19 (1D3), allophycocyanin- and PE-anti-B220 (RA3-6B2), biotinylated GL7, unconjugated RANKL (IK22-5), and unconjugated anti-GP2 antibody (2F11-C3, MBL, Woburn, MA). Rhodamine-UEA-I was purchased from Vector Laboratories. The anti-RANKL Ab (IK22-5) used for in vivo RANKL neutralization experiment; mice were treated 250 µg of IK22-5 i.p. every 2 days.

Immunofluorescence staining of frozen sections

Frozen sections of PPs were cut on a cryostat and prepared for staining experiments as previously described. (21) The sections were air dried overnight, and fixed for 10 min in acetone at -20°C. Abs diluted in TNB buffer (PerkinElmer Life Sciences, Waltham MA) were applied for one hour at room temperature. Biotinylated antibodies were detected using streptavidin-conjugated Alexa 488 (Invitrogen, Carlsbad, CA). Unconjugated antibodies were detected with a secondary anti-rat Alexa 546-conjugated antibody (Invitrogen). 4',6-diamidino-2-phenylindole, DAPI, (Sigma-Aldrich, St. Louis, MO) at 10 ng/ml was used as a nuclear counterstain. The slides were mounted in ProLong anti-fade reagent (Invitrogen). Images were acquired using a Nikon 80i fluorescence microscope.

Whole mount staining of PPs for detection of UEA-I⁺ M cells

For detection of M cells, PPs were stained for whole mount imaging as previously described. (20) Individual PPs were excised and vortex mixed in 0.5% Tween 20-PBS followed by staining with rhodamine-UEA-I in TNB buffer for 40 minutes at 4°C. PPs were then wet mounted under a 20 mm x 20 mm cover slip in 200 µl PBS. A count of UEA-I⁺ M cells was done for every dome on the individual PPs to calculate the average number of M cells per dome. Because the outlines of individual UEA-I⁺ M cells were best delineated in images acquired using a 60x objective, some figures include composite images representing single follicles were assembled by stitching of up to 4 overlapping individual 60x images using Photo Stitch 3.0 (Canon).

In vivo assessment of M cell uptake of fluorescent beads

The uptake of 200 nm diameter fluorescent polystyrene latex nanoparticles (Fluoresbrite YG: Polysciences) by M cells in FAE of individual PP was assessed by oral gavage. Mice were fed 200 μ l aliquots of 1×10^{11} 200 nm beads, 16 hours later PPs were excised and embedded in OCT. Frozen sections were cut, briefly stained with DAPI (Sigma-Aldrich) without fixation, and examined by microscopy.

Quantitative analysis of fluorescent bead uptake by PP M cells

Analysis of the degree of bead uptake into PPs was done by threshold analysis using ImageJ v1.37 software (<http://rsb.info.nih.gov/ij>) as previously described (20). The percentage of the pixels with a signal intensity that exceeded this cutoff was calculated for the area occupied by each PP follicle.

ELISA for measurement of fecal IgA

To quantitate total fecal IgA, fecal pellet samples were collected and extracted by making a 1/10 suspension (w/v) with PBS. After the suspension was vortexed and spun for 10 min at 12,000 x g, the supernatant was stored at -70C. Polyclonal goat anti-mouse IgA Ab (Southern Biotechnology) was used as a capture Ab. The bound mouse IgA was detected with peroxidase-labeled goat anti-mouse IgA Ab (Southern Biotechnology) using TMB (BD Biosciences) as the peroxidase substrate. A mouse IgA, k isotype control mAb (BD Biosciences) was used to establish a standard curve.

Statistical analysis

Differences between the mean values for groups were analyzed by either two-tailed Student's t test, two-tailed Mann-Whitney test, or two-tailed ANOVA (for multiple groups) using Prism (GraphPad Software). A P value of less than 0.01 was considered significant.

Results

Acute antibody-mediated deletion of B cells does not interfere with M cell differentiation

We used mice that express an hCD20 transgene as an experimental model for examining the effect of acute depletion of B cells on M cell differentiation in PPs. The presence of hCD20 on all mature B cells in these mice allows depletion of B cells following in vivo treatment with rituximab, an anti-hCD20 monoclonal antibody (22). To validate the use of this transgenic model for our studies of M cells in small intestinal PPs, we first compared the structure and function of PPs in hCD20 transgenic mice and littermate controls. As expected, no significant differences were observed in the number of PPs, the architectural arrangement of B and T cell areas in PPs, the number of UEA-I⁺ M cells per PP follicle, or the concentration of fecal IgA (Fig. S1).

To induce and maintain systemic depletion of B cells, hCD20 transgenic mice and littermate controls lacking the transgene were treated with 2 mg of rituximab every 4 days for a total of 16 days. The lifespan of small intestinal epithelial cells besides Paneth cells (including M cells) is approximately 3 to 4 days(23). Maintaining the B cell-depleted state for 16 days assured that all M cells identified at the end of this period had arisen and differentiated under B cell-depleted conditions. Rituximab treatment led to a >97% decrease in B220⁺ CD19⁺ B cells in PPs as assessed by flow cytometry (Fig. 1A), indicating that the efficiency of depletion of B cells from PPs was similar to that observed in the spleen. While a few residual B cells remained in the PPs, these B cells were no longer organized into follicles (Fig. 1B) and the areas normally containing B cells were mostly filled in with Thy-1⁺ T cells (data not shown). We checked for the

presence of M cells in the PPs from B cell-depleted mice by staining sections for the M cell-specific marker GP2 and visualizing UEA-I+ cells on whole mounts of PP domes. Despite the loss of the vast majority B cells from PPs after rituximab treatment, there were still GP2⁺ M cells on the dome of the PPs (Fig. 1B) and radially-arranged columns of M cells extending from the crypts towards the apex of the PP dome (Fig. 1C). The mean number of M cells per PP dome was slightly reduced (Fig. 1D), but the difference was not statistically significant. To determine if the GP2⁺ and UEA-I⁺ M cells detected in the B cell-depleted mice retained their ability to transcytose particulate antigens, mice were gavaged with 200 nm diameter fluorescent beads. Sections of PPs showed a similar degree of uptake of beads in the B cell-depleted and control mice (Fig. 1E), which was confirmed by quantitative image analysis (Fig. 1F). Thus, depletion of B cells from PPs does not interfere with either the differentiation or function of M cells in the PP FAE.

RANKL deficient mice have a much greater reduction in total Peyer's patch M cells than B cell-deficient mice

Two independent gene-targeted models of B cell-deficient mice (μ MT and $J_H^{-/-}$) were found to have a substantial decrease in the number of PP M cells (11). The extent of loss of PP M cells in the $J_H^{-/-}$ mice was estimated to be between 150- and 800-fold. Because our studies of mice acutely depleted of B cells using rituximab revealed only a minimal decrease in the number of M cells per PP follicle, we did a quantitative comparison of the degree of loss of M cells in rituximab-treated hCD20 transgenic mice, μ MT mice and $J_H^{-/-}$ mice in comparison with the relevant control mice. $RANKL^{-/-}$ mice that lack most M cells and their littermate $RANKL^{+/+}$ controls were also included in this

analysis. For each strain the total number of PP M cells was calculated as the product of the average number of PPs, the average number of domes per PP, and the average number of M cells per PP dome. This analysis revealed that both models of B cell deficient mice had fewer grossly detectable PP, fewer follicles per PP, and only about one third the number of UEA-I⁺ M cells per PP dome (Fig. 2A). The residual PP M cells in B cell deficient mice retained expression of GP2 (Fig. 2B). Overall, we found a 14-fold decrease in the total number of PP M cells in J_H^{-/-} mice and a 4-fold decrease of PP M cells in μMT mice, when compared to control mice of the appropriate strain (Table 1). In contrast, PP from RANKL^{-/-} mice retained B cell follicles (Fig. 2C), but had a much larger 83-fold decrease in the estimated total number of PP M cells.

Density of M cells remains relatively constant in wild type, B cell-depleted and B cell-deficient mice

A consistent correlation was observed between the number of M cells in each PP dome and the size of the PP domes when B cell-depleted and B cell-deficient mice were compared with the respective wild type controls (Fig. 3A-C). For example, wild type BALB/c mice had an average of 171 M cells per dome distributed over an average PP dome surface area of 0.46 mm² for a density of 332 cells/mm². J_H^{-/-} and μMT mice had significantly smaller domes (0.11 and 0.24 mm², respectively) and significantly fewer M cells per dome (30 and 51), but the density of PP M cells (323 and 343 cells/mm²) remained remarkably similar to that calculated in the wild type controls. In stark contrast, RANKL^{-/-} mice had a slightly reduced dome surface area coupled with a huge decrease in the number of PP M cells, resulting in the density of residual M cells dropping to 33/mm²

or just one-tenth the density of wild type mice. Results parallel to the density obtained by UEA-I staining were obtained when uptake into PP of 200 nm diameter fluorescent nanoparticles administered by oral gavage was used as a functional assay for transcytosis by PP M cells. The observed amount of uptake of the nanoparticles was not diminished in mice with acute depletion or absence of B cells, but was severely compromised in RANKL^{-/-} mice (Fig. 3D). Preservation of essentially the same density of M cells on the FAE surface and the normal functional capacity of these M cells despite the acute depletion of most B cells or the total developmental absence of B cells is a strong indication that B cells are not supplying additional signals required for the differentiation of M cells within the PP FAE.

M cell differentiation is not restored in chimeric mice with RANKL expression restricted to hematopoietic cells

Immunohistochemical analysis of RANKL expression in PP showed that the principal cells that express RANKL are stromal cells concentrated in the subepithelial dome area. However, RANKL expression has also been reported on activated T cells and specific subsets of B cells. Thus, T and/or B cells in the PP environment are another potential local source of RANKL that could contribute to M cell differentiation. To establish whether RANKL sufficient hematopoietic cells could direct the normal differentiation of PP M cells when the stromal cells were unable to produce RANKL, two reciprocal chimeric mouse models were established in which RANKL was absent on either the hematopoietic or non-hematopoietic cells. To examine whether RANKL supplied by hematopoietic cells would restore the deficiency in M cells in RANKL^{-/-}

mice, RANKL^{-/-} or C57BL/6 CD45.2 hosts were lethally irradiated and reconstituted with bone marrow from C57BL/6 CD45.1 donors. Because bone marrow could not be harvested from the osteopetrotic long bones of RANKL^{-/-} mice, the reciprocal chimeras were established using E16 RANKL^{-/-} fetal liver cells were used as a source of hematopoietic cells and transferred into irradiated C57BL/6 CD45.1 mice. After eight weeks, both types of chimeric mice and controls were analyzed for the extent of PP M cell development by whole mount UEA-I staining (Fig. 4A). RANKL^{-/-} mice reconstituted with CD45.1 bone marrow had an average of 15 UEA-I⁺ M cells per PP, or just one-tenth the number of M cells on the PP dome of control mice (Fig. 4B). This low number of UEA-I⁺ cells per PP dome is similar to the number of UEA-I⁺ M cells previously reported in RANKL^{-/-} mice (20). In contrast C57BL/6 CD45.1 mice reconstituted with RANKL^{-/-} fetal liver cells had an average of 131 M cells per PP dome, indicating that RANKL provided by only non-hematopoietic stromal cells was sufficient to support PP M cell development.

M cell development in J_H^{-/-} mice can be blocked with neutralizing RANKL antibody

The normal pattern of RANKL expression in the subepithelial dome of PPs is maintained in B cell deficient mice (Fig. 2D). We previously showed that development of PP M cells in wild type mice was blocked by administration of neutralizing RANKL antibody (20). To determine if PP M cell development in J_H^{-/-} mice is also fully dependent on the availability of RANKL, we attempted to block M cell development in J_H^{-/-} mice by administration of 250 µg neutralizing RANKL antibody every other day for 8 days. On day 8, the number of PP M cells was vastly decreased compared to control J_H^{-/-} mice (Fig.

5A). This loss in PP M cells in $J_H^{-/-}$ mice after RANKL depletion correlated with an equivalent decrease in the efficiency with which fluorescent beads were taken up into PPs (Fig. 5B).

Discussion

Concurrent with the initial discovery of the unusual ultrastructural appearance of specialized antigen-sampling M cells in the intestinal epithelium of mammals was the realization that M cell differentiation is generally restricted to a subset of the enterocytes covering intestinal lymphoid structures including PPs and ILFs (24, 25). These early observations about M cells paved the way for development of the basic hypothesis that cells and/or soluble factors concentrated in these organized lymphoid structures (and not present throughout the entire intestinal epithelium) provide the essential signals needed for the differentiation of M cells from precursor cells in the follicle-associated epithelium (26, 27). A series of experimental observations made using *in vivo* and *in vitro* systems gave some preliminary support to the idea that the B lymphocytes present in the follicles of organized lymphoid tissues have a critical role in M cell differentiation (12). A key *in vitro* finding was the description of a cell culture model using the human Caco-2 intestinal epithelial cell line in which M cell-like cells could be induced *in vitro* by co-culture of polarized Caco-2 cells on a permeable support with B lymphocytes or a B lymphoblastoid cell line such as Raji cells. Since its introduction, this Caco-2 cell culture system and various modifications of it have been widely used as an experimental approach to study the biology of M cells. A complementary *in vivo* finding was the observation that strains of knockout mice that lack all B cells also have a decreased number of PP M cells (11). However, when viewed as a whole, these *in vitro* and *in vivo* studies have not yet led to the identification of specific factors produced by B cells that act to foster M cell differentiation either *in vitro* or *in vivo*. Furthermore, the results seen

in the Caco-2 system have yet to be replicated in other intestinal cell culture systems, as murine intestinal epithelial cells cultured with B cells alone did not convert into transcytosing cells (28). Recently new candidate molecules that are capable of regulating M cell differentiation and maturation have emerged from analysis of other knockout mouse models. Our laboratory identified RANKL as a TNF superfamily cytokine produced by stromal cells concentrated beneath the FAE of PP and ILF that is necessary for PP M cell differentiation and capable of inducing widespread villous M cell differentiation on the RANK-expressing villous epithelium of the small intestine after systemic RANKL treatment (20). CD137 (4-1BB) is a TNF receptor superfamily member that has been implicated in regulating the degree of M cell maturation in both mouse PPs and in the murine nasal epithelium (29). The identification of these specific candidate molecules involved in the regulation of M cell differentiation has led to a need to reassess some of the earlier observations concerning the relationship between B cells and M cell differentiation to determine if some or all of the M cell-promoting effects previously attributed to B cells are explained by cytokines including RANKL and 4-1BBL.

One of the limitations of studying PP M cell differentiation in any of the knockout mouse models with a lifelong global deficiency in B cells is that the entire developmental sequence for PPs is substantially altered beginning in early embryonic life by the absence of any B lymphocytes. This altered early development and the significantly reduced adult size of PP could conceivably impair M cell differentiation independent of a true requirement for the presence of B cells to drive M cell differentiation (16, 17). In this study we sought to reexamine the role of B lymphocytes in M cell differentiation using a newer transgenic mouse model of acute B cell deficiency in mice in which the vast

majority of resident B cells are removed by initiating treatment with a depleting monoclonal antibody (rituximab) specific for a human B cell antigen (CD20) encoded by a transgene only expressed by B lymphocytes. This model allowed us to acutely deplete almost all B cells from adult mice and then observe the consequences for M cell differentiation after the state of B cell depletion was maintained for multiple weeks by additional rituximab injections. Since the lifespan of M cells and most other subsets of differentiated enterocytes is in the range of only 3 to 4 days (23), any M cells still present in the FAE of PP after two or more weeks of acute B cell depletion must be able to differentiate in the presence of few if any PP B cells.

The major conclusion emerging from our quantitative analysis of the status of PP M cells in both the acute B cell depletion model and the B cell knockout mouse strains is that while either acute loss or total absence of B cells reduced the size of PPs, the area of the FAE domes, and the number of M cells per dome, the density of UEA-I⁺ M cells (calculated as cells per unit area) within the FAE remained relatively constant even when B cells were mostly or totally absent. In contrast, either absence of RANKL or antibody-mediated neutralization of RANKL resulted in a precipitous drop in the density of UEA-I⁺ M cells. While there are subsets of both B cells and T cells that can make RANKL, our analysis of chimeric mice revealed that hematopoietic cell expression of RANKL alone is not enough to support a normal level of M cell development. However, expression of RANKL restricted to nonhematopoietic stromal cells was sufficient to allow a full degree of M cell development. This result in chimeric mice coupled with the demonstration by immunohistochemical staining that most expression of RANKL within PP is confined to stromal cells preferentially located in the subepithelial dome area emphasize the crucial

role of the PP stroma in providing a critical cytokine signal for M cell differentiation in the PP FAE.

Our findings on the B cell-independence of M cell differentiation and the central role of RANKL suggest that new types of in vitro and in vivo experimental models are needed to unlock some of the remaining mysteries of M cell differentiation. In vitro culture conditions using a combination of specific growth factors have been defined that permit primary intestinal stem cells expressing the Lgr5 receptor to proliferate in vitro in three dimensional “organoid” cultures to yield both daughter intestinal stem cells and a mix of the major differentiated enterocyte subsets (absorptive enterocytes, goblet cells, enteroendocrine cells, and Paneth cells) (30, 31). The establishment of this culture system was a major experimental advance that will allow increased use of in vitro systems to unravel the transcription factors and signaling pathways that regulate the differentiation of specific lineages of enterocytes including goblet cells, enteroendocrine cells, and Paneth cells, instead of cell culture systems that rely on transdifferentiation of immortalized cell lines into the differentiated cell of choice . Supplementation of these organoid cultures with additional defined growth factors and cytokines putatively involved in M cell differentiation may yield cultures in which some of cells can adopt an M cell fate rather than ending up in one of the other types of differentiated enterocyte lineages. Furthermore, an improved understanding of the full breadth of the PP M cell transcriptome by microarray studies has yielded a series of new M cell-specific markers such as GP2 (32) that can now be used to more rigorously assess whether any cells that closely mimic natural PP M cells can be generated via modifications of the basic “organoid” culture system. Analysis of the expression levels of these same M cell-

specific genes can also be as a validation tool to evaluate the various culture systems that are based on use of established intestinal epithelial cell lines such as Caco-2.

One still unsettled issue about M cell differentiation concerns the nature of the immediate precursor cells that can differentiate into M cells. Some laboratories have proposed the existence of a transdifferentiation pathway that is capable of converting normal mature absorptive enterocytes in the FAE into M cells (33, 34). Other models for M cell development have posited that the commitment of a subset of enterocytes to become M cells is instead largely restricted to the proliferative zone within the crypt where both intestinal stem cells and transit amplifying cells reside (35, 36). This latter model is better aligned with current concepts on how the other specialized enterocyte subsets differentiate from uncommitted precursors(23). In fact, a series of transcription factors have been described that play key roles in regulating the conversion of undifferentiated enterocytes into one of the differentiated subsets of enterocytes (37, 38). An in vitro system in which the degree of differentiation of uncommitted proliferating enterocytes precursors into cells expressing signature M cell genes could be controlled by simply modifying the cocktail of growth factors used would have great potential to identify what types and sequence of cell fate decisions are involved in the generation of M cells.

The appreciation of the pivotal role of the RANKL-RANK signaling pathway for M cell development also has the potential to yield new in vivo mouse models featuring selective intestinal M cell deficiency. While RANKL deficient mice show a profound loss of intestinal M cells (20), their phenotype includes multiple other complex deficits that result from the pleiotropic roles of RANKL in multiple processes including

osteoclastogenesis, lymph node development, lactation by mammary epithelium, medullary thymic epithelial cell development, and hair follicle growth (39). Preparation of genetically engineered mice in which blockade of the RANKL-RANK signaling pathway is restricted to the intestinal epithelium through the use of conditional and inducible knockout approaches has the potential to yield mice that lack functional intestinal M cells without all or most of the other phenotypic manifestations seen in the global RANKL knockout mice.

References

1. Garside P, Millington O, Smith KM. The Anatomy of Mucosal Immune Responses. *Annals of the New York Academy of Sciences*. 2004;1029(1):9-15.
2. Kucharzik T, LÜGering N, Rautenberg K, LÜGering A, Schmidt MA, Stoll R, et al. Role of M Cells in Intestinal Barrier Function. *Annals of the New York Academy of Sciences*. 2000;915(1):171-83.
3. Owen RL. Uptake and transport of intestinal macromolecules and microorganisms by M cells in Peyer's patches-- a personal and historical perspective. *Semin Immunol*. 1999;11(3):157-63.
4. Gebert A, Rothkotter HJ, Pabst R. M cells in Peyer's patches of the intestine. *Int Rev Cytol*. 1996;167:91-159.
5. Neutra MR, Frey A, Kraehenbuhl JP. Epithelial M cells: gateways for mucosal infection and immunization. *Cell*. 1996;86(3):345-8.
6. Neutra MR, Mantis NJ, Frey A, Giannasca PJ. The composition and function of M cell apical membranes: Implications for microbial pathogenesis. *Semin Immunol*. 1999;11(3):171-81.
7. Hamada H, Hiroi T, Nishiyama Y, Takahashi H, Masunaga Y, Hachimura S, et al. Identification of multiple isolated lymphoid follicles on the antimesenteric wall of the mouse small intestine. *J Immunol*. 2002;168(1):57-64.
8. Hall P, Coates P, Ansari B, Hopwood D. Regulation of cell number in the mammalian gastrointestinal tract: the importance of apoptosis. *Journal of cell science*. 1994;107(12):3569-77.
9. Roberts DJ. Molecular mechanisms of development of the gastrointestinal tract. *Developmental Dynamics*. 2000;219(2):109-20.
10. van den Brink GR, de Santa Barbara P, Roberts DJ. Epithelial Cell Differentiation— a Matter of Choice. *Science*. 2001;294(5549):2115.

11. Golovkina TV, Shlomchik M, Hannum L, Chervonsky A. Organogenic role of B lymphocytes in mucosal immunity. *Science*. 1999;286(5446):1965-8.
12. Kerneis S, Bogdanova A, Kraehenbuhl JP, Pringault E. Conversion by Peyer's patch lymphocytes of human enterocytes into M cells that transport bacteria. *Science*. 1997;277(5328):949-52.
13. Kerneis S, Caliot E, Stubbe H, Bogdanova A, Kraehenbuhl J, Pringault E. Molecular studies of the intestinal mucosal barrier physiopathology using cocultures of epithelial and immune cells: a technical update. *Microbes Infect*. 2000;2(9):1119-24.
14. El Bahi S, Caliot E, Bens M, Bogdanova A, Kerneis S, Kahn A, et al. Lymphoepithelial interactions trigger specific regulation of gene expression in the M cell-containing follicle-associated epithelium of Peyer's patches. *J Immunol*. 2002;168(8):3713-20.
15. Luther SA, Tang HL, Hyman PL, Farr AG, Cyster JG. Coexpression of the chemokines ELC and SLC by T zone stromal cells and deletion of the ELC gene in the *plt/plt* mouse. *Proc Natl Acad Sci U S A*. 2000;97(23):12694-9.
16. Debard N, Sierro F, Browning J, Kraehenbuhl J-P. Effect of mature lymphocytes and lymphotoxin on the development of the follicle-associated epithelium and M cells in mouse Peyer's patches. *Gastroenterology*. 2001;120(5):1173-82.
17. Tumanov AV, Kuprash DV, Mach JA, Nedospasov SA, Chervonsky AV. Lymphotoxin and TNF produced by B cells are dispensable for maintenance of the follicle-associated epithelium but are required for development of lymphoid follicles in the Peyer's patches. *J Immunol*. 2004;173(1):86-91.
18. Lugerling A, Floer M, Westphal S, Maaser C, Spahn TW, Schmidt MA, et al. Absence of CCR6 inhibits CD4⁺ regulatory T-cell development and M-cell formation inside Peyer's patches. *Am J Pathol*. 2005;166(6):1647-54.
19. Mach J, Hsieh T, Hsieh D, Grubbs N, Chervonsky A. Development of intestinal M cells. *Immunol Rev*. 2005;206:177-89.

20. Knoop KA, Kumar N, Butler BR, Sakthivel SK, Taylor RT, Nochi T, et al. RANKL is necessary and sufficient to initiate development of antigen-sampling M cells in the intestinal epithelium. *J Immunol.* 2009;183(9):5738-47.
21. Taylor RT, Patel SR, Lin E, Butler BR, Lake JG, Newberry RD, et al. Lymphotoxin-independent expression of TNF-related activation-induced cytokine by stromal cells in cryptopatches, isolated lymphoid follicles, and Peyer's patches. *J Immunol.* 2007;178(9):5659-67.
22. Ahuja A, Shupe J, Dunn R, Kashgarian M, Kehry MR, Shlomchik MJ. Depletion of B cells in murine lupus: efficacy and resistance. *J Immunol.* 2007;179(5):3351-61.
23. van der Flier LG, Clevers H. Stem Cells, Self-Renewal, and Differentiation in the Intestinal Epithelium. *Annual Review of Physiology.* 2009;71(1):241-60.
24. Bockman DE, Cooper MD. Pinocytosis by epithelium associated with lymphoid follicles in the bursa of Fabricius, appendix, and Peyer's patches. An electron microscopic study. *Am J Anat.* 1973;136(4):455-77.
25. Wolf JL, Bye WA. The membranous epithelial (M) cell and the mucosal immune system. *Annual review of medicine.* 1984;35:95-112.
26. Pringault E. Emerging concepts in M cell function and Peyer's patch development. *Semin Immunol.* 1999;11(3):155-6.
27. Kraehenbuhl JP, Neutra MR. Epithelial M cells: differentiation and function. *Annu Rev Cell Dev Biol.* 2000;16:301-32.
28. Kanaya T, Miyazawa K, Takakura I, Itani W, Watanabe K, Ohwada S, et al. Differentiation of a murine intestinal epithelial cell line (MIE) toward the M cell lineage. *Am J Physiol Gastrointest Liver Physiol.* 2008;295(2):G273-84.
29. Hsieh EH, Fernandez X, Wang J, Hamer M, Calvillo S, Croft M, et al. CD137 is required for M cell functional maturation but not lineage commitment. *Am J Pathol.* 2010;177(2):666-76.

30. Barker N, Huch M, Kujala P, van de Wetering M, Snippert HJ, van Es JH, et al. Lgr5(+ve) stem cells drive self-renewal in the stomach and build long-lived gastric units in vitro. *Cell Stem Cell*. 2010;6(1):25-36.
31. Sato T, van Es JH, Snippert HJ, Stange DE, Vries RG, van den Born M, et al. Paneth cells constitute the niche for Lgr5 stem cells in intestinal crypts. *Nature*. 2011;469(7330):415-8.
32. Terahara K, Yoshida M, Igarashi O, Nochi T, Pontes GS, Hase K, et al. Comprehensive gene expression profiling of Peyer's patch M cells, villous M-like cells, and intestinal epithelial cells. *J Immunol*. 2008;180(12):7840-6.
33. Kerneis S, Pringault E. Plasticity of the gastrointestinal epithelium: the M cell paradigm and opportunism of pathogenic microorganisms. *Semin Immunol*. 1999;11(3):205-15.
34. Sierro F, Pringault E, Assman PS, Kraehenbuhl JP, Debard N. Transient expression of M-cell phenotype by enterocyte-like cells of the follicle-associated epithelium of mouse Peyer's patches. *Gastroenterology*. 2000;119(3):734-43.
35. Gebert A, Fassbender S, Werner K, Weissferdt A. The development of M cells in Peyer's patches is restricted to specialized dome-associated crypts. *Am J Pathol*. 1999;154(5):1573-82.
36. Lelouard H, Sahuquet A, Reggio H, Montcourrier P. Rabbit M cells and dome enterocytes are distinct cell lineages. *Journal of cell science*. 2001;114(Pt 11):2077-83.
37. Yang Q, Bermingham NA, Finegold MJ, Zoghbi HY. Requirement of Math1 for secretory cell lineage commitment in the mouse intestine. *Science*. 2001;294(5549):2155-8.
38. Gregorieff A, Stange DE, Kujala P, Begthel H, van den Born M, Korving J, et al. The ets-domain transcription factor Spdef promotes maturation of goblet and paneth cells in the intestinal epithelium. *Gastroenterology*. 2009;137(4):1333-45 e1-3.
39. Kong YY, Yoshida H, Sarosi I, Tan HL, Timms E, Capparelli C, et al. OPGL is a key regulator of osteoclastogenesis, lymphocyte development and lymph-node organogenesis. *Nature*. 1999;397(6717):315-23.

Table 1. Extent of M cell depletion seen in three mutant mouse models

Mice	Number of PP Actual (Normalized) ^a	Domes per PP Actual (Normalized)	M Cells per Dome Actual (Normalized) ^b	Relative Number of M Cells ^c	Fold Decrease in M Cells ^d
RANKL ^{+/+}	8.6 (1.00)	5.4 (1.00)	117 (1.00)	1.000	1
RANKL ^{-/-}	5.3 (0.61)	2.2 (0.40)	6 (0.05)	0.012	83
C57BL/6	7.5 (1.00)	5.1 (1.00)	116 (1.00)	1.000	1
μMT	5.7 (0.76)	3.4 (0.66)	51 (0.50)	0.253	4
BALB/c	8.0 (1.00)	5.5 (1.00)	155 (1.00)	1.000	1
J _H ^{-/-}	5.0 (0.62)	3.1 (0.56)	30 (0.20)	0.070	14

^a The number of PP was counted in RANKL^{+/+} mice (n=4), RANKL^{-/-} mice (n=8), C57BL/6 mice (n=2), μMT mice (n=5), BALB/c mice (n=4), and J_H^{-/-} mice (n=4). The results are normalized to background control levels set at 1.00.

^b The number of UEA-I⁺ M cells were counted dome in the follicle with the most M cells in each PP examined. Scatter plots of these results are presented in Figure 5A.

^c The three normalized fractions (number of PP, domes, M cells) were multiplied to yield the fraction of M cells relative to wild type mice, an approach modeled on that described previously by Golovkina et al.³²

^d Ratio of total number of M cells in control mice to total number in the mutant strain.

Figures

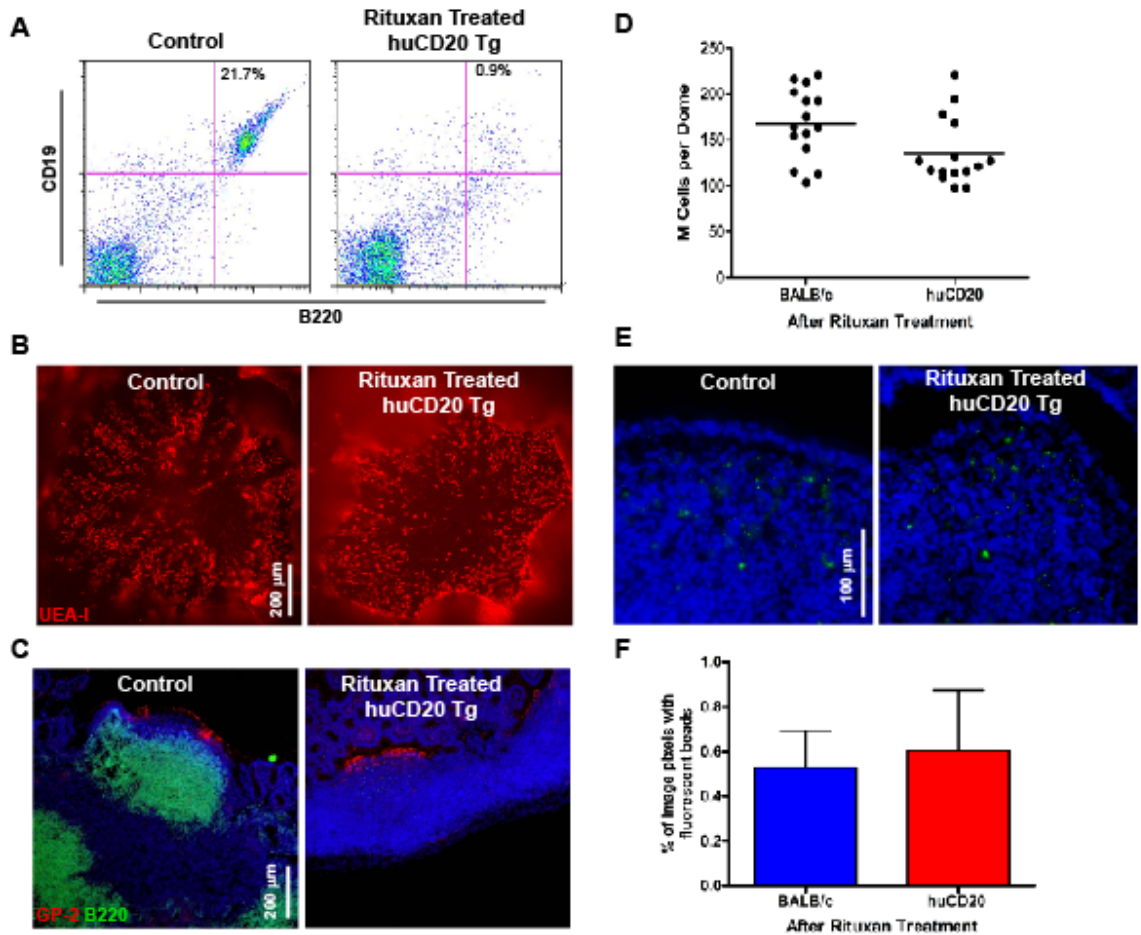


Figure 1. Mice maintain functional M cells after B cell depletion. (a) Cells from PPs were stained for CD19 and B220 to measure the number of B cells after Rituxan depletion via flow cytometry. (b) Sections of PPs were stained for GP2 and B220 (top row) to visualize M cells on the FAE and the B cell follicles after B cell depletion. DAPI was used as a counterstain, scale bar = 200 μ m. (c) Whole mount staining of PPs with Rhodamine-UEA-I and (d) scatter plot summarizing the number of UEA-I+ M cells per PP dome showed no significant difference after B cell depletion as calculated by a Mann-

Whitney test. Scale bar = 200 μm . (e) Sections of PPs from mice gavaged with 200-nm fluorescent beads were stained with DAPI to show the M cells after B cell depletion are able to take up particles, scale bar 100 μm . (f) Bar graph summarizing beads taken up into PP domes shows no significant difference after B cell depletion as calculated by a Mann-Whitney test. N = 3 mice per group.

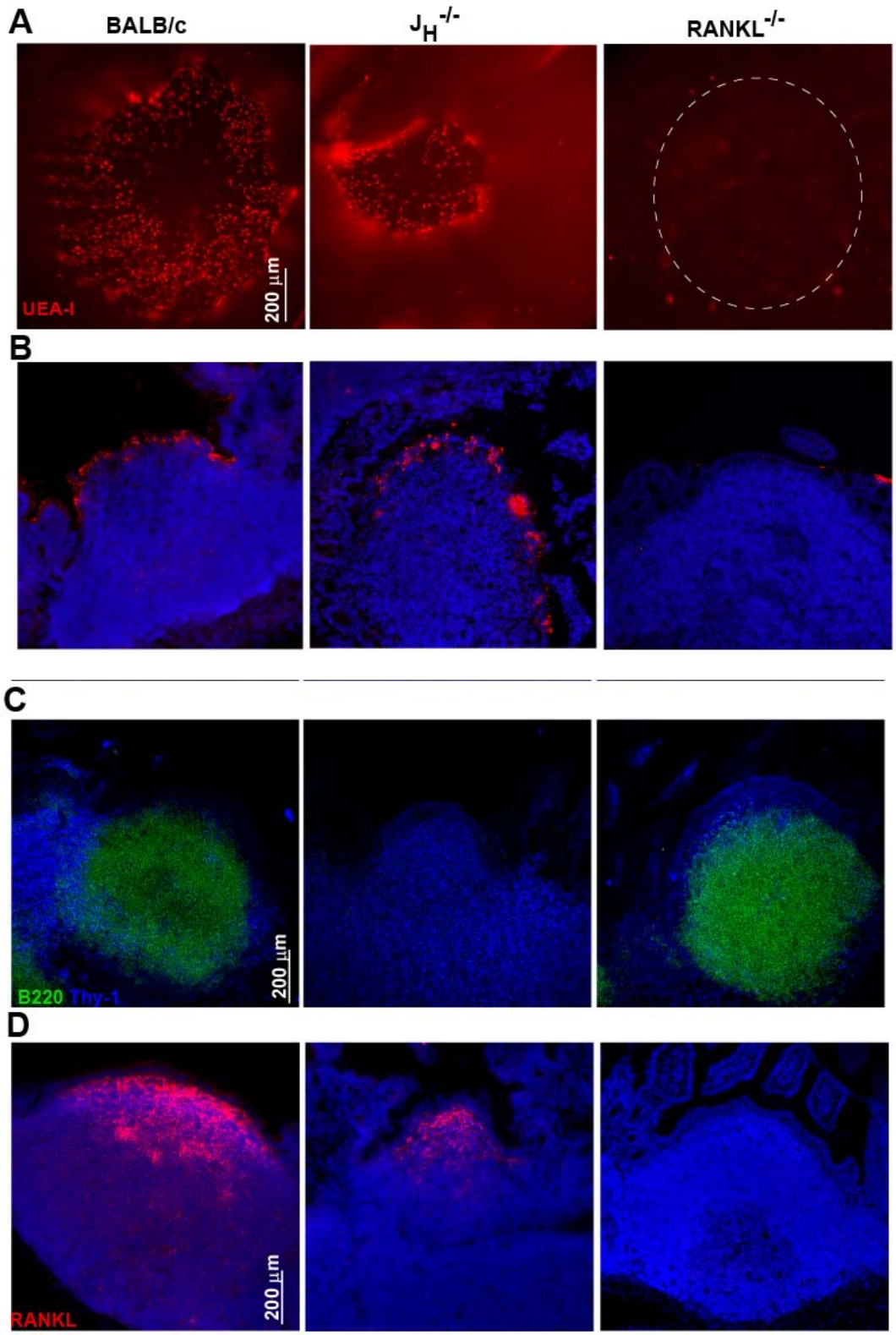


Figure 2. $J_H^{-/-}$ mice lack B cells, yet still have M cells, while $RANKL^{-/-}$ mice lack M cells in the presence of B cells. (a) Whole mount staining of PPs with rhodamine-UEA-I show

some UEA-I⁺ M cells on the surface of B cell deficient PPs but no M cells on the surface of RANKL^{-/-} PPs, scale bar = 200 μm. (b) Sections of PPs were stained for GP2 to visualize M cells on the FAE. (c) Sections of PPs were stained for Thy-1 and B220 to visualize the B cell follicles, scale bar = 200 μm. (d) Sections of PPs were stained for RANKL expression, scale bar = 200 μm.

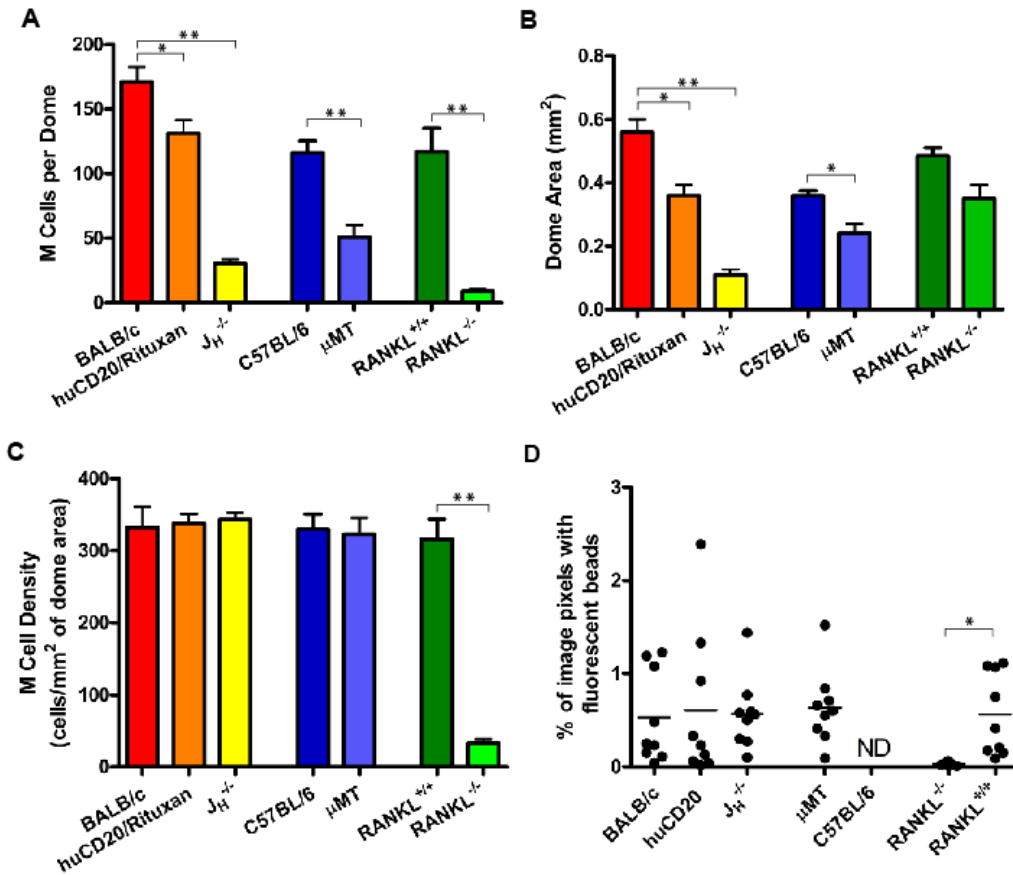


Figure 3. M cell density is similar in wild type, B cell depleted, and $J_H^{-/-}$ mice. (a) Bar graph summarizing average number of M cells per PP dome in BALB/c, acute-B cell depleted mice, $J_H^{-/-}$ mice, and RANKL^{-/-} mice. (b) Bar graph summarizing average area of the PP dome in BALB/c, acute-B cell depleted mice, $J_H^{-/-}$ mice, and RANKL^{-/-} mice. (c) Bar graph summarizing M cell density in BALB/c, acute-B cell depleted mice, $J_H^{-/-}$ mice, and RANKL^{-/-} mice. M cell density was calculated by dividing number of M cells per dome by area of dome for an M cell density in mm². (d) Scatter plot summarizing beads found within PPs as a measure of functional M cells. ND indicates data not gathered. Asterisk indicates significant difference of $p < 0.05$, two asterisks indicate significant difference of $p < 0.001$ when compared to control groups indicated by connecting lines calculated by independent student T tests.

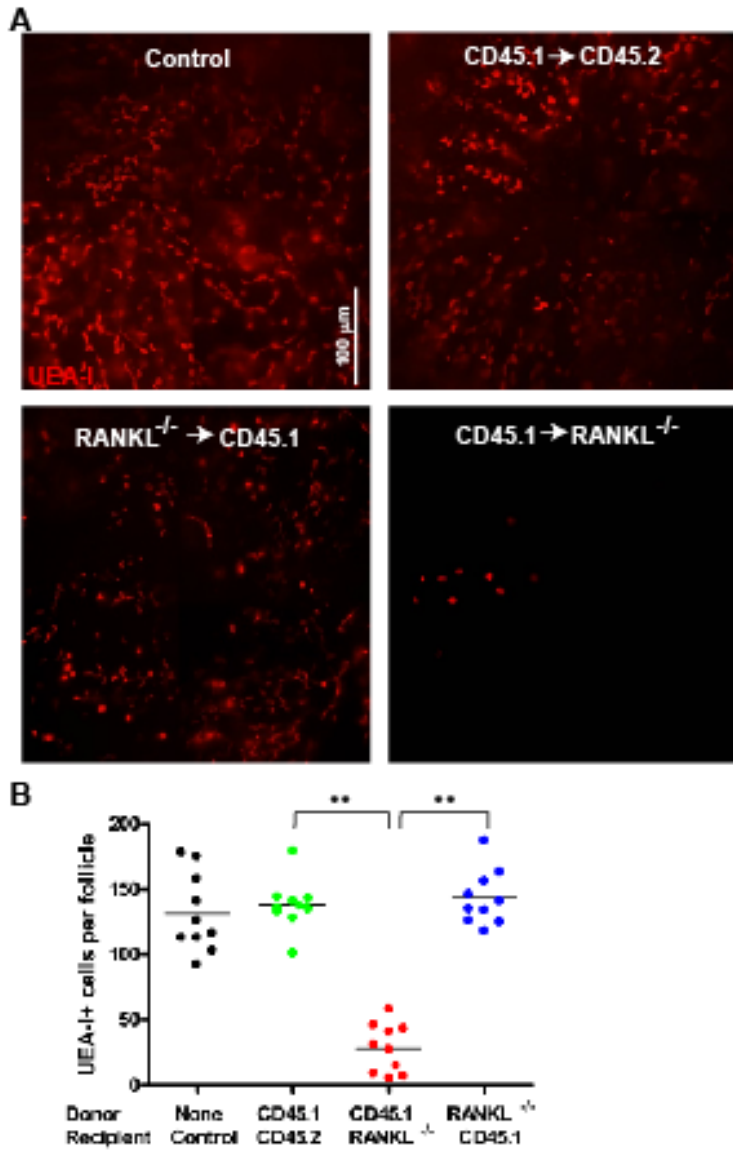


Figure 4. RANKL necessary for M cell differentiation is supplied by a non-hematopoietic source. (a) Whole mount composite images of PPs from chimeras ($RANKL^{-/-} \rightarrow CD45.1$, $CD45.1 \rightarrow RANKL^{-/-}$, or $CD45.1 \rightarrow CD45.1$) stained with rhodamine-UEA-I, representing single follicles were assembled by stitching of up to 4 overlapping individual images scale bar = 100 μ m. (b) Bar graph summarizing average number of M cells per follicle in chimera models, two asterisks denotes significant difference of $p < 0.0001$ calculated by ANOVA with Tukey correction. N = 2 mice per group.

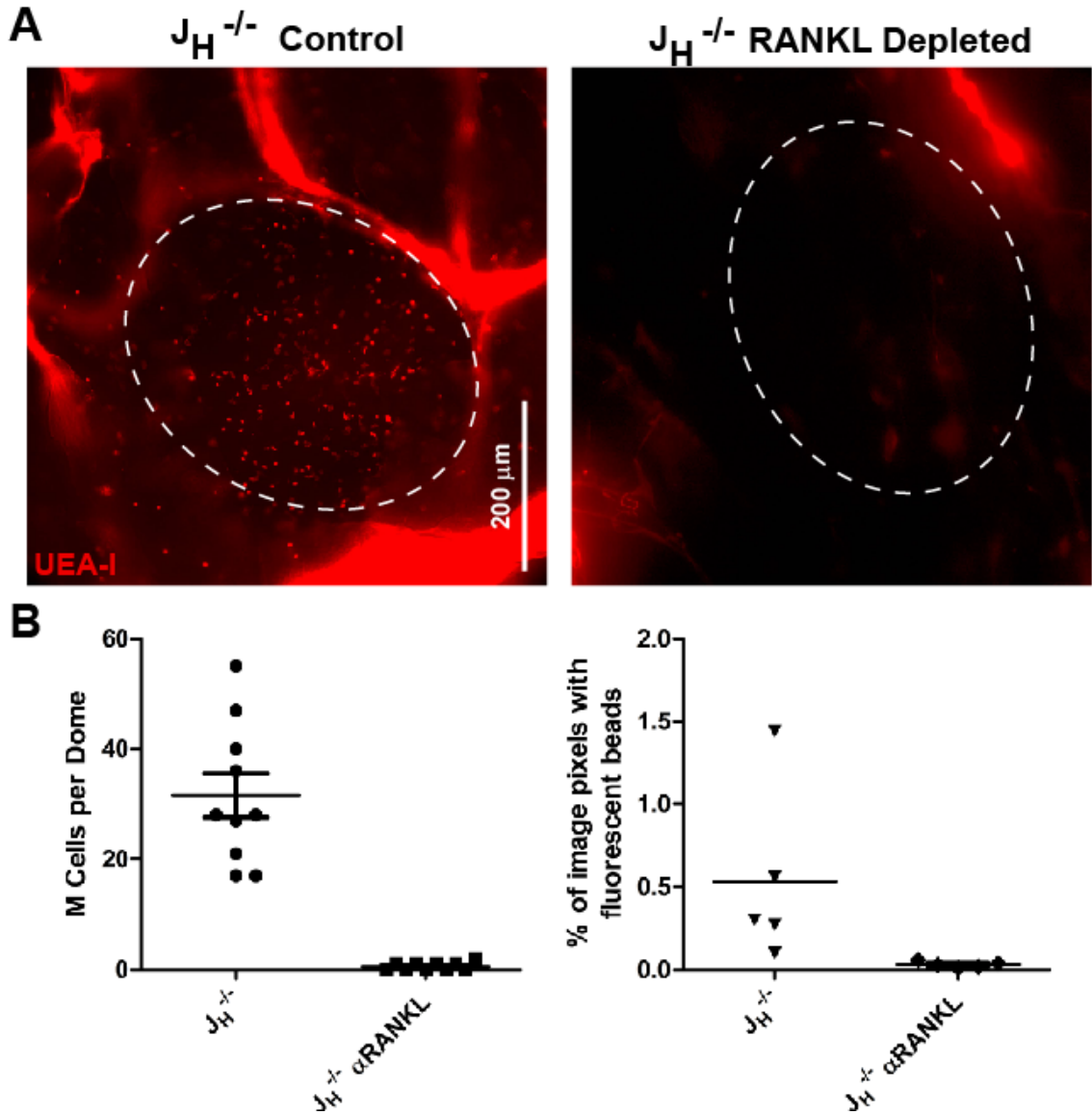
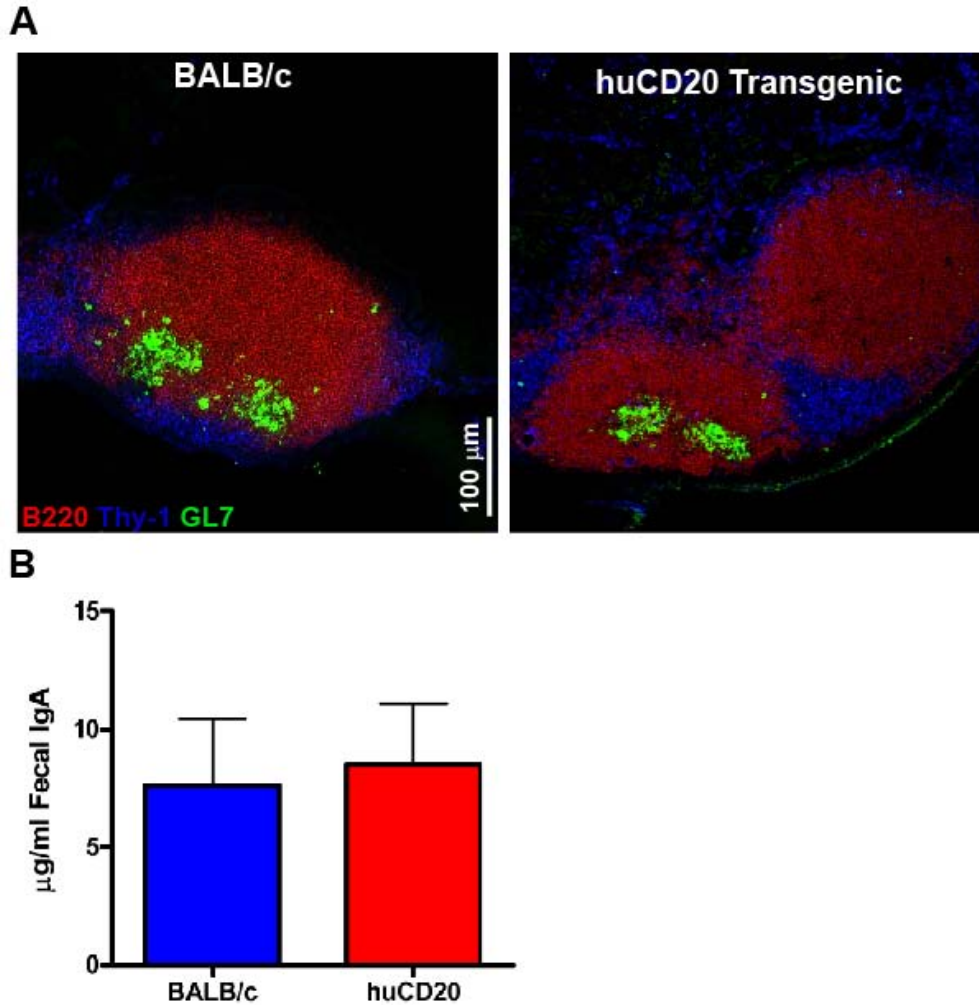


Figure 5. M cell development in $J_H^{-/-}$ mice can be blocked with neutralizing RANKL antibody. (a) Whole mount staining of PPs with rhodamine-UEA-I show some UEA-I⁺ M cells on the surface of B cell deficient PPs but no M cells after anti-RANKL treatment, scale bar = 200 μ m. (b) Representative images of PPs from mice gavaged with beads illustrates functional M cells in $J_H^{-/-}$ mice, but not in $J_H^{-/-}$ mice treated with neutralizing RANKL antibody, scale bar = 100 μ m. Images are representative of 4 mice per group.



Supplementary Figure 1. The human CD20 Transgene does not affect gut humoral responses. (a) PP sections were stained with B220, Thy-1, and GL7 to visualize B cell zones, T cell zones and germinal centers. (b) Bar graph summarizing the average concentration of IgA in fecal matter, no significant difference was seen as calculated by a Mann-Whitney test. N = 5 mice per group.

Chapter 3

Escape of the enteric microflora from the normal homeostatic control of secretory IgA results in expanded development of small intestinal villous M cells

Kathryn A. Knoop, Daniel C. Rios, Betsy R. Butler, Nachiket Kumar, and Ifor R. Williams

This manuscript is in progress

The experiments in this study were performed by Kathryn A. Knoop with assistance from Danny Rios, Nachiket Kumar, and Betsy Butler.

This manuscript was written by Kathryn A. Knoop and edited by Ifor Williams.

Abstract

The differentiation of intestinal epithelial cells into M cells specialized for antigen-sampling is a RANKL-dependent process that predominantly occurs in the follicle-associated epithelium overlying lymphoid aggregates such as intestinal Peyer's patches. A lesser number of M cells can be found on the villous epithelium of wild type mice, with an average density of just 0.07 villous M (vM) cells/villus in wild type mice as detected by whole mount UEA-I staining. In wild type mice the density of vM cells is relatively constant along the length of the small intestine. In sharp contrast, mice lacking all B cells ($J_H^{-/-}$ and μ MT strains) or IgA ($IgA^{-/-}$ and $AID^{-/-}$ strains) exhibit a substantial increase in the density of vM cells in the last 3 cm of the ileum to 10-17 vM cells/villus. This expansion of vM cells in the distal ileum can be completely blocked by oral ampicillin treatment for 3 days, indicating that the escape of the commensal enteric flora from the normal homeostatic control of secretory IgA is one contributing factor. Treatment of $J_H^{-/-}$ mice with neutralizing anti-RANKL for 4 days also blocked the differentiation of vM cells in the distal ileum, indicating that RANKL also contributes to the differentiation and/or survival of these vM cells. The increase of vM cells in the distal ileum of mice when secretory IgA is absent supports a model in which the commensal microflora and RANKL coordinately regulate the extent of vM cell differentiation in the small intestine.

Introduction

The small intestine is an active area of interaction between the gut immune system and the diverse population of commensal bacteria in the lumen. The density of the microflora increases from approximately 10^4 bacteria/ml of luminal contents in the duodenum to approximately 10^8 bacteria/ml in the distal ileum (1). Though not as dense as the microflora in the colon, this enteric microflora has a profound impact on the development of the mucosal immune system (2). The composition of the enteric flora differs greatly between separate specific pathogen free mouse facilities (3), and individual mouse models (4). Though most commensal species aid mammals in digestion and nutrient absorption (1), alterations in the composition of the enteric flora can contribute to the emergence of clinical disease (5). A single-cell layer of epithelium is the main physical barrier between the enteric flora in the lumen and the rest of the body, acting as an “interactive barrier” (6), which can itself respond to the bacteria. The small intestinal epithelium undergoes complete self-renewal approximately every three days. The source of the new epithelial cells are proliferating stem cells in the crypts surrounding villi and PPs. Each stem cell has the capacity to differentiate into one of several different specialized cell types depending on the set of signals and factors to which the stem cells are exposed. The villous epithelium is comprised of absorptive enterocytes, enteroendocrine cells, Paneth cells, or goblet cells, while the follicle-associated epithelium that overlies PPs is principally made up of absorptive enterocytes and M cells.

Microfold cells (M cells) are specialized epithelial cells that constantly transcytose particulate antigens from the lumen (7). Lacking the longer brush border of

enterocytes, M cells have shortened microvilli containing a distinct set of surface glycolipids and glycoproteins which can be used to identify these cells (8-10). M cells can be identified using the lectin *Ulex europaeus* agglutinin I (UEA-I), though UEA-I also binds to goblet cells, mucus, and fucosylated epithelial cells (11). M cells can also be identified by the expression of glycoprotein 2 (GP2), a receptor for the FimH proteins found on a subset of Gram-negative enteric bacteria (12).

Though much of the sampling is passive, M cells use pinocytosis, macropinocytosis, receptor-mediated endocytosis, and other methods to sample a diverse range of antigens of varying sizes (12-14). Once the antigens pass through the cells, the payload is picked up by lymphocytes or dendritic cells that can access an intraepithelial pocket within the M cells (15, 16). Since M cells represent a major pathway by which particulate antigens are introduced into the PPs, M cells are central to the development of immune responses to both pathogenic bacteria and commensal bacteria; a reduction in M cells can lead to little or no IgA production (17, 18). Secretory IgA is one of the primary methods of controlling the luminal flora (19, 20); even non-pathogenic bacteria require IgA production to keep the density within a manageable number and away from other inflammatory mechanisms of the epithelium (21). Commensal bacteria can be safely sampled through M cells and deposited to dendritic cells, which can migrate to the mesenteric lymph node to initiate IgA production (22).

While the majority of M cells are found over PP, M cells may also develop on villi (23). Though villous M cells are very rare in wild type mice, they are similar to PP M cells, UEA-I+ and able to transcytose antigens similar to PP M cells. We have previously shown Receptor Activated NF- κ B Ligand, RANKL, to be a critical factor in

the development of M cells (18). RANKL is expressed on stromal cells below the FAE, in direct contact with the RANK⁺ epithelium. In wild type mice, RANKL expression is restricted to the PP dome, restricting the development of M cells to the FAE. Upon systemic treatment with recombinant RANKL, the villous epithelium, which is also RANK⁺ can be induced to develop M cells on 100% of the villi (18), showing the potential of the stem cells in the villous crypts to develop into M cells with the proper stimuli.

RANKL^{-/-} mice have very few M cells on the PP domes, but interestingly the density of PP M cells in these mice increases from almost no M cells in the proximal small intestine to around 15 M cells on the largest dome of the most distal PP (18). Although the proximal to distal gradient in the density of PP M cells per dome observed in RANKL^{-/-} mice is not seen in wild type mice, this gradient of M cell density mirrors the density of the commensal flora, suggesting that at least under some conditions, signals from the commensal flora may directly influence M cell development.

In this study we present evidence indicating that the enteric flora specifically found in mice lacking IgA can induce the development of M cells on villi in the distal ileum. These villous M cells are similar to PP M cells and fully functional. Appearing just after weaning when the density of the enteric flora rapidly expands, these commensal-induced villous M cells require signals from live bacteria, temporarily disappearing after antibiotic treatment. As these commensal-induced villous M cells also require RANKL, we find a population of M cells controlled by both commensal bacteria and RANKL.

Materials and Methods

Mice

$J_H^{-/-}$ mice were purchased from Taconic Farms (Hudson, NY). BALB/c and μ MT mice used in experiments were purchased from Jackson Labs (Bar Harbor, ME). $IgA^{-/-}$ mice originally made by Dr. Innocent N. Mbawuke at Baylor University were obtained from Dr. Charles Parkos (24). $AID^{-/-}$ mice were obtained from Dr. Sidonia Fagarasan (25). All animal studies were reviewed and approved by the Emory University Institutional Animal Care and Use Committee.

Oral gavage of cecal contents

To induce villous M cells prior to weaning of neonates, 10 day old $J_H^{-/-}$ or $J_H^{+/-}$ mice were gavaged with the cecal contents from a 10 week old $J_H^{-/-}$ mouse. Briefly, the cecum from a $J_H^{-/-}$ was removed, opened, and the contents were scraped into 2mls PBS. Mixture was vortexed for ten seconds to homogenize solution. Neonates were gavaged with 100 μ l of cecal contents and analyzed 1 week later for villous M cells.

Cholera toxin induction of fucosylated epithelial cells

Fucosylation on epithelial cells was induced by oral gavage of 10 μ g of cholera toxin (Vector Labs, Burlingame, CA) in 200 μ l PBS. 24 hours later tissue from the small intestine was embedded in OCT and frozen sections prepared for staining with fluorescent antibodies.

RANKL induction of villous M cells

Villous M cell development was induced by systemic injections of recombinant RANKL made as previously described (18). Mice were initially injected with 50 µg of protein SC and 50 µg of protein IP, followed by daily injections of 50 µg of protein SC for three additional days. On day four, small intestines were frozen for sections and fluorescence imaging.

Antibodies and Lectins

Rhodamine-UEA-I was purchased from Vector Laboratories. The anti-RANKL Ab (IK22-5) was used for in vivo RANKL neutralization experiment; mice were treated 250 µg of IK22-5 i.p. every 2 days for a total of 4 injections.

Immunofluorescence staining of frozen sections

Frozen sections of small intestines were cut on a cryostat and prepared for staining experiments as previously described (26). The sections were air dried overnight, and fixed for 10 min in acetone at -20°C. Abs diluted in TNB buffer (PerkinElmer Life Sciences, Waltham MA) were applied for one hour at room temperature. Unconjugated antibodies were detected with a secondary anti-rat Alexa 546-conjugated antibody (Invitrogen, Carlsbad, CA). 4',6-diamidino-2-phenylindole, DAPI, (Sigma-Aldrich, St. Louis, MO) at 10 ng/ml was used as a nuclear counterstain. The slides were mounted in ProLong anti-fade reagent (Invitrogen). Images were acquired using a Nikon 80i fluorescence microscope.

Whole mount staining of small intestines for detection of UEA-I⁺ M cells

For detection of M cells, small intestines were stained for whole mount imaging as previously described (18). Segments of small intestines were excised, opened longitudinal, and vortex mixed in 0.5% Tween 20-PBS. The tissue was then fixed in buffered formalin for 20 minutes, washed in PBS, and then stained with rhodamine-UEA-I and DAPI in TNB buffer for 40 minutes at 4°C. Segments of small intestine were then wet mounted under a 20 mm x 40 mm cover slip in 200 µl PBS.

In vivo assessment of M cell uptake of fluorescent beads and bacteria

The uptake of 1 µm diameter fluorescent polystyrene latex nanoparticles (Fluoresbrite YG: Polysciences, Warrington, PA) or Salmonella Typhimurium labeled with Alexa-546 (Invitrogen) by M cells on villi was assessed by using a modification of previously described isolated small intestinal loop models (18), by deliberately tying 5 cm-long loops between 5 to 0 cm from the cecum, and 15 to 10 cm from the cecum. Frozen sections were cut, briefly stained with DAPI (Sigma-Aldrich) without fixation, and examined by microscopy.

Quantitative analysis of fluorescent bead uptake by villous M cells

Analysis of the degree of bead uptake into villi was done by threshold analysis using ImageJ software (<http://rsb.info.nih.gov/ij>) as previously described (18). The percentage of the pixels with a signal intensity that exceeded the selected threshold was calculated for the area occupied by small intestinal villi.

ELISA for measurement of fecal IgA

To quantitate total fecal IgA, fecal pellet samples were collected and extracted by making a 1/10 suspension (w/v) with PBS. After the suspension was vortexed and spun for 10 min at 12,000 x g, the supernatant was stored at -70C. Polyclonal goat anti-mouse IgA Ab (Southern Biotechnology) was used as a capture Ab. The bound mouse IgA was detected with peroxidase-labeled goat anti-mouse IgA Ab (Southern Biotechnology) using TMB (BD Biosciences) as the peroxidase substrate. A mouse IgA, k isotype control mAb (BD Biosciences) was used to establish a standard curve.

Statistical analysis

Differences between the mean values for groups were analyzed by either two-tailed Student's t-test, two-tailed Mann-Whitney test, or two-tailed ANOVA (for multiple groups) using Prism (GraphPad Software). A p value of less than 0.01 was considered significant.

Results

Mice lacking B cells have an increased density in M cells on villi in the distal ileum

Development of M cells is generally restricted to the FAE of PP. Rarely in wild type mice, M cells capable of sampling antigen may also appear on the villi (23).

BALB/c mice contain a low density of villous M cells of an average of 0.07 M cells per villus, throughout the small intestine. Interestingly, we observed by whole mount UEA-I staining a much larger number of M cells per villus in the distal ileum of $J_H^{-/-}$ mice (Figure 1a). The increase in villous M cell density was most evident beginning approximately 6 cm from the cecum (Figure 1b). Between 6 cm and 3 cm from the cecum, the villous M cell density in $J_H^{-/-}$ was 7 cells per villus. This density further increased on villi located 3 cm or less from the cecum to 15 cells per villus (Figure 1b). This increase in villous M cell density was not seen in BALB/c which maintained an average density of 0.07 cells per villi.

To demonstrate that the UEA-I⁺ cells in $J_H^{-/-}$ mice are indeed villous M cells, functional assays were set up to measure uptake of particulate antigens into villi. Loops of the distal small intestine were tied off and injected with 1 μ m diameter fluorescent beads or Alexa546 labeled *Salmonella typhimurium*. Only villi from the distal ileum of $J_H^{-/-}$ mice contained beads, while villi from the proximal ileum of $J_H^{-/-}$ or the proximal or distal ileum of BALB/c mice were unable to take up beads (Figure 1c). The amount of beads found within villi corresponded to number of UEA-I cells (Figure 1d), indicating these cells are functional villous M cells.

The absence of IgA is sufficient to cause an increase in villous M cells in the distal ileum

To determine if the expansion of villous M cells in the distal ileum was a general phenomena associated with absence of B cells, μ MT mice were used as a second model of B cell deficient mice on a different strain background. μ MT mice also had an increased density of villous M cells in the distal ileum, with the greatest density of 15 M cells per villus occurring in the far distal ileum (Figure 2). We next sought to determine if the expansion of villous M cells seen in both $J_H^{-/-}$ and μ MT mice also occurred in mice that retain B cells but specifically lack the ability to make IgA. $AID^{-/-}$ mice lack the ability to class switch or undergo somatic hypermutation, and therefore lack IgA, IgG, and high affinity IgM antibodies. These mice also had a similar increase in villous M cell density in the distal ileum to the two B cell deficient strains (figure 2). Using knockout mice that only lacked IgA, we showed that absence of just IgA was sufficient to bring about expansion of the number of villous M cells in the distal ileum (figure 2).

Oral antibiotic treatment of $J_H^{-/-}$ mice leads to loss of distal ileum villous M cells

To determine if the enteric microflora is involved in driving the expansion of villous M cells in $J_H^{-/-}$ mice, the mice were treated in their drinking water with a mixture of three antibiotics: ampicillin, neomycin, and metronidazole. The density of villous M cells started decreasing after 1 day of antibiotics (figure 3). After 3 days on antibiotics, villous M cells could no longer be found (Figure 3). $J_H^{-/-}$ mice were given single antibiotics in their drinking water for 3 days; while each of the individual antibiotics alone reduced the number of villous M cells, only ampicillin alone was as effective as the combination of antibiotics (data not show).

Villous M cells first appear in $J_H^{-/-}$ mice at the time of weaning

$J_H^{-/-}$ mice were examined at different ages to determine when the villous M cells occurred in the distal ileum first appeared. Neonates and mice up through two weeks of age had no M cells on villi in the distal ileum. At 3 weeks, $J_H^{-/-}$ mice had a density of 5 M cells per villus, which continued to increase until 5 weeks when the density of M cells in the distal ileum reached the density seen in adult mice (Figure 4a).

To determine if the development of villous M cells in the distal ileum of $J_H^{-/-}$ mice could be accelerated by premature introduction of the bacterial species normally resident in the intestine of $J_H^{-/-}$ mice, 10 day old $J_H^{-/-}$ mice were gavaged with cecal contents harvested from a 12 week-old $J_H^{-/-}$ mouse. One week later, the mice gavaged with cecal contents had an increased density of villous M cells in the distal ileum compared to control littermates gavaged with PBS alone (Figure 4b).

RANKL supports the expansion of villous M cells in $J_H^{-/-}$ mice

We previously showed that antibody-mediated neutralization of RANKL blocks the development of PP M cells (18). To determine if RANKL was involved in the development of the villous M cells in the distal ileum, $J_H^{-/-}$ mice were treated with neutralizing anti-RANKL antibody every other day for 8 days. Neutralization of RANKL significantly decreased the density of villous M cells to 1.0 M cells per villus, which is just above the average level seen in wild type mice (Figure 5).

Discussion

The commensal enteric flora has an obligate role in the normal maintenance of homeostasis in the mammalian intestine (27). This is evident by the many changes that occur in mice housed under germfree conditions when they are subsequently colonized by commensal bacteria (28). Introduction of a normal microflora into gnotobiotic mice leads to increases in the number of mucosal B cells and specific subsets of T cells (e.g. Th17 cells) along with the development of isolated lymphoid follicles (ILFs), organized intestinal lymphoid structures containing B cells (29). The epithelium undergoes similar maturation events once mice becomes in contact with commensal bacteria. In germfree mice, the epithelium has an average turnover time of 115 hours; following colonization with commensal bacteria the transit time of epithelial cells from the crypts to the tips of the villi shortens to 53 hours and mucus production increases (30, 31). Thus, the intestinal epithelium is able to recognize the presence of the commensal bacteria and modify its pattern of gene expression in response (32). Here we report the interaction of commensal bacteria with the intestinal epithelium also has the potential to promote the development of villous M cells.

The distal ileum has the highest density of commensal bacteria in the entire small intestine. In mice without IgA, the enteric flora is altered, with a roughly 100-fold increase in several species of anaerobes (33). One anaerobic type of bacteria that inhabits the distal small intestine and is expanded in IgA^{-/-} and AID^{-/-} mice is the segmented filamentous bacteria, and these bacteria have been shown to preferentially stimulate the development of Th17 cells (3). The expansion of at least some species within the normal

commensal flora is likely responsible for inducing increased numbers of villous M cells in the terminal ileum of B cell- and IgA-deficient mice. When these bacteria are depleted as a result of oral antibiotic treatment, the main stimulus driving villous M cell differentiation in the terminal ileum is lost and the number of villous M cells observed rapidly decreases. The increased number of villous M cells in $J_H^{-/-}$ mice is first noted around the time of weaning when the normal enteric flora colonizes the neonates and begins its expansion towards adult levels. Prior to weaning, the epithelium in the distal small intestine is still able to generate increased numbers of villous M cells if the proper signals are provided. Gavaging part of the cecal contents from adult $J_H^{-/-}$ mice into 10 day old $J_H^{-/-}$ mice results in induction of villous M cells approximately one week prior to their normal time of appearance.

The villous M cells in the distal ileum of $J_H^{-/-}$ mice were found to require RANKL for their development as do normal PP M cells. Though we were unable to detect any RANKL expression in subepithelial stromal cells beneath the distal ileum villi of $J_H^{-/-}$ mice (data not shown), neutralizing RANKL by antibody treatment significantly decreased the density of villous M cells. In the small intestine, RANKL is normally expressed by stromal cells in the subepithelial dome of PP and ILFs (26). RANKL also circulates in serum as a soluble cytokine after cleavage from the cell surface mediated by metalloproteases (34). Based on the crucial role of RANKL in the development of PP M cells and the ability of exogenous RANKL to induce villous M cells throughout the small intestine, it is reasonable to hypothesize that RANKL could also foster the maintenance of villous M cells initially induced by other stimuli. In wild type mice, the normal circulating level of RANKL is generally insufficient to induce the development of villous

M cells that are not located immediately adjacent to a cellular source of RANKL. However, for villous M cells induced in the distal ileum of $J_H^{-/-}$ mice by the commensal flora, the low levels of circulating serum RANKL might be sufficient to help sustain these M cells. Expression of the metalloprotease MMP-7 by the intestinal epithelium is induced after bacterial colonization (35). Other metalloproteases become more active in the gut during inflammation for the purpose of activating defensins or inducing epithelial wound repair (36). Thus, changes in the density and composition of the commensal enteric flora could potentially increase the activity of the metalloproteases which cleave the transmembrane form of RANKL found on cells, thus increasing the local soluble level of RANKL in the vicinity of the area of enhanced metalloprotease expression.

In B cell-deficient mice, the enteric flora quickly becomes altered with generally around a 100-fold increase in the density of several types of anaerobes (33). The specific bacterial species represented in the commensal enteric flora in different mouse breeding facilities could potentially influence the degree to which this flora is capable of inducing villous M cells in the distal ileum. For example, 7 week old μ MT mice examined one day after arrival from Jackson Laboratories had essentially no villous M cells in the distal ileum (data not shown), while μ MT mice of the same age bred at Emory University routinely showed villous M cells. There are precedents for mice from The Jackson Laboratory having a more restricted enteric flora with less of an immunostimulatory effect (e.g. on Th17 development) than mice purchased from other commercial vendors or maintained in specific-pathogen free facilities at universities (2). Housing μ MT mice purchased from The Jackson Laboratory in the Emory mouse colony together with Emory-bred μ MT mice for just 3 weeks allowed these μ MT mice an opportunity to

acquire the same commensal flora found in the Emory-bred mice and led to the induction of villous M cells in the distal ileum.

The intestinal epithelium recognizes commensal and pathogenic bacteria through a variety of pattern recognition receptors including plasma membrane TLRs, endosomal TLRs (37), intracellular NLRs (38), formyl peptide receptors, and receptors for short chain fatty acids such as acetate and butyrate. Under homeostatic conditions, balanced proinflammatory and anti-inflammatory signaling occurs (39). Bacteria can also directly modulate epithelial signaling: while pathogenic bacteria generally activate inflammatory pathways once they breach the epithelial barrier, various commensal bacteria species can actually inhibit epithelial inflammatory signaling by disrupting NF- κ B signaling (40). Some of these same bacterial signals may also function to initiate M cell development when secretory IgA is lacking leading to expansion of some classes of bacteria in the intestinal lumen. Further investigation will be needed to reveal the precise mechanism(s) by which commensal bacteria can induce M cells and how these signaling pathways overlap in part with the signaling mechanisms initiated by RANKL.

PP and ILF M cells are found naturally as part of the antigen-sampling mechanism of the FAE that allows the introduction of antigen into the inductive lymphoid tissues of the mucosa. RANKL-induced villous M cells represent an experimentally generated group of M cells that are capable of temporarily increasing antigen sampling throughout the small intestine. The newly described commensal-induced villous M cells characterize an innate response of the epithelium to an elevated bacterial loads in the intestinal lumen. One of the many common factors between PP M cells, RANKL-induced villous M cells, and commensal-induced villous M cells is their

dependence on RANKL for their continued differentiation and survival. Like PP M cells and RANKL-induced villous M cells, commensal-induced villous M cells disappear rapidly after RANKL is neutralized. We believe that these 3 populations of intestinal M cells found in different locations and circumstances are derived from a common lineage of antigen-sampling M cells that differentiate from uncommitted intestinal cells in the proliferative zone in a process that requires at least a threshold level of RANKL to be present.

References

1. Hooper LV, Midtvedt T, Gordon JI. How host-microbial interactions shape the nutrient environment of the mammalian intestine. *Annual Review of Nutrition*. 2002;22(1):283-307.
2. Ivanov II, Frutos RdL, Manel N, Yoshinaga K, Rifkin DB, Sartor RB, et al. Specific Microbiota Direct the Differentiation of IL-17-Producing T-Helper Cells in the Mucosa of the Small Intestine. *Cell Host & Microbe*. 2008;4(4):337-49.
3. Ivanov II, Atarashi K, Manel N, Brodie EL, Shima T, Karaoz U, et al. Induction of Intestinal Th17 Cells by Segmented Filamentous Bacteria. *Cell*. 2009;139(3):485-98.
4. Vijay-Kumar M, Aitken JD, Carvalho FA, Cullender TC, Mwangi S, Srinivasan S, et al. Metabolic Syndrome and Altered Gut Microbiota in Mice Lacking Toll-Like Receptor 5. *Science*. 2010;328(5975):228-31.
5. Linskens RK, Huijsdens XW, Savelkoul PHM, Vandenbroucke-Grauls CMJE, Meuwissen SGM. The Bacterial Flora in Inflammatory Bowel Disease: Current Insights in Pathogenesis and the Influence of Antibiotics and Probiotics. *Scandinavian Journal of Gastroenterology*. 2001;36(234):29-40.
6. Sansonetti PJ. War and peace at mucosal surfaces. *Nat Rev Immunol*. 2004;4(12):953-64.
7. Owen RL, Jones AL. Epithelial cell specialization within human Peyer's patches: an ultrastructural study of intestinal lymphoid follicles. *Gastroenterology*. 1974;66(2):189-203.
8. Giannasca PJ, Giannasca KT, Falk P, Gordon JI, Neutra MR. Regional differences in glycoconjugates of intestinal M cells in mice: potential targets for mucosal vaccines. *Am J Physiol Gastrointest Liver Physiol*. 1994;267(6):G1108-21.
9. Gebert A, Rothkotter HJ, Pabst R. M cells in Peyer's patches of the intestine. *Int Rev Cytol*. 1996;167:91-159.

10. Owen RL. Uptake and transport of intestinal macromolecules and microorganisms by M cells in Peyer's patches-- a personal and historical perspective. *Semin Immunol.* 1999;11(3):157-63.
11. Terahara K, Nochi T, Yoshida M, Takahashi Y, Goto Y, Hatai H, et al. Distinct fucosylation of M cells and epithelial cells by Fut1 and Fut2, respectively, in response to intestinal environmental stress. *Biochem Biophys Res Commun.* 2011;404(3):822-8.
12. Hase K, Kawano K, Nochi T, Pontes GS, Fukuda S, Ebisawa M, et al. Uptake through glycoprotein 2 of FimH+ bacteria by M cells initiates mucosal immune response. *Nature.* 2009;462(7270):226-30.
13. Pappo J, Ermak TH. Uptake and translocation of fluorescent latex particles by rabbit Peyer's patch follicle epithelium: a quantitative model for M cell uptake. *Clin Exp Immunol.* 1989;76(1):144-8.
14. Schulte R, Kerneis S, Klinke S, Bartels H, Preger S, Kraehenbuhl JP, et al. Translocation of *Yersinia enterocolitica* across reconstituted intestinal epithelial monolayers is triggered by *Yersinia* invasin binding to beta1 integrins apically expressed on M-like cells. *Cell Microbiol.* 2000;2(2):173-85.
15. Neutra MR, Frey A, Kraehenbuhl JP. Epithelial M cells: gateways for mucosal infection and immunization. *Cell.* 1996;86(3):345-8.
16. Neutra MR, Mantis NJ, Frey A, Giannasca PJ. The composition and function of M cell apical membranes: Implications for microbial pathogenesis. *Semin Immunol.* 1999;11(3):171-81.
17. Hashizume T, Togawa A, Nochi T, Igarashi O, Kweon MN, Kiyono H, et al. Peyer's patches are required for intestinal immunoglobulin A responses to *Salmonella*. *Infect Immun.* 2008;76(3):927-34.
18. Knoop KA, Kumar N, Butler BR, Sakthivel SK, Taylor RT, Nochi T, et al. RANKL is necessary and sufficient to initiate development of antigen-sampling M cells in the intestinal epithelium. *J Immunol.* 2009;183(9):5738-47.

19. Michalek SM, McGhee JR, Kiyono H, Colwell DE, Eldridge JH, Wannemuehler MJ, et al. The IgA response: inductive aspects, regulatory cells, and effector functions. *Annals of the New York Academy of Sciences*. 1983;409:48-71.
20. Macpherson AJ, Uhr T. Induction of protective IgA by intestinal dendritic cells carrying commensal bacteria. *Science*. 2004;303(5664):1662-5.
21. Garrett WS, Gordon JI, Glimcher LH. Homeostasis and Inflammation in the Intestine. *Cell*. 2010;140(6):859-70.
22. Macpherson AJ, Uhr T. Compartmentalization of the mucosal immune responses to commensal intestinal bacteria. *Ann N Y Acad Sci*. 2004;1029:36-43.
23. Jang MH, Kweon M-N, Iwatani K, Yamamoto M, Terahara K, Sasakawa C, et al. Intestinal villous M cells: An antigen entry site in the mucosal epithelium. *Proceedings of the National Academy of Sciences of the United States of America*. 2004;101(16):6110-5.
24. Mbawuike IN, Pacheco S, Acuna CL, Switzer KC, Zhang Y, Harriman GR. Mucosal Immunity to Influenza Without IgA: An IgA Knockout Mouse Model. *The Journal of Immunology*. 1999;162(5):2530-7.
25. Muramatsu M, Kinoshita K, Fagarasan S, Yamada S, Shinkai Y, Honjo T. Class Switch Recombination and Hypermutation Require Activation-Induced Cytidine Deaminase (AID), a Potential RNA Editing Enzyme. *Cell*. 2000;102(5):553-63.
26. Taylor RT, Patel SR, Lin E, Butler BR, Lake JG, Newberry RD, et al. Lymphotoxin-independent expression of TNF-related activation-induced cytokine by stromal cells in cryptopatches, isolated lymphoid follicles, and Peyer's patches. *J Immunol*. 2007;178(9):5659-67.
27. Hooper LV, Gordon JI. Commensal Host-Bacterial Relationships in the Gut. *Science*. 2001;292(5519):1115-8.
28. Macpherson AJ, Uhr T. Compartmentalization of the Mucosal Immune Responses to Commensal Intestinal Bacteria. *Annals of the New York Academy of Sciences*. 2004;1029(1):36-43.

29. Shroff K, Meslin K, Cebra J. Commensal enteric bacteria engender a self-limiting humoral mucosal immune response while permanently colonizing the gut. *Infect Immun.* 1995;63(10):3904-13.
30. Matsuzawa T, Wilson R. The Intestinal Mucosa of Germfree Mice after Whole-Body X-Irradiation with 3 Kilorontgens. *Radiation Research.* 1965;25(1):15-24.
31. Szentkuti L, Riedesel H, Enss M, Gaertner K, von Engelhardt W. Pre-epithelial mucus layer in the colon of conventional and germ-free rats. *The Histochemical Journal.* 1990;22(9):491-7.
32. Artis D. Epithelial-cell recognition of commensal bacteria and maintenance of immune homeostasis in the gut. *Nat Rev Immunol.* 2008;8(6):411-20.
33. Fagarasan S, Muramatsu M, Suzuki K, Nagaoka H, Hiai H, Honjo T. Critical roles of activation-induced cytidine deaminase in the homeostasis of gut flora. *Science.* 2002;298(5597):1424-7.
34. Lum L, Wong BR, Josien R, Becherer JD, Erdjument-Bromage H, Schlondorff J, et al. Evidence for a role of a tumor necrosis factor- α (TNF- α)-converting enzyme-like protease in shedding of TRANCE, a TNF family member involved in osteoclastogenesis and dendritic cell survival. *J Biol Chem.* 1999;274(19):13613-8.
35. López-Boado YS, Wilson CL, Hooper LV, Gordon JI, Hultgren SJ, Parks WC. Bacterial Exposure Induces and Activates Matrilysin in Mucosal Epithelial Cells. *The Journal of Cell Biology.* 2000;148(6):1305-15.
36. Parks WC, Wilson CL, Lopez-Boado YS. Matrix metalloproteinases as modulators of inflammation and innate immunity. *Nat Rev Immunol.* 2004;4(8):617-29.
37. Medzhitov R. Recognition of microorganisms and activation of the immune response. *Nature.* 2007;449(7164):819-26.

38. Girardin SE, Boneca IG, Carneiro LAM, Antignac A, Jéhanno M, Viala J, et al. Nod1 Detects a Unique Muropeptide from Gram-Negative Bacterial Peptidoglycan. *Science*. 2003;300(5625):1584-7.
39. Mantovani A, Locati M, Polentarutti N, Vecchi A, Garlanda C. Extracellular and intracellular decoys in the tuning of inflammatory cytokines and Toll-like receptors: the new entry TIR8/SIGIRR. *J Leukoc Biol*. 2004;75(5):738-42.
40. Neish AS, Gewirtz AT, Zeng H, Young AN, Hobert ME, Karmali V, et al. Prokaryotic Regulation of Epithelial Responses by Inhibition of I κ B- α Ubiquitination. *Science*. 2000;289(5484):1560-3.

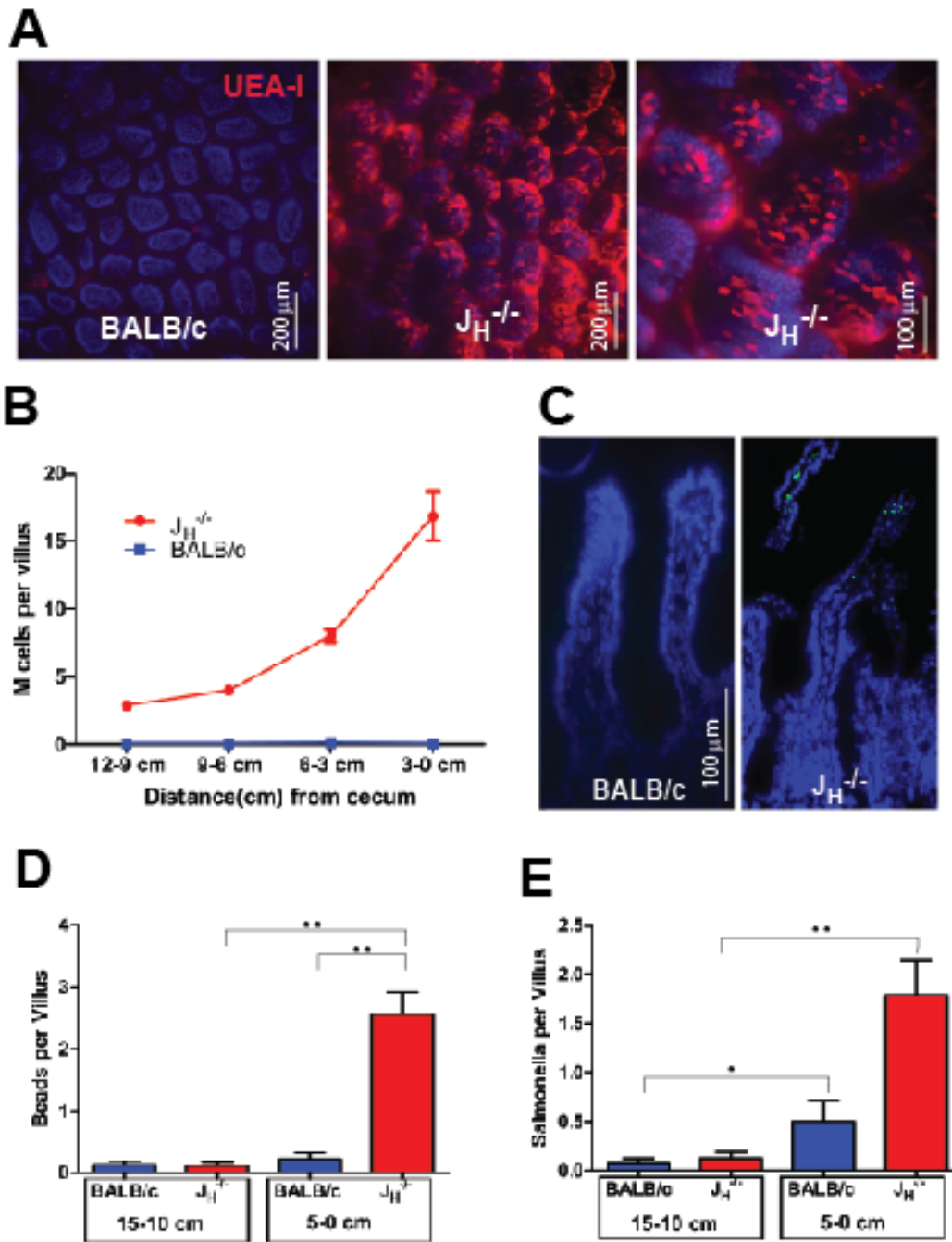


Figure 1. Villous M cells develop in large numbers in the distal ileum of $J_H^{-/-}$ mice. A, Small intestines from $J_H^{-/-}$ or BALB/c mice were stained with UEA-I⁺ to visualize M cells. B, Graph showing the number of M cells per villus as compared to distance from

the cecum. N=4 per group. C, Isolated small intestinal loops were prepared in anesthetized $J_H^{-/-}$ or BALB/c mice that were injected with 1×10^{11} 200 nm fluorescent beads. D, Graph summary of fluorescent beads taken up into villi, as determined by ImageJ analysis. E, Graph summary of salmonella labeled with Alexa 546 taken up into villi.

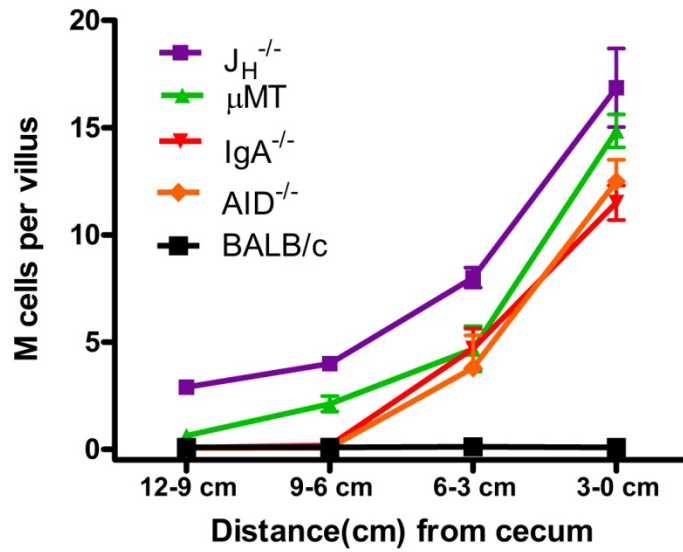


Figure 2. Mice lacking IgA have an increased villous M cell density. A, B cell deficient mice: $J_H^{-/-}$ and μMT , and IgA deficient mice: $IgA^{-/-}$ and $AID^{-/-}$ have an increase in UEA-I⁺ cells in the distal ileum calculated by whole mount staining. N=3 per group.

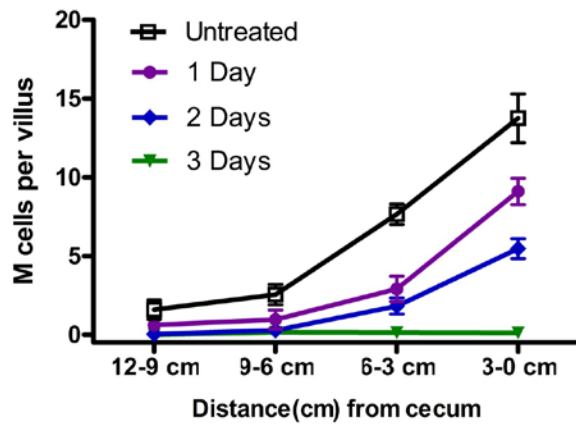


Figure 3. Elimination of enteric flora reduces villous M cell development. $J_H^{-/-}$ mice were placed on mixed antibiotics containing ampicillin, metronidazole, and neomycin for 1, 2, or 3 days. After 3 days villous M cells are significantly decreased. N=4 per group.

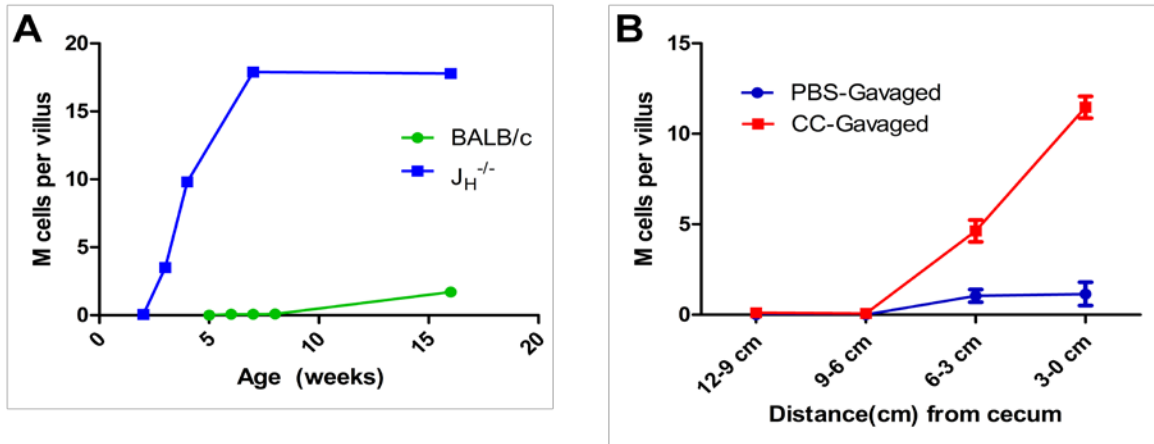


Figure 4. Villous M cells appear in $J_H^{-/-}$ mice during weaning. A, Small intestines from BALB/c or $J_H^{-/-}$ mice at different ages were stained with UEA-I. N=2 at each time point. B, 10 day old $J_H^{-/-}$ mice were gavaged with PBS or cecal contents from 12 week old $J_H^{-/-}$ mice. 1 week later, small intestines were stained with UEA-I. N=3 per group.

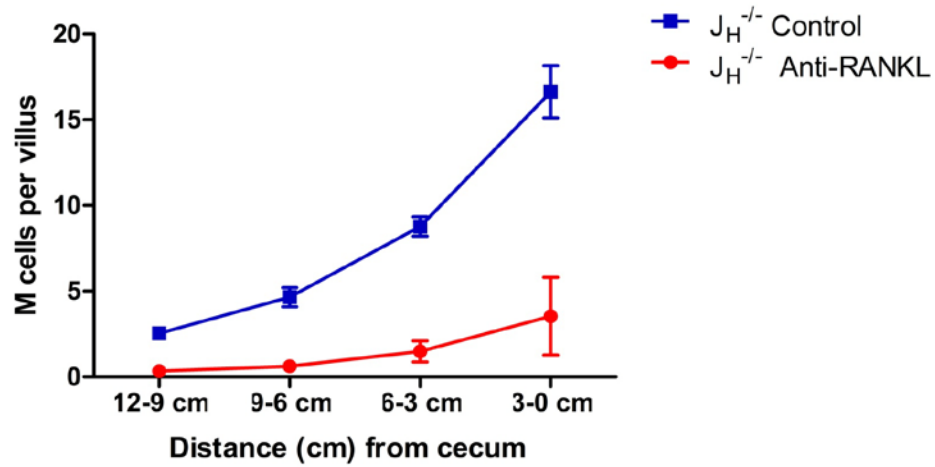


Figure 5. Villous M cells in $J_H^{-/-}$ mice require RANKL. After $J_H^{-/-}$ mice were treated with neutralizing RANKL antibody with 250 μ g every other day for 8 days, small intestines were stained with UEA-I, and had significantly less villous M cell compared to an untreated $J_H^{-/-}$ mice. N=4 mice.

Chapter 4

Other Examples of an Association of Stromal RANKL and GP2⁺ M cells in Organized Intestinal Lymphoid Tissues

The work in this chapter is unpublished. All experiments were performed by Kathryn A. Knoop. This chapter was written by Kathryn A. Knoop

Significance

While M cells are mostly studied as part of the PP FAE, they are known to develop on the epithelium overlaying lymphoid tissue found in other parts of the body (1, 2). Some of these lymphoid tissues are induced upon infection such as the Bronchial Associated Lymphoid Tissue (3). Other lymphoid tissues which develop as part of the normal developmental program can be found in the large intestine: the cecal patch, and the colonic patch and ILFs. The cecal patch is a multi-follicle organ found on the tip of the cecum, opposite of junction where the small intestine ends and colon begins. The colonic patch is a multi-follicle organ developing on the proximal end of the colon, approximately 2 cm from the cecum differing from colonic ILFs, which commonly develop throughout the length of the colon. The cecal and colonic patches are structurally similar to Peyer's patches, requiring cytokines such as lymphotoxin during embryonic development (4-7). The colon also develops several ILFs, which can be more prevalent than ILFs in the small intestine (5) (8). These large intestinal lymphoid tissues all contain FAE and M cells (9, 10).

As RANKL was only recently shown to be necessary in small intestinal M cell development, these observations have not been shown in the large intestine. If RANKL is a critical factor in small intestinal M cell development, it would stand to reason RANKL would have a similar role in M cell development in GALT in the large intestine. The purpose of this study was to examine if RANKL is found in a similar pattern on stromal cells below the FAE which contains antigen-sampling M cells.

Methods and Materials

Mice

BALB/c mice used in experiments were purchased from Jackson Labs (Bar Harbor, ME). All mice used in the experiments were at least 8 weeks old. RANKL^{-/-} mice on a C57BL/6 background were obtained from a breeding colony maintained in a conventional specific pathogen free mouse facility at Emory University. All animal studies were reviewed and approved by the Emory University Institutional Animal Care and Use Committee.

Antibodies and Lectins

Unconjugated anti-GP2 antibody (2F11-C3) was purchased from MBL (Woburn, MA). Rhodamine-UEA-I was purchased from Vector Laboratories. Anti-RANKL (IK22-5) was purchased from eBioscience.

Immunofluorescence staining of frozen sections

Frozen sections of large intestines were cut on a cryostat and prepared for staining experiments as previously described. (11) The sections were air dried overnight, and fixed for 10 min in acetone at -20°C. Abs diluted in TNB buffer (PerkinElmer Life Sciences, Waltham MA) were applied for one hour at room temperature. Unconjugated antibodies were detected with a secondary anti-rat Alexa 546-conjugated antibody (Invitrogen). 4',6-diamidino-2-phenylindole, DAPI, (Sigma-Aldrich, St. Louis, MO) at 10 ng/ml was used as a nuclear counterstain. The slides were mounted in ProLong anti-

fade reagent (Invitrogen). Images were acquired using a Nikon 80i fluorescence microscope.

Results and Discussion

Though RANKL was shown to be necessary for the development of M cells in the small intestine (12), this pathway has not been seen in other lymphoid tissues which contain M cells. The first hint of the importance of RANKL in PP function came with the observation of the arch-like pattern of RANKL on stromal cells just below the FAE (11). We hypothesized that if RANKL is a critical factor in the development of M cells, RANKL should be found below the FAE of other lymphoid tissues where M cells are found.

The large intestine contains several GALT structures of varying sizes. Cecal patches contain multiple follicles, similar to PP(4). ILFs develop in the colon, similar to the small intestines (5). Sections of large intestinal lymphoid tissue were stained for RANKL expression. RANKL was found on stromal cells in both the cecal patch and colonic ILFs (Figure 1), in the same pattern seen in small intestine PP and ILF, in an arch just below the FAE, suggesting a similar function in the development of M cells on large intestinal FAE.

The epithelium in the large intestine is slightly different than the small intestine. One difference impacting this study is the fucosylation patterns of epithelial cells. In the small intestine, only M cells have α 1,2 fucose linkage on their apical surface, making UEA-I a good reagent for identifying M cells in the small intestine. However, in the large intestines all of the enterocytes contain α 1,2 fucose on their surface, making all of the epithelium UEA-I reactive. GP2 is an M cell specific receptor (13, 14) ; been shown to be specific for small intestinal M cells, but believed to be a universal M cell marker.

Sections of both BALB/c cecal patches and colonic ILFs revealed GP2⁺ M cells develop on the FAE of the structures (Figure 1).

RANKL^{-/-} mice have a conspicuous absence of M cells on small intestinal PP FAE(12), demonstrating that without RANKL M cells fail to develop. To look for a similar phenotype in the large intestine of RANKL^{-/-} mice, sections of colon were next examined for M cells through staining for GP2⁺. No GP2⁺ cells were found on the FAE of colonic ILFs (Figure 2), indicating without RANKL, M cells are unable to develop in the large intestine as well as the small intestine.

Finding RANKL directly below M cells extends the association between RANKL and M cells to GALT structures outside the small intestine. Similar to our previous findings, the lack of RANKL in the large intestine causes a lack of M cells on large intestinal lymphoid structures, suggesting RANKL is critical in the development of all intestinal M cells. As with our previous report, we suggest there is a direct stimulation of the epithelium with the RANKL⁺ stromal cells to initiate and maintain M cells on the FAE.

References

- 1 Gebert, A. & Pabst, R. M cells at locations outside the gut. *Semin Immunol* **11**, 165-170, (1999).
- 2 Kraehenbuhl, J. P. & Neutra, M. R. Epithelial M cells: differentiation and function. *Annu. Rev. Cell Dev. Biol.* **16**, 301-332 (2000).
- 3 Moyron-Quiroz, J. E. *et al.* Role of inducible bronchus associated lymphoid tissue (iBALT) in respiratory immunity. *Nat Med* **10**, 927-934, (2004).
- 4 Yoshida, H. *et al.* IL-7 receptor α^+ CD3 $^-$ cells in the embryonic intestine induces the organizing center of Peyer's patches. *Int Immunol* **11**, 643-655 (1999).
- 5 Hamada, H. *et al.* Identification of multiple isolated lymphoid follicles on the antimesenteric wall of the mouse small intestine. *J Immunol* **168**, 57-64 (2002).
- 6 Dohi, T. *et al.* Elimination of colonic patches with lymphotoxin β receptor-Ig prevents Th2 cell-type colitis. *J Immunol* **167**, 2781-2790 (2001).
- 7 Fukuda, K. *et al.* Mesenchymal expression of Foxl1, a winged helix transcriptional factor, regulates generation and maintenance of gut-associated lymphoid organs. *Developmental Biology* **255**, 278-289 (2003).
- 8 Kweon, M.-N. *et al.* Prenatal blockage of lymphotoxin β receptor and TNF receptor p55 signaling cascade resulted in the acceleration of tissue genesis for isolated lymphoid follicles in the large intestine. *J Immunol* **174**, 4365-4372 (2005).
- 9 Jepson, M. A. *et al.* Targeting to intestinal M cells. *J Anat* **189** (Pt 3), 507-516 (1996).
- 10 Neutra, M. R., Mantis, N. J., Frey, A. & Giannasca, P. J. The composition and function of M cell apical membranes: Implications for microbial pathogenesis. *Semin Immunol* **11**, 171-181, (1999).

- 11 Taylor, R. T. *et al.* Lymphotoxin-independent expression of TNF-related activation-induced cytokine by stromal cells in cryptopatches, isolated lymphoid follicles, and Peyer's patches. *J Immunol* **178**, 5659-5667 (2007).
- 12 Knoop, K. A. *et al.* RANKL is necessary and sufficient to initiate development of antigen-sampling M cells in the intestinal epithelium. *J Immunol* **183**, 5738-5747 (2009).
- 13 Hase, K. *et al.* Uptake through glycoprotein 2 of FimH⁺ bacteria by M cells initiates mucosal immune response. *Nature* **462**, 226-230 (2009).
- 14 Terahara, K. *et al.* Comprehensive gene expression profiling of Peyer's patch M cells, villous M-like cells, and intestinal epithelial cells. *J. Immunol.* **180**, 7840-7846 (2008).

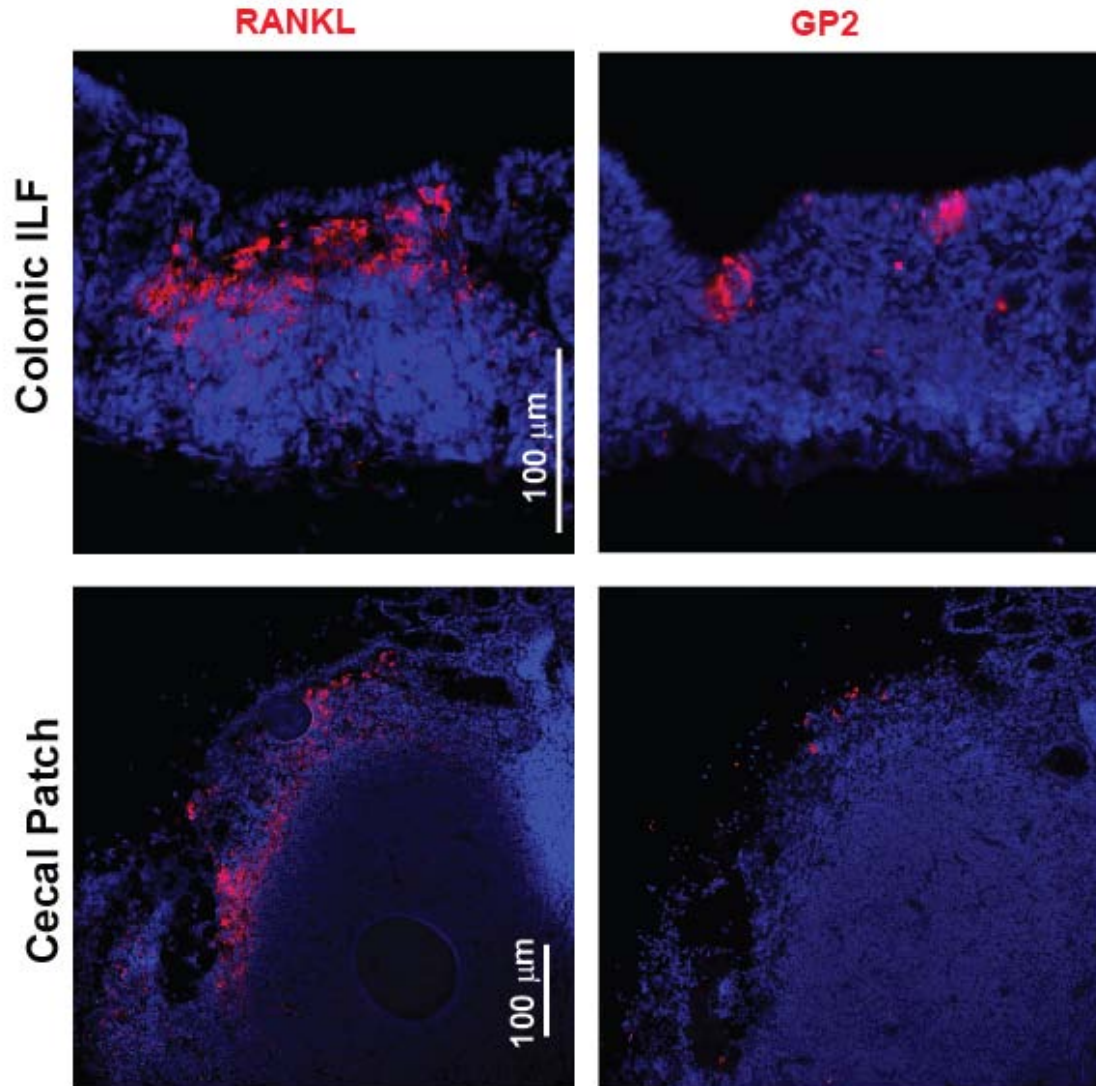


Figure 1. Large intestinal GALT contain GP2⁺ M cells above RANKL⁺ stroma. Sections of a colonic ILF (top panel) or the cecal patch (bottom panel) from BALB/c mice were stained for RANKL (left column) or GP2 (right column). RANKL is found in a pattern similar to that seen in PP. GP2⁺ M cells can be seen on the FAE of both structures. Scale bar 100 μm.

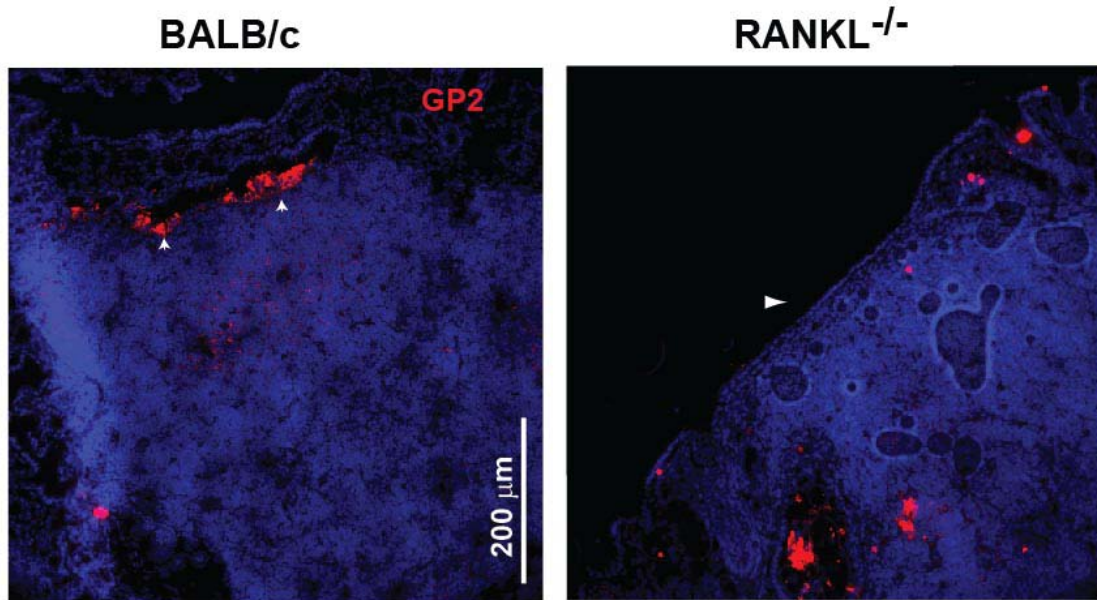


Figure 2. Colonic ILFs in RANKL^{-/-} mice lack M cells. Sections of colonic ILFs from a BALB/c mouse (left) or a RANKL^{-/-} mouse (right) were stained for GP2. While numerous GP2⁺ M cells were seen in BALB/c mice, indicated by the small white arrow, RANKL^{-/-} mice lacked M cells on the colonic FAE, indicated by the narrow white arrow. Scale bar 200 μm.

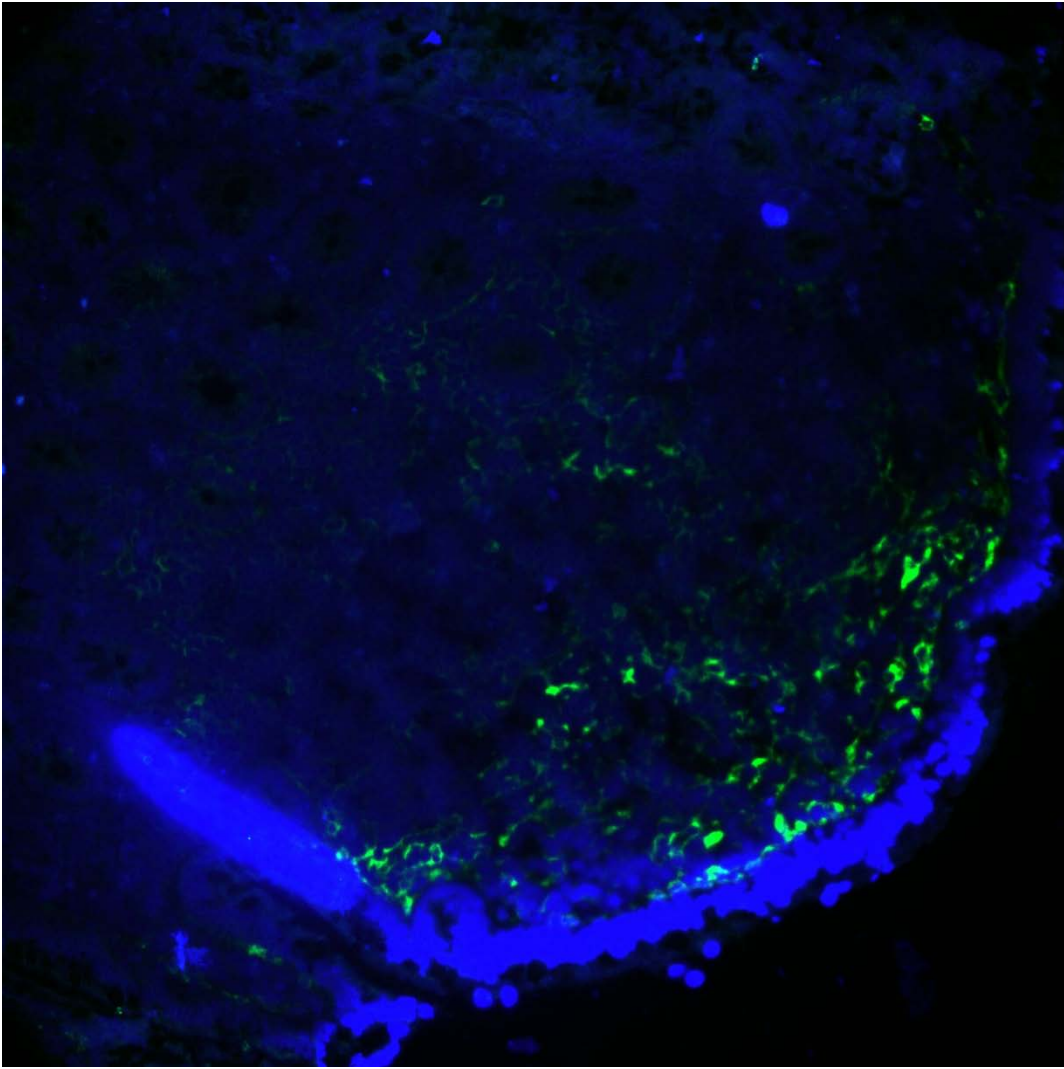


Figure 3. Human PPs express RANKL on stromal cells in the subepithelial dome.

Sections of human PPs were stained for RANKL, which was found in a pattern similar to mouse PP. Scale bar 200 μm .

Chapter 5

Distinct developmental requirements for isolated lymphoid follicle formation in the small and large intestine: RANKL is essential only in the small intestine

Kathryn A. Knoop¹, Betsy R. Butler¹, Nachiket Kumar¹, Rodney Newberry², and Ifor R. Williams¹

¹Department of Pathology and Laboratory Medicine, Emory University School of Medicine, Atlanta, GA 30322

²Department of Internal Medicine, Washington University School of Medicine, St. Louis, MO 63110

Submitted to American Journal of Pathology, February 1st, 2011.

All experiments in this study were performed by Kathryn A. Knoop, with assistance from Betsy R. Butler.

This manuscript was written by Kathryn A. Knoop and edited by Ifor R. Williams.

Abstract

Cryptopatches (CPs) and isolated lymphoid follicles (ILFs) are organized intestinal lymphoid tissues that develop postnatally in mice and include stromal cells expressing RANKL. We found that RANKL^{-/-} mice had a 4-fold reduction in the overall density of CPs in the small intestine, with the largest decrease in the proximal small intestine. No B cells were present in CPs from the small intestine of RANKL^{-/-} mice and ILF formation was completely blocked. In sharp contrast, colonic ILFs containing B cells were present in RANKL^{-/-} mice. Stromal cells within CPs in the small intestine of RANKL^{-/-} mice did not express CXCL13 and often lacked other normally expressed stromal cell antigens, while colonic lymphoid aggregates in RANKL^{-/-} mice retained stromal CXCL13 expression. The CXCL13-dependent maturation of precursor CPs into ILFs is differentially regulated in the small intestine and colon, with an absolute requirement for RANKL only in the small intestine.

Introduction

Lymphoid organogenesis is dependent on a series of complex interactions involving multiple cell adhesion molecules, chemokines, cytokines, and their receptors.(1) The development of each type of organized lymphoid tissue is characterized by a differential degree of reliance on individual mediators. For example, receptor activator of NF- κ B ligand (RANKL) is a TNF superfamily cytokine which is essential for the development of some types of lymphoid tissue (e.g. lymph nodes), but dispensable for other lymphoid structures such as Peyer's patches (PPs) and thymus.(2, 3) In lymph node development, RANKL has an obligate role in the establishment of the positive feedback loops involving lymphotoxin (LT) $\alpha_1\beta_2$ -producing lymphoid tissue inducer (LTi) cells and LT β R-expressing lymphoid tissue organizer cells.(4, 5)

Besides PPs, the gut-associated lymphoid tissue of mice also includes two additional types of smaller organized lymphoid tissues, cryptopatches (CPs) and isolated lymphoid follicles (ILFs).(6) CPs, the smaller of these lymphoid tissues, are found in the deep lamina propria adjacent to the crypts where they develop postnatally starting on day 14. Under normal homeostatic conditions there are approximately 1500 CPs in the small intestine and 150 in the colon.(6-8) An ILF is a single B cell follicle that develops a germinal center on maturation and can serve as an inductive site for IgA responses.(9) A single ILF fills up an entire villus and is covered by a follicle-associated epithelium containing M cells that is similar to the follicle-associated epithelium of PPs. Recently it has been suggested that CPs and ILFs are not distinct types of intestinal lymphoid tissue, but rather two extremes on a continuum of solitary intestinal lymphoid tissue (SILT).(10)

Current evidence suggests that the number of SILT structures in the intestine is normally stable after postnatal development is completed.(8) Instead, changes to the size and composition of the SILT occur in response to changes in the status of the commensal flora. While CPs are present in germ-free mice, the development of ILFs from these precursor CPs requires signals originating with the commensal enteric flora.(7, 11, 12)

We have previously shown that RANKL is expressed on stromal cells found throughout CPs, but is preferentially expressed by stromal cells located in the subepithelial dome of ILFs and PPs.(13) We also showed RANKL appears on stromal cells later in ontogeny than other stromal cell antigens including FDC-M1, VCAM-1, and CD157, and can still be induced when $LT\alpha_1\beta_2$ signaling through the $LT\beta R$ is blocked. In this study, we utilized $RANKL^{-/-}$ mice to further investigate the role of RANKL in the development of CPs and ILFs and found that in the absence of RANKL small intestinal but not colonic CPs fail to express CXCL13, recruit B cells or develop into ILFs.

Materials and Methods

Mice

RANKL^{-/-} mice on a C57BL/6 background were obtained from a breeding colony maintained in a conventional specific pathogen free mouse facility at Emory University. This colony was established with mice provided by Dr. Yongwon Choi at the University of Pennsylvania (Philadelphia, PA). Mice heterozygous for the RANKL null mutation were also backcrossed to BALB/cByJ mice (The Jackson Laboratory, Bar Harbor, ME) for at least four generations to allow intercrossing of male C57BL/6 RANKL^{+/-} mice and female BALB/c RANKL^{+/-} mice and production of RANKL^{-/-} mice and littermate controls on a background roughly equivalent to (C57BL/6 X BALB/c)F1 mice. A higher fraction of RANKL^{-/-} mice offspring on the F1 background survived into adulthood. All experiments using RANKL^{-/-} mice were done with mice on a C57BL/6 background and/or mice on a (C57BL/6 X BALB/c)F1 background, as indicated in the figure legends. Since equivalent results were obtained with RANKL^{-/-} mice on both backgrounds, the quantitative data were pooled for the figures. All control mice used were littermates to the RANKL^{-/-} mice, and these controls included both wild type mice (RANKL^{+/+}) and heterozygous mice (RANKL^{+/-}). Genotyping of mice for the RANKL null mutation was done using a three PCR primer system as previously described.(14) The mice used were at least 8 weeks old. All animal studies were reviewed and approved by the Emory University Institutional Animal Care and Use Committee.

Antibodies

The mAbs used for immunofluorescence detection of mouse cells on frozen sections included PE- and FITC-anti-Thy-1 (53-2.1, eBioscience, San Diego, CA), PE-anti-CD157 (BP-3, eBioscience), biotin-anti-VCAM-1 (429, BD Biosciences, San Diego, CA), PE-anti-CD11c (HL3, eBioscience), allophycocyanin- and FITC-anti-B220 (RA3-6B2, eBioscience), and unconjugated FDC-M1 (BD Biosciences). Biotinylated antibodies were detected using streptavidin conjugated to Alexa488 or Alexa647 (Invitrogen). Unconjugated primary rat antibodies were detected with biotin-anti-rat IgG (Invitrogen) followed by tyramide signal amplification (PerkinElmer, Waltham, MA). CXCL13 was detected with polyclonal goat anti-CXCL13 (R&D Systems, Minneapolis, MN) followed by horseradish peroxidase-conjugated anti-goat IgG (R&D Systems) and tyramide signal amplification.

Immunofluorescence staining of frozen sections

The small intestine and colon were excised, placed in cold PBS and opened longitudinally. For horizontal sections of the small intestine or colon, three small sheets of tissue (approximately 15 x 20 mm) were stacked and covered with TissueTek OCT freezing medium (VWR Scientific, Randor, PA). Swiss rolls of small intestine or colon were prepared for vertical sections. PPs were excised from surrounding tissue and blocked separately. The tissue blocks were quickly frozen in cold 2-methylbutane on dry ice. Frozen sections of 6 μm thickness were cut with a cryostat, air dried overnight, and fixed for 10 min in acetone at -20°C . Endogenous peroxidase activity was quenched with 0.3% H_2O_2 in PBS for 30 min at 37°C . Sections were rinsed with PBS and blocked with TNB buffer (PerkinElmer). To obtain optimal staining results when staining intestinal

tissues for the soluble chemokine CXCL13, the tissue was fixed in situ by perfusion of mice with 3 ml of PBS, followed by 5 ml of 4% paraformaldehyde and then 3 ml of 5% sucrose as previously described.(15)

Quantitative analysis of CP and ILF development

CPs and ILFs in mice were quantitated by counting the number of intestinal lymphoid aggregates on H&E or anti-B220 stained sections and using ImageJ software (<http://rsb.info.nih.gov/ij/>) to calculate their density (expressed as aggregates per cm² of crypt lamina propria area) and the area of individual aggregates. In some experiments the observed lymphoid aggregates were also assigned to 1 of 6 classes based on size (Class I: < 5000 μm²; Class II: 5000-10,000 μm²; Class III: 10,000-15,000μm²; Class IV: 15,000-20,000 μm²; Class V: 20,000-50,000 μm²; Class VI: > 50,000 μm²), as previously described.(8, 12)

In utero treatment of mice with LTβR-Ig

To generate mice without PPs that develop increased numbers of intestinal ILFs postnatally, timed pregnant C57BL/6 RANKL^{+/-} mice, which had been mated to C57BL/6 RANKL^{-/-} mice, were injected i.v. with purified human LTβR-Ig fusion protein as described previously.(13) Injections of 100 μg of LTβR-Ig were given on embryonic days 14 and 16. The RANKL^{+/-} and RANKL^{-/-} offspring were sacrificed at 8 weeks of age and tissue from the small intestine was analyzed. In all of the in utero treated mice, the absence of PPs was verified by gross examination.

Recombinant mouse RANKL

A fusion protein of GST and mouse RANKL (137-316) was generated using a bacterial expression construct as previously described.(16) The GST-RANKL fusion protein was administered to RANKL null mice by initial i.p. and s.c. injections of 100 µg of GST-RANKL followed by s.c. injections of 100 µg per day for the next 4 days. Recombinant GST prepared from empty pGEX-5X-1 vector was used as a control for GST-RANKL.

Statistical analysis

Differences between the mean values for groups were analyzed by either two-tailed ANOVA (for multiple groups) or two-tailed Student's t-test as calculated using Prism (GraphPad Software, San Diego, CA). A p value of less than 0.01 was considered significant.

Results

The small intestine of RANKL^{-/-} mice has a reduced density of CPs with decreased size

CPs can be easily identified in sections from the small intestine by staining for Thy-1-expressing LTi cells. The mean density of small CP-sized aggregates in the pericryptal lamina propria of control mice was 19.5 aggregates per cm², with no difference in density between the jejunum and ileum. In RANKL^{-/-} mice, the overall density of CPs was significantly reduced (Figure 1A and B) to 4.8 aggregates per cm². In addition, the density of CPs in RANKL^{-/-} mice was higher in the distal small intestine compared to the proximal small intestine (Figure 1B). CPs from RANKL^{-/-} mice were also smaller compared to CPs in control mice (Figure 1C). Control small intestinal CPs had a mean area of 21,626 μm², while CPs in RANKL^{-/-} mice averaged just 5410 μm², or approximately a 4-fold decrease.

RANKL^{-/-} mice do not develop B cell-containing ILF

Surprisingly, all of the small intestinal lymphoid aggregates observed in the RANKL^{-/-} mice lacked B cells (Figure 2A). Because no small intestinal lymphoid aggregates aside from PPs contained B cells in RANKL^{-/-} mice, all non-PP lymphoid aggregates in RANKL^{-/-} mice can be classified as CPs. To further assess the apparent size difference of CPs between control and RANKL^{-/-} mice, a classification system for SILT based on their cross-sectional area originally developed by Pabst et al.(12) was applied to the analysis of small intestinal lymphoid aggregates from RANKL^{-/-} and control mice. Both class I and II SILT are typically CPs with few, if any, B220⁺ cells. Classes III, IV,

and V have progressively larger B220⁺ clusters and can be deemed immature ILFs. Mature ILFs with full-sized B cell follicles typically fall into the Class VI category. While the SILT structures in control mice showed the expected degree of diversity and were distributed amongst all 6 classes, 80% of the RANKL^{-/-} aggregates fell into Class I and Class II, consistent with most of these structures being small CPs (Figure 1C). The RANKL^{-/-} aggregates falling into Classes III, IV, and V, which are typically the immature ILF classes, lacked B cells and therefore do not qualify as ILFs. Even the largest lymphoid aggregates in the RANKL^{-/-} mice that filled up an entire villus contained no B cells (Figure 2B). The classification of 20% of the lymphoid aggregates from RANKL^{-/-} mice as Class III to V based solely on their area points out the ability of these CPs to expand without attracting B cells.

In utero LTβR-Ig treatment fails to restore ILF development in RANKL^{-/-} mice

Because ILF development is dependent on the status of the commensal gut flora, most conventionally housed mice on a C57BL/6 background fail to develop large numbers of ILFs. ILF development in wild type mice can be enhanced by in utero treatment with LTβR-Ig, which blocks formation of PPs leading to a compensatory increase in the number of ILFs.(13, 17) Pregnant RANKL^{+/-} female mice which had been bred with RANKL^{-/-} male mice were treated with LTβR-Ig. The resultant RANKL^{-/-} and control RANKL^{+/-} offspring lacked PPs, indicating the treatment successfully blocked PP development. Similar to previous studies(17), in utero LTβR-Ig treatment of RANKL^{+/-} mice resulted in a 3-fold increase in the number of aggregates (Figure 3A). These aggregates included a high percentage of ILFs that had a greater average size than

aggregates in untreated mice (Figure 3B). This increase skewed the distribution of lymphoid aggregates, with an increased number of Class IV to VI structures (Figure 3C). However, the RANKL^{-/-} mice showed no increase in the number of small intestinal lymphoid aggregates after in utero LTβR-Ig treatment (Figure 3A). The aggregates present in the LTβR-Ig treated RANKL^{-/-} mice were not increased in size compared to untreated RANKL^{-/-} mice (Figure 3B and C) and still lacked any B cells (data not shown).

RANKL^{-/-} mice develop colonic aggregates that include B cell follicles

Previous studies on CP and ILF development have largely focused on either the small intestine or the colon, rather than comparing formation of these lymphoid aggregates in both tissues. We investigated whether the defects in CP and ILF development found in the small intestine of RANKL^{-/-} mice were also present in the colon. The colonic lamina propria in RANKL^{-/-} and littermate control mice had a similar density of Thy-1⁺ clusters (Figure 4A and B). On average RANKL^{-/-} colonic aggregates were roughly one third of the size of control colonic aggregates, with an average area of 27,954 μm² compared to 84,160 μm², respectively. Assigning these aggregates to Classes I-VI using the SILT classification revealed that the smaller classes of aggregates (Class II-IV) were increased in frequency at the expense of the Class VI aggregates. Despite the smaller average size of colonic lymphoid aggregates in RANKL^{-/-} mice, these aggregates had a frequency of B220⁺ cells similar to colonic lymphoid aggregates in control mice (Figure 4C). The colonic ILFs in RANKL^{-/-} mice included some mature ILFs covered by

a follicle-associated epithelium, demonstrating that the full spectrum of ILF development can be completed in the colon in the absence of RANKL.

The density and distribution of CD11c⁺ cells are not perturbed in RANKL^{-/-} CP

CD11c⁺ dendritic cells account for 20-30% of the cells in the small intestinal CP of adult mice (7). These CD11c⁺ cells are concentrated at the border of CPs, with the Thy-1⁺ LTi cells predominating centrally.(7, 18) During the postnatal development of CP, clusters of CD11c⁺ cells associate with CP before the influx of B cells to generate ILF begins.(19) We examined the distribution of CD11c⁺ cells in RANKL^{-/-} CPs to ascertain whether a failure to recruit normal numbers of CD11c⁺ cells or a perturbation in the distribution of CD11c⁺ cells might be a contributor to the failure of RANKL^{-/-} CPs to progress to ILF development. CPs in adult RANKL^{-/-} mice had a density and distribution of CD11c⁺ cells that was unchanged from CPs in control mice (Figure 5).

CXCL13 is not expressed within CPs in the small intestine of RANKL^{-/-} mice

CXCL13 is a chemokine expressed by stromal cells in organized lymphoid structures including CPs and ILFs that plays a critical role in the recruitment of B cells.(20) Intestinal tissue from RANKL^{-/-} mice and controls was stained with antibodies to CXCL13. In control mice, CXCL13 was found on stromal cells in all B cell follicles in the gut, including both small intestinal and colonic aggregates (Figure 6). In RANKL^{-/-} mice, CXCL13 was not detected in RANKL^{-/-} small intestinal aggregates (Figure 6A),

but remained present in the colonic lymphoid aggregates that contained B cell-containing follicles (Figure 6B).

Stromal cells in small intestinal CPs from RANKL^{-/-} mice fail to express several LTβR-dependent stromal cell antigens

We previously reported that all CPs in wild type mice include stromal cells that express FDC-M1, VCAM-1, and CD157.(13) While all CPs in the RANKL^{-/-} small intestine included FDC-M1⁺ stromal cells, most of these CPs did not include any stromal cells expressing VCAM-1 or CD157 (Figure 7A). None of the small intestinal CPs from RANKL^{-/-} mice examined had both VCAM-1⁺ and CD157⁺ stromal cells, the pattern found in all control CPs. In 84% of the CPs from RANKL^{-/-} mice, no stromal cell expression of VCAM-1 or CD157 was detected. In the other 16% of CPs, only CD157⁺ stromal cells were found. In contrast with the stromal cell abnormalities observed in small intestinal CPs from RANKL^{-/-} mice, colonic lymphoid aggregates from RANKL^{-/-} mice and control mice contained stromal cells expressing VCAM-1 and CD157 to the same extent as in small intestinal CPs and ILFs from control mice (Figure 7B). To determine if the altered pattern of stromal cell antigen expression in the small intestinal CPs of RANKL^{-/-} mice could be corrected by providing an exogenous source of RANKL, RANKL^{-/-} mice were treated with 100 µg of GST-RANKL for 5 days. While this treatment was previously shown to be sufficient to restore M cell differentiation in the PPs of RANKL^{-/-} mice,(16) it failed to normalize stromal cell antigen expression in the small intestinal CPs or bring about recruitment of B cells into the CPs (data not shown).

Discussion

The early stages of lymphoid tissue development involve exchange of a series of cytokine-mediated signals between LT_i cells and lymphoid tissue organizer cells.

RANKL has a critical role in these interactions as evidenced by the complete absence of lymph nodes in RANKL deficient mice.(2, 3) Not all secondary lymphoid tissues fail to develop in the absence of RANKL. Intestinal PPs are present in RANKL^{-/-} mice, although they are smaller and exhibit a profound deficiency in the formation of M cells.(16) The contribution of RANKL to the development of the organized lymphoid tissues of the intestine that develop postnatally (i.e. CPs and ILFs) has not been previously examined.

The absence of RANKL results in multiple abnormalities in CP and ILF development in the small intestine, but does not compromise development of these structures in the colon. Small intestinal CPs from RANKL^{-/-} mice are both fewer in number and smaller compared to CPs from wild type mice. Furthermore, the CPs that remain in the small intestine of RANKL^{-/-} mice do not include any B cells and no ILFs form in the small intestine. Even when in utero LT β R-Ig treatment was used as a stimulus to enhance the extent of postnatal ILF development, no small intestinal ILF development was observed in RANKL^{-/-} mice. In contrast, colonic CPs from RANKL^{-/-} mice were present at a normal density and are capable of maturing into ILFs. The development of colonic ILFs but not small intestinal ILFs in RANKL^{-/-} mice demonstrates that ILF development is differentially regulated in the small intestine and colon.

The most striking feature of the RANKL^{-/-} small intestinal CPs was the complete absence of any B cell clusters within these CPs. Our results indicate that loss of CXCL13 expression in the stroma of the CPs may be a pivotal factor in the inability of these structures to recruit and incorporate B cells allowing maturation into ILFs. CXCL13 has been identified as an important factor in the initiation of lymphoid tissue development by virtue of its ability to attract LT_i cells to sites of lymphoid organogenesis.(21-23) In embryonic lymph node development, stimulation of neurons elicits retinoic acid production leading to CXCL13 expression by lymph node organizer cells, thus triggering the initial formation of the lymph node anlagen without a requirement for LT- α .(24) CXCL13 also contributes to the formation of B cell follicles in nasopharynx-associated lymphoid tissue and omental milky spots.(25) (26) Intestinal CPs and ILFs also depend on CXCL13 for B cell recruitment and maturation into ILFs. CXCL13^{-/-} mice have normal numbers of CPs, but lack B220⁺ ILFs, thus showing the dependence on CXCL13 for the accumulation and organization of B cells, but not the initial development of CPs.(19) Knocking out the CXCR5 receptor for CXCL13 results in a similar phenotype: CXCR5^{-/-} mice lack mature ILFs, although some aggregates still have a limited number of B cells.(8) Increasing the local concentration of CXCL13 through transgenic expression by gut epithelial cells results in an increase in B cell accumulation and ILF development in the jejunum and ileum.(27) Although the overexpression of CXCL13 in these mice also increased the number of ROR γ ⁺ LT_i cells, there was no increase in the absolute number of intestinal aggregates. The conspicuous absence of CXCL13 in small intestinal aggregates in RANKL^{-/-} mice reveals that expression of CXCL13 by stromal cells in small intestinal CPs is dependent on RANKL. This dependency does not extend to

colonic lymphoid aggregates from the RANKL^{-/-} mice, since CXCL13 expression is maintained and ILFs still develop.

The requirement for RANKL to achieve CXCL13 expression in small intestinal CPs may be a consequence of RANKL's demonstrated ability to promote LT $\alpha_1\beta_2$ expression. During the fetal development of lymph nodes, RANKL is not required for the earliest steps in lymph node development. Instead RANKL participates in a positive feedback loop involving LT $\alpha_1\beta_2$ that is required for lymph node development to continue.(28) CP development is thought to closely resemble fetal lymph node development in many respects and CPs also contain ROR γ^+ LTi cells.(29, 30) RANKL is also not required for the initial step in CP development, as RANKL^{-/-} mice still have some CPs, although the reduced number of CPs in RANKL^{-/-} mice reveals RANKL is an important factor in achieving full CP development. Growth of developing CPs relies on the continued crosstalk between LTi cells, which express RANKL and CXCR5, and VCAM-1⁺ organizer cells that express RANK and CXCL13 upon LT β R signaling.(31, 32) Decreased LT $\alpha_1\beta_2$ expression caused by absence of RANKL may lead to loss of CXCL13 expression, which in turn inhibits further CP development and prevents their maturation into ILFs.

Our results also show the small intestinal CPs that develop in RANKL^{-/-} mice fail to express stromal antigens such as VCAM-1 and CD157 that are normally present on the stroma of CPs in wild type mice.(13) In previous studies, we showed that *aly/aly* mice lacking functional NF- κ B-inducing kinase (NIK) or wild type mice in which LT $\alpha_1\beta_2$ signaling was blocked with LT β R-Ig also had defective stromal antigen expression in CPs, failing to express VCAM-1, CD157, and FDC-M1, but retaining RANKL

expression. The CPs from the *aly/aly* mice also failed to develop into ILFs. In aggregate, these findings point to a requirement in the small intestine for multiple factors including RANKL and $LT\alpha_1\beta_2$ for normal stromal cell differentiation in CPs and the development of ILFs from these CPs.

A major difference between the small intestine and the colon is the increase in the density of the commensal flora in the colon. Although signals derived from the enteric microflora are not required for CP development, commensal bacteria influence the size of CPs as germ-free wild type mice were found to have smaller CPs.(12) Sensing of the enteric microflora by NOD1 was identified as a critical signal driving the differentiation of CPs into immature ILFs.(33) While RANKL^{-/-} mice are normally colonized by gut commensals, we previously showed they have less than 2% of the normal number of antigen-sampling M cells compared to wild type mice.(16) This profound M cell deficit in RANKL^{-/-} mice likely results in decreased antigen-sampling of the commensal flora, thereby impairing the NOD1-initiated differentiation of CPs into immature ILFs. Follicular dendritic cells isolated from PP have the capacity to respond directly to environmental stimuli including retinoic acid and intestinal bacteria by increasing production of both CXCL13 and BAFF(34), indicating that stromal cells are able to directly sense the presence of the commensal enteric flora. In wild type mice, the density of CPs is relatively uniform in different portions of the small intestine despite a gradient in the density of the enteric microflora between the proximal and distal end. The increase in the density of CPs in the distal small intestine of RANKL^{-/-} mice compared to the proximal small intestine parallels the increase in the density of the commensal flora. The proximal to distal gradient of CP density in the small intestine of RANKL^{-/-} mice and the

lack of stromal CXCL13 expression suggest that the density of the commensal flora has the potential to influence the extent of CP development in the small intestine, but this effect is normally overridden by the contribution of other signals. In the colon, the density of the commensal flora may be high enough that direct induction of CXCL13 expression on stromal cells in lymphoid aggregates is sufficient to override the requirement for RANKL evident in the small intestine. The contribution of RANKL to colonic lymphoid aggregate development is limited to influencing the extent of B cell recruitment and the final size attained by ILFs.

In summary, we have shown that the development of ILFs from precursor CPs in the small intestine is dependent upon RANKL for the expression of CXCL13. Surprisingly, this requirement for RANKL for ILF development did not extend to colonic lymphoid aggregates. The differential dependence on RANKL for development of lymphoid structures in the small intestine and colon suggests that other molecules involved in CP and ILF development may also be differentially utilized between these tissues. These observations reveal a new role for RANKL in CP and ILF formation and clearly illustrate that the molecular pathways that contribute to the initiation and maturation of these lymphoid aggregates are not identical in the small intestine and colon.

Acknowledgements

This work was supported by grants from the National Institutes of Health (DK64730 to I.R.W. and DK64399 supporting the Imaging Core Facility of the Emory Digestive Diseases Research Development Center) and the Crohn's & Colitis Foundation of America (Senior Research Award to I.R.W.).

References

1. Mebius RE. Organogenesis of lymphoid tissues. *Nat Rev Immunol.* 2003;3(4):292-303.
2. Kong YY, Yoshida H, Sarosi I, Tan HL, Timms E, Capparelli C, et al. OPGL is a key regulator of osteoclastogenesis, lymphocyte development and lymph-node organogenesis. *Nature.* 1999;397(6717):315-23.
3. Yoshida H, Naito A, Inoue J, Satoh M, Santee-Cooper SM, Ware CF, et al. Different cytokines induce surface lymphotoxin-ab on IL-7 receptor-a cells that differentially engender lymph nodes and Peyer's patches. *Immunity.* 2002;17(6):823-33.
4. Ruddle NH, Akirav EM. Secondary lymphoid organs: responding to genetic and environmental cues in ontogeny and the immune response. *J Immunol.* 2009;183(4):2205-12.
5. Roozendaal R, Mebius RE. Stromal Cell–Immune Cell Interactions. *Annu Rev Immunol.* 2011;29(1).
6. Taylor RT, Williams IR. Lymphoid organogenesis in the intestine. *Immunol Res.* 2005;33(2):167-82.
7. Kanamori Y, Ishimaru K, Nanno M, Maki K, Ikuta K, Nariuchi H, et al. Identification of novel lymphoid tissues in murine intestinal mucosa where clusters of c-kit+ IL-7R+ Thy1+ lympho-hemopoietic progenitors develop. *J Exp Med.* 1996;184(4):1449-59.
8. Velaga S, Herbrand H, Friedrichsen M, Jiong T, Dorsch M, Hoffmann MW, et al. Chemokine receptor CXCR5 supports solitary intestinal lymphoid tissue formation, B cell homing, and induction of intestinal IgA responses. *J Immunol.* 2009;182(5):2610-9.
9. Lorenz RG, Newberry RD. Isolated lymphoid follicles can function as sites for induction of mucosal immune responses. *Ann N Y Acad Sci.* 2004;1029:44-57.

10. Pabst O, Herbrand H, Worbs T, Friedrichsen M, Yan S, Hoffmann MW, et al. Cryptopatches and isolated lymphoid follicles: dynamic lymphoid tissues dispensable for the generation of intraepithelial lymphocytes. *Eur J Immunol.* 2005;35(1):98-107.
11. Lorenz RG, Chaplin DD, McDonald KG, McDonough JS, Newberry RD. Isolated lymphoid follicle formation is inducible and dependent upon lymphotoxin-sufficient B lymphocytes, lymphotoxin b receptor, and TNF receptor I function. *J Immunol.* 2003;170(11):5475-82.
12. Pabst O, Herbrand H, Friedrichsen M, Velaga S, Dorsch M, Berhardt G, et al. Adaptation of solitary intestinal lymphoid tissue in response to microbiota and chemokine receptor CCR7 signaling. *J Immunol.* 2006;177(10):6824-32.
13. Taylor RT, Patel SR, Lin E, Butler BR, Lake JG, Newberry RD, et al. Lymphotoxin-independent expression of TNF-related activation-induced cytokine by stromal cells in cryptopatches, isolated lymphoid follicles, and Peyer's patches. *J Immunol.* 2007;178(9):5659-67.
14. Kim D, Mebius RE, MacMicking JD, Jung S, Cupedo T, Castellanos Y, et al. Regulation of peripheral lymph node genesis by the tumor necrosis factor family member TRANCE. *J Exp Med.* 2000;192(10):1467-78.
15. Dauner JG, Chappell CP, Williams IR, Jacob J. Perfusion fixation preserves enhanced yellow fluorescent protein and other cellular markers in lymphoid tissues. *Journal of Immunological Methods.* 2009;340(2):116-22.
16. Knoop KA, Kumar N, Butler BR, Sakthivel SK, Taylor RT, Nochi T, et al. RANKL is necessary and sufficient to initiate development of antigen-sampling M cells in the intestinal epithelium. *J Immunol.* 2009;183(9):5738-47.
17. Newberry RD, McDonough JS, McDonald KG, Lorenz RG. Postgestational lymphotoxin/lymphotoxin b receptor interactions are essential for the presence of intestinal B lymphocytes. *J Immunol.* 2002;168(10):4988-97.

18. Luger A, Kucharzik T, Soler D, Picarella D, Hudson JT, 3rd, Williams IR. Lymphoid precursors in intestinal cryptopatches express CCR6 and undergo dysregulated development in the absence of CCR6. *J Immunol.* 2003;171(5):2208-15.
19. McDonald KG, McDonough JS, Dieckgraefe BK, Newberry RD. Dendritic Cells Produce CXCL13 and Participate in the Development of Murine Small Intestine Lymphoid Tissues. *Am J Pathol.* 2010;176(5):2367-77.
20. Ohl L, Henning G, Krautwald S, Lipp M, Hardtke S, Bernhardt G, et al. Cooperating mechanisms of CXCR5 and CCR7 in development and organization of secondary lymphoid organs. *J Exp Med.* 2003;197(9):1199-204.
21. Honda K, Nakano H, Yoshida H, Nishikawa S, Rennert P, Ikuta K, et al. Molecular basis for hematopoietic/mesenchymal interaction during initiation of Peyer's patch organogenesis. *J Exp Med.* 2001;193(5):621-30.
22. Finke D, Acha-Orbea H, Mattis A, Lipp M, Kraehenbuhl J. CD4+CD3- cells induce Peyer's patch development: role of $\alpha 4\beta 1$ integrin activation by CXCR5. *Immunity.* 2002;17(3):363-73.
23. Luther SA, Ansel KM, Cyster JG. Overlapping Roles of CXCL13, Interleukin 7 Receptor α , and CCR7 Ligands in Lymph Node Development. *J Exp Med.* 2003;197(9):1191-8.
24. van de Pavert SA, Olivier BJ, Goverse G, Vondenhoff MF, Greuter M, Beke P, et al. Chemokine CXCL13 is essential for lymph node initiation and is induced by retinoic acid and neuronal stimulation. *Nat Immunol.* 2009;10(11):1193-9.
25. Rangel-Moreno J, Moyron-Quiroz J, Kusser K, Hartson L, Nakano H, Randall TD. Role of CXC chemokine ligand 13, CC chemokine ligand (CCL) 19, and CCL21 in the organization and function of nasal-associated lymphoid tissue. *J Immunol.* 2005;175(8):4904-13.
26. Rangel-Moreno J, Moyron-Quiroz JE, Carragher DM, Kusser K, Hartson L, Moquin A, et al. Omental Milky Spots Develop in the Absence of Lymphoid Tissue-Inducer Cells and Support B and T Cell Responses to Peritoneal Antigens. *Immunity.* 2009;30(5):731-43.

27. Marchesi F, Martin AP, Thirunarayanan N, Devany E, Mayer L, Grisotto MG, et al. CXCL13 expression in the gut promotes accumulation of IL-22-producing lymphoid tissue-inducer cells, and formation of isolated lymphoid follicles. *Mucosal Immunol.* 2009;2(6):486-94.
28. Vondenhoff MF, Greuter M, Goverse G, Elewaut D, Dewint P, Ware CF, et al. LTbR signaling induces cytokine expression and up-regulates lymphangiogenic factors in lymph node anlagen. *J Immunol.* 2009;182(9):5439-45.
29. Eberl G, Marmon S, Sunshine MJ, Rennert PD, Choi Y, Littman DR. An essential function for the nuclear receptor RORgamma(t) in the generation of fetal lymphoid tissue inducer cells. *Nat Immunol.* 2004;5(1):64-73.
30. Eberl G. Inducible lymphoid tissues in the adult gut: recapitulation of a fetal developmental pathway? *Nat Rev Immunol.* 2005;5(5):413-20.
31. Katakai T, Suto H, Sugai M, Gonda H, Togawa A, Suematsu S, et al. Organizer-like reticular stromal cell layer common to adult secondary lymphoid organs. *J Immunol.* 2008;181(9):6189-200.
32. Suto H, Katakai T, Sugai M, Kinashi T, Shimizu A. CXCL13 production by an established lymph node stromal cell line via lymphotoxin-beta receptor engagement involves the cooperation of multiple signaling pathways. *Int Immunol.* 2009;21(4):467-76.
33. Bouskra D, Brezillon C, Berard M, Werts C, Varona R, Boneca IG, et al. Lymphoid tissue genesis induced by commensals through NOD1 regulates intestinal homeostasis. *Nature.* 2008;456(7221):507-10.
34. Suzuki K, Maruya M, Kawamoto S, Sitnik K, Kitamura H, Agace WW, et al. The Sensing of Environmental Stimuli by Follicular Dendritic Cells Promotes Immunoglobulin A Generation in the Gut. *Immunity.* 2010;33(1):71-83.

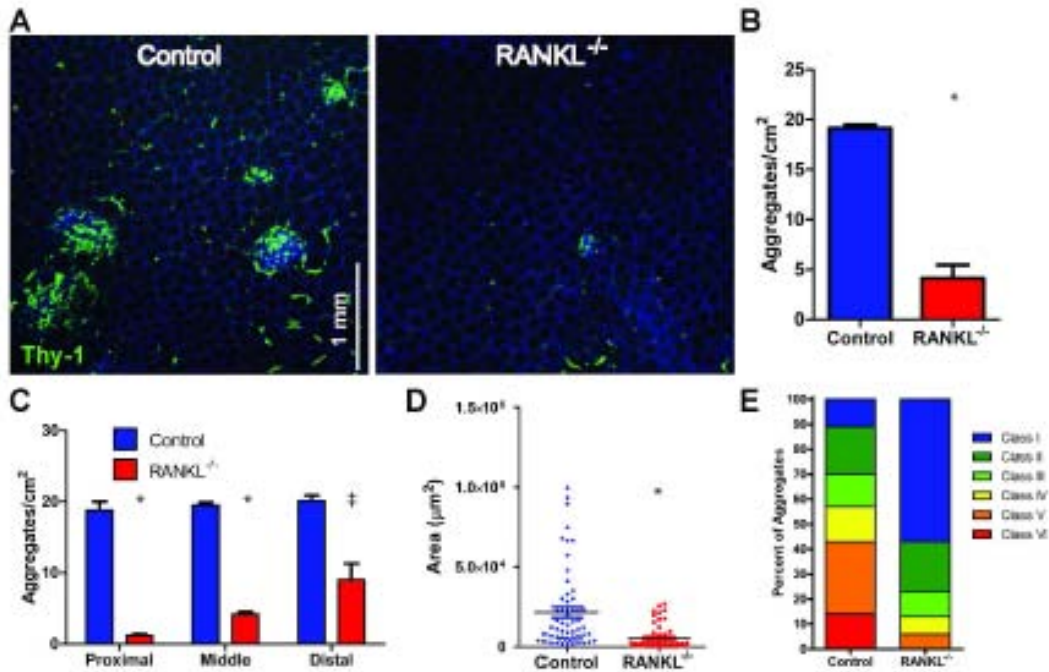


Figure 1. Cryptopatches are less frequent and smaller in the small intestine of RANKL^{-/-} mice. (a) Horizontal sections of the pericryptal lamina propria in the distal ileum from RANKL^{-/-} mice and littermate controls were stained with anti-Thy-1 and DAPI. Scale bar, 1 mm. (b) RANKL^{-/-} mice had a reduced density of small intestinal lymphoid aggregates. (c) The reduction in the mean density of small intestinal lymphoid aggregates in RANKL^{-/-} mice was greatest in the proximal small intestine (proximal = 0-10 cm; middle = 10-20 cm; distal = beyond 20 cm). (d) The average size of small intestinal lymphoid aggregates was reduced in RANKL^{-/-} mice. (e) Divided bar graph depicting the size distribution of small intestinal lymphoid aggregates in RANKL^{-/-} and control mice by assigning them to 1 of 6 previously described classes based on their size. (10) This analysis used 3 RANKL^{-/-} mice on a C57BL/6 background and 2 RANKL^{-/-} mice on an F1 equivalent background with a matched number of littermate controls. *, $p \leq 0.001$; ‡, $p \leq 0.01$ (compared to control mice by t-test).

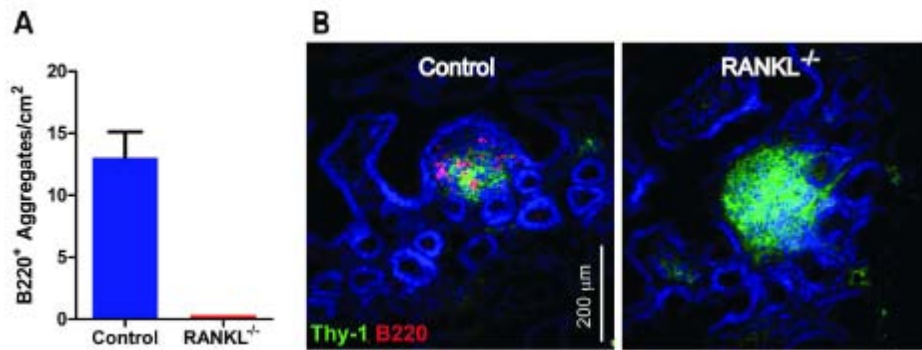


Figure 2. Cryptopatches in the small intestine of $RANKL^{-/-}$ mice do not contain any B cells. (a) Density of lymphoid aggregates containing $B220^{+}$ cells in the small intestine of $RANKL^{-/-}$ and littermate control mice. (b) Horizontal sections of the pericryptal lamina propria in the distal ileum were stained with anti-Thy-1, anti-B220, and DAPI. Representative images show that $B220^{+}$ cells were absent in all of the $RANKL^{-/-}$ lymphoid aggregates. Scale bar, 200 μm . This analysis used 3 $RANKL^{-/-}$ mice on a C57BL/6 background and 2 $RANKL^{-/-}$ mice on an F1 equivalent background with a matched number of littermate controls.

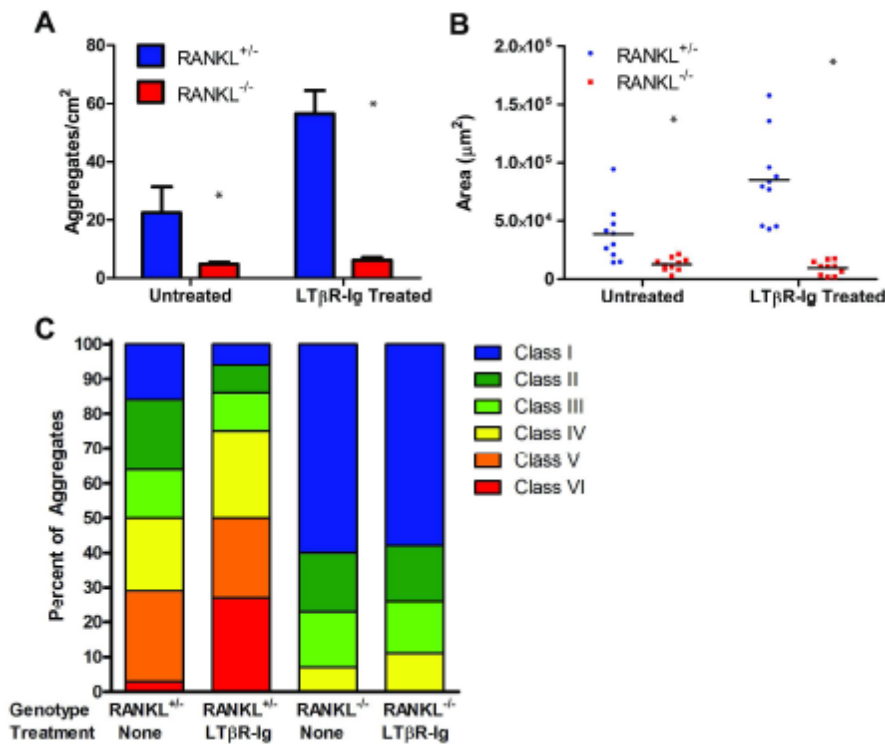


Figure 3. In utero LTβR-Ig treatment does not restore isolated lymphoid follicle development in the small intestine of RANKL^{-/-} mice. In utero LTβR-Ig treatment increased both the density (a) and average size of lymphoid aggregates (b) in RANKL^{+/-} mice, but the density and size of the aggregates were not increased in RANKL^{-/-} mice. (c) Divided bar graph depicting the size distribution of small intestinal lymphoid aggregates shows the shift to larger classes after LTβR-Ig treatment in RANKL^{+/-} mice, but not RANKL^{-/-} mice. This analysis used 3 mice of each genotype on a C57BL/6 background. *, p ≤ 0.001 (compared to RANKL^{+/-} mice by ANOVA).

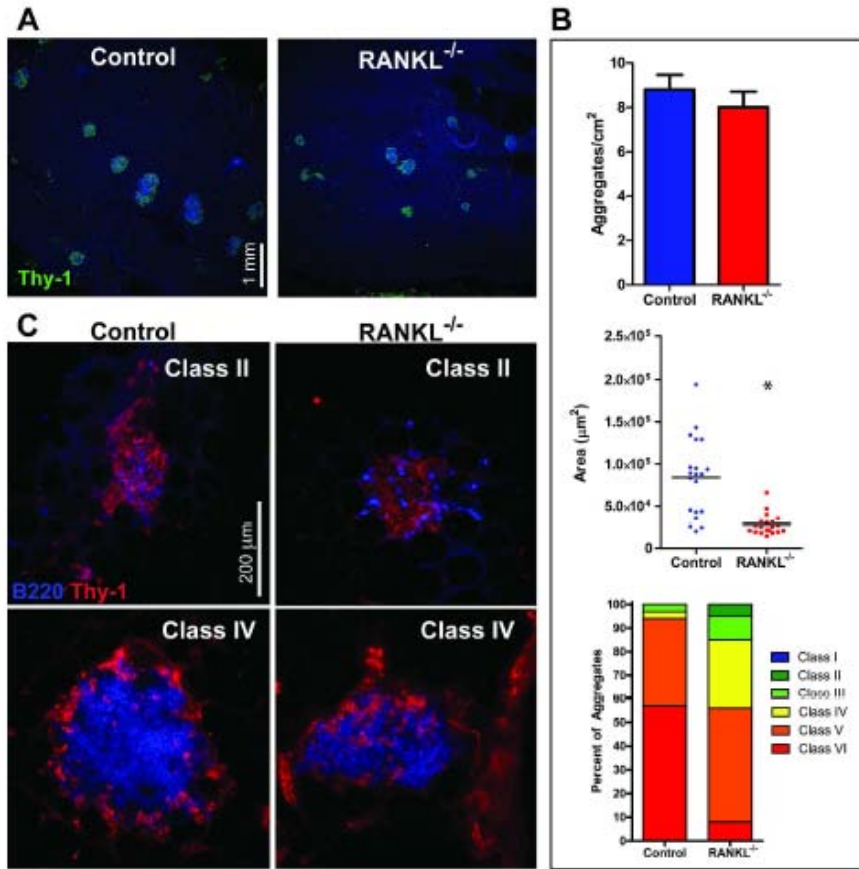


Figure 4. Colonic lymphoid aggregates in $RANKL^{-/-}$ mice include B cell follicles. (a) Horizontal sections of colon were stained with anti-Thy-1 and DAPI revealing a similar density of lymphoid aggregates in $RANKL^{-/-}$ and littermate control mice. Scale bar, 1 mm. (b) The density of colonic lymphoid aggregates in $RANKL^{-/-}$ mice was not significantly different from control mice, but the average size of the lymphoid aggregates was significantly reduced. (c) Representative images of Class II and Class IV lymphoid aggregates show that follicles of $B220^{+}$ cells were present in both the lymphoid aggregates of both $RANKL^{-/-}$ and control mice. Scale bar, 200 μm . This analysis used 3 $RANKL^{-/-}$ mice on a C57BL/6 background and 2 $RANKL^{-/-}$ mice on an F1 equivalent background with a matched number of littermate controls. *, $p \leq 0.001$ (compared to control mice by t-test).

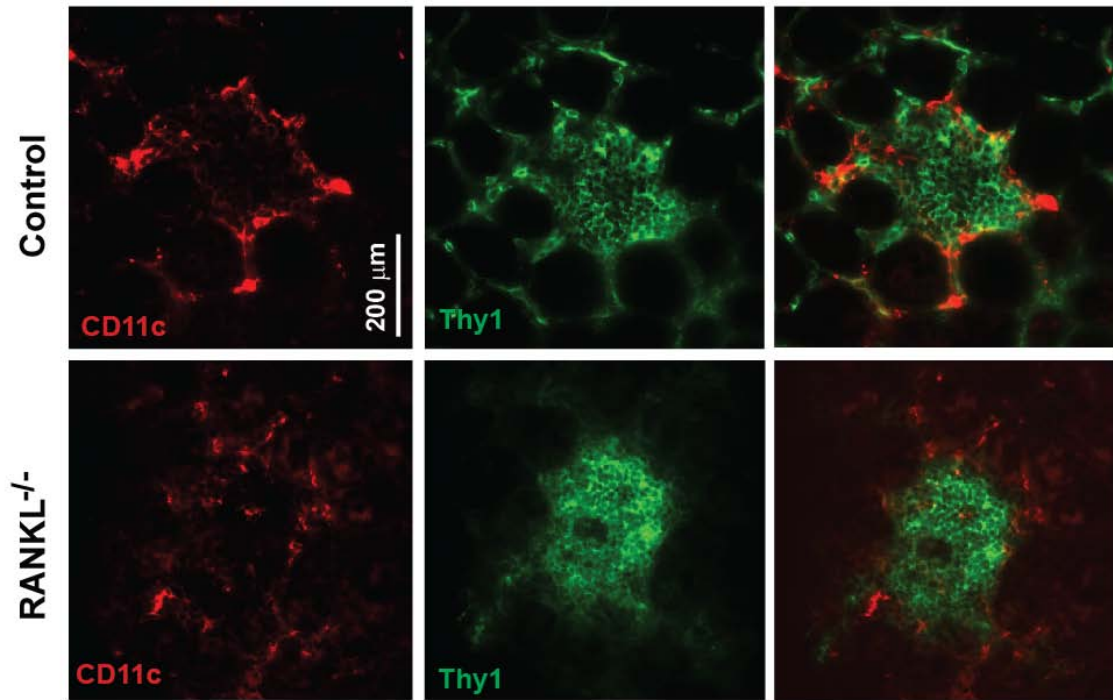


Figure 5. RANKL^{-/-} cryptopatches have a normal density and distribution of CD11c⁺ cells. Cryptopatches in horizontal sections of small intestine from RANKL^{-/-} and control small intestine were stained for Thy-1 and CD11c. The density and peripheral distribution of CD11c⁺ cells were similar in RANKL^{-/-} cryptopatches and control cryptopatches. Scale bar, 200 μm. The representative images shown are from a RANKL^{-/-} mouse on an F1 equivalent background and a littermate control, but similar results were obtained with 2 RANKL^{-/-} mice and controls on a C57BL/6 background.

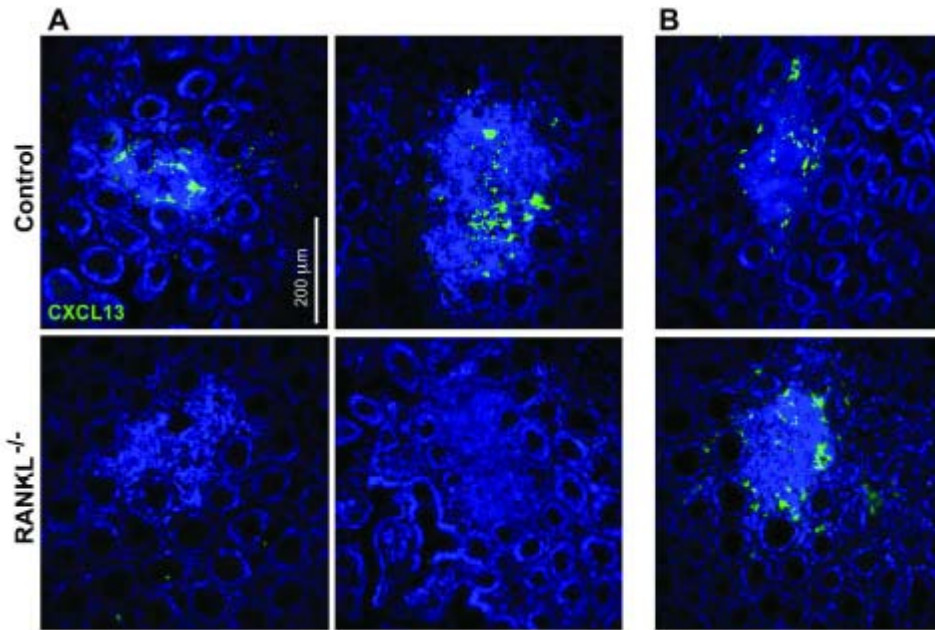


Figure 6. CXCL13-expressing cells are absent from small intestinal lymphoid aggregates in RANKL^{-/-} mice. Horizontal sections of small intestine (a) and colon (b) were stained for CXCL13 expression. Representative images demonstrate that CXCL13-expressing cells were only detected in the colon of RANKL^{-/-} mice. Scale bar, 200 μm. This analysis used 3 RANKL^{-/-} mice on an F1 equivalent background and 3 littermate controls.

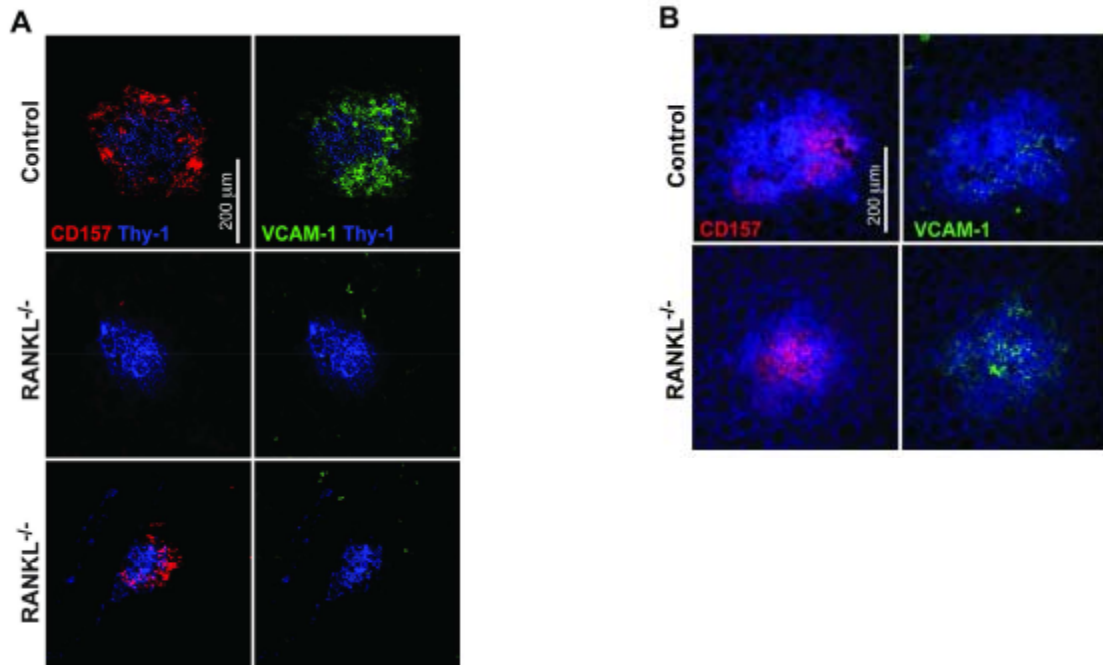


Figure 7. Stromal cells in small intestinal but not colonic cryptopatches from RANKL^{-/-} mice do not express several LTβR-dependent antigens. (a) Horizontal sections of small intestine stained for VCAM-1 and CD157 revealed that most RANKL^{-/-} cryptopatches lack expression of both of these antigens found on stromal cells in all cryptopatches in littermate control mice. Scale bar, 200 μm. (b) Horizontal sections of colon stained with anti-VCAM-1, anti-CD157 and DAPI showed all aggregates in RANKL^{-/-} mice and control mice included both VCAM-1⁺ and CD157⁺ stromal cells. Scale bar, 200 μm. This analysis used 5 RANKL^{-/-} mice on either a C57BL/6 or an F1 equivalent background and 5 littermate controls.

DISCUSSION

This body of work introduces a novel model of M cell development in which the major signal is derived from RANKL and secondary contributions may come from the enteric flora. This model proposes B cells have no direct role in M cell development, contrary to previous models. Instead, RANKL expressed on the stromal cells in the dome of the PP and ILFs directly stimulate the RANK⁺ epithelium. Moreover, the enteric flora can initiate villous M cell development alongside RANKL. Additionally, this work has shown a second role for RANKL in the development of gut lymphoid tissue in the development of cryptopatches and their transition into ILFs. RANKL has a more prominent role in the development of both gut lymphoid tissues and their antigen sampling function than previously shown.

Two important questions that have confounded the M cell field are: do M cells represent transdifferentiated enterocytes in a transient antigen-sampling state and what factors drive M cell development. Through the study of RANKL^{-/-} mice, recombinant RANKL, and neutralizing RANKL antibody, the second question has been unequivocally answered (Chapter 1). Under normal conditions, most RANKL in PP and ILF is expressed by stromal cells below the FAE. Hence M cell development is restricted to PP and ILF domes, though all of the small intestinal epithelium expresses RANK. Once RANKL is introduced into the system through injections of recombinant RANKL, all of the small intestinal epithelium is exposed to the protein, and M cells are induced from both normal crypts and follicle-associated crypts further proving the inductive capacity of RANKL in the development of M cells.

RANKL is important for the full development of two other epithelial cell types, medullary thymic epithelium and mammary epithelium. mTEC development is initiated upon ligation of the receptor, RANK, indicating RANKL acts directly upon these cells (93). Activation of RANK on mammary epithelial cells induces proliferation, and activates anti-apoptotic genes through NF- κ B signaling (98). It would stand to reason the RANKL/RANK has a similar effect on the gut epithelium, where RANKL directly binds RANK on the epithelium, and when ligated, RANK promotes cell survival, as the RANKL-RANK signaling drives the cell into an M cell.

Answering the first question, the results presented in Chapter 1 suggests M cells are a fully differentiated epithelial cell type and not a transient phase of enterocyte development. In RANKL^{-/-} mice treated with recombinant RANKL, the number of M cells is only restored to wild type levels after five days. Likewise villous M cells only fully cover the villi, reaching the tip, after four days of recombinant RANKL injections. Conversely, BALB/c mice treated with neutralizing antibody show a decrease in M cells after four days, with full depletion of M cells after 8 days (Chapter 1). Taken together, these results suggest M cells are differentiated cells that must be induced at the stem cell or transient amplifying cell level. To explain the lag time in the development of M cells after recombinant RANKL treatment, RANKL must signal to the cells in the crypts and the resultant M cells require a few days to travel up the dome or villi. If M cells were able to transdifferentiate from enterocytes, M cells would appear much quicker after RANKL injections as initial reports suggested enterocytes can flip into M cells as quickly as twelve hours (99). Removing RANKL from the system does not cause the M cells to revert into enterocytes. Instead it takes several days for the new epithelial cells, all

enterocytes differentiating without the M cell-inducing signals from RANKL, to replace the old M cell containing FAE.

Approximately 5-10% of the epithelium overlaying PP domes are M cells which are arranged in radial strips. This number is generally not increased in BALB/c mice after RANKL injections (data not shown), indicating the number of M cells on the PP dome is held constant. Correspondingly, after recombinant RANKL injections, roughly 5% of the small intestinal epithelium becomes M cells signifying that intestinal stem cells in every crypt, villous or follicle-associated, can potentially give rise to progeny that become M cells. It is unclear if this constant number of M cells is controlled by RANKL itself, or some other regulatory mechanism. Intestinal epithelial cells use mechanisms such as Notch signaling and lateral inhibition to ensure that specialized cells types do not dominate the epithelium (100). Stem cells could use similar mechanisms to ensure too much of the epithelium does not become M cells thus putting the host in jeopardy by dangerously increasing antigen uptake.

Traditionally the intestinal epithelial cells are divided into two categories, secretory and absorptive epithelial cells; absorptive epithelium only includes regular enterocytes. Paneth cells, goblet cells, and enteroendocrine cells are grouped together in the secretory group based on function and similar induction signals (48). Deciding where M cells fall into these categories will depend on what cell type they most resemble and which precursor cell M cells develop from during differentiation. Currently M cells are thought to most resemble absorptive enterocytes (59), though it is unknown if they share a common precursor, or when these cell types separate during differentiation. With the

use of RANKL, a large number of M cells can be induced to better study them at the cellular level to answer these questions.

Previously it was reported that B cell deficient mice had decreased number of M cells (55). We found that two models of B cell deficient mice, $J_H^{-/-}$ and μ MT mice, maintained a constant ratio of M cells developing on the PP dome as 5-10% of the FAE (Chapter 2). BALB/c mice have a density of 328 M cells per mm^2 , and this density is unchanged in B cell deficient mice with 326 and 323 M cells per mm^2 in $J_H^{-/-}$ and μ MT mice, respectively. The PPs of B cell deficient mice lack B cell follicles, so these mice have a shrunken and underdeveloped FAE. The smaller amount of FAE includes fewer M cells, accounting for the decreased absolute number of M cells in B cell deficient mice. We also looked at a novel model of acute B cell depletion, which involved >97% depletion of B cells from PP for over two weeks. These mice had a modest decrease in the number of M cells, but again maintained a density of 363 M cells per mm^2 demonstrating the presence of B cells is not required for the normal development of M cells. In all models of B cell deficiencies, both genetic and acute, RANKL expression on the subepithelial stromal cells is undisturbed, indicating B cells are not required for the expression of RANKL. This confirms RANKL, not B cells, is the critical factor for M cell development, and that B cells are not required for the maintenance of M cells.

It appears there are additional signals besides RANKL that contribute to the development of M cells as we consistently observed a trace number of residual UEA-I⁺ and GP2⁺ M cells in a few of the PP follicles in $\text{RANKL}^{-/-}$ mice (chapter 1). Interestingly the most distal PP in $\text{RANKL}^{-/-}$ mice was invariably the PP with the largest number of residual M cells per follicle, though the number of M cells found in the $\text{RANKL}^{-/-}$ distal

PP with the M cell marker GP2 found even fewer M cells implying most of these UEA-I⁺ cells in the distal PP of RANKL^{-/-} mice may be goblet cells or aggregates of adherent mucus. In addition, both J_H^{-/-} and μMT mice have increased PP M cells in the distal PPs (data not shown) suggesting that an increased density of luminal commensal bacteria can accentuate the extent of M cell differentiation locally. An increase in the number of M cells in the distal PP is also seen in cows (101), perhaps as a function to increase antigen uptake where there is more antigen to be sampled and more bacteria to monitor.

Unexpectedly B cell deficient mice also have an exaggerated increase in the density of villous M cells in the distal ileum, again where the density of bacteria is the greatest (Chapter 3). These proximal to distal gradients in the number of PP M cells or villous M cells are much less apparent or absent in wild type mice, which have a microflora that is tightly regulated through the homeostatic mechanisms of the mucosal immune system. Mice lacking AID have a 100-fold increase in anaerobes (102). The increased anaerobic bacteria could induce both the increased PP M cells and villous M cells in the distal ileum, characterizing an innate response of the epithelium enabling it respond to excessive bacterial loads by increasing antigen sampling in order to increase IgA production and restore the enteric flora to more controllable density. Interestingly, the development of these villous M cells is dependent on RANKL to some extent; further showing RANKL is a critical factor in intestinal M cell development, even when other factors are contributing to this development.

Other TNF family members may contribute to the induction of M cell differentiation and account for the low level of residual M cell formation in the absence of RANKL, given that TNF family members are known to have overlapping and partially

redundant functions in other developmental contexts (103). Cooperation of RANKL with the TNF family member CD40L has recently been established for the induction of mTEC differentiation (93, 94). A role for the TNF superfamily member CD137 in the maturation of M cells has been suggested (104).

Interesting parallels exist between the role of RANKL in inducing differentiation of UEA-I⁺ M cells in the FAE of PP and its role in inducing the differentiation of UEA-I⁺ mTEC in the thymus. The RANKL-induced mTECs are critical for establishment of central T cell tolerance, while RANKL-induced M cells contribute to the establishment of peripheral T cell tolerance to bacterial antigens at mucosal surfaces normally colonized by commensal bacteria. The role of RANKL in the transition of CPs into ILFs is also indicative of a contribution of RANKL to peripheral tolerance. Similar our model of M cell development, the data suggests signals from both RANKL and the commensal bacteria can drive small lymphoid aggregate development, through to differing degrees in the small and large intestine. CPs in the small intestine do develop in the absence of RANKL, though they are smaller and less frequent compared to wild type mice (chapter 5). Interestingly, CPs in RANKL^{-/-} mice develop in a gradient similar to M cells, increasing in density toward the distal ileum, suggesting that the density of the commensal flora also has the potential to influence the extent of CP development in the small intestine. The absence of RANKL, however, prevents the formation of B cell follicles within small lymphoid aggregates, halting the transition of CP to ILFs. This may be due to the lack of CXCL13 expression in small intestinal CPs from RANKL^{-/-} mice, and the subsequent lack of B cell recruitment to the aggregates. Surprisingly, RANKL is not required for the expression of CXCL13 and the development of ILF in the large

intestine where the density of the commensal flora may be high enough that direct induction of CXCL13 expression on stromal cells in lymphoid aggregates is sufficient to override the requirement for RANKL evident in the small intestine.

Development of both M cells and intestinal lymphoid aggregates depends on RANKL and the commensal bacteria, indicating RANKL has an important role in the maintenance of mucosal tolerance based on its contribution to normal antigen sampling mechanisms. These roles of RANKL can be seen in the distribution pattern of RANKL in the different stages of the lymphoid aggregates. In CPs, RANKL is found throughout the aggregates, necessary for the continual development of the aggregate along with the expression of CXCL13. As the follicle is developed, RANKL expression moves to the subepithelial dome, as it is no longer needed for the development of the aggregate, just the development of M cells. The restriction of RANKL to below the FAE ensures there is the proper amount of RANKL in the stimulation of M cells, yet keeping RANKL concentrations to a minimum in the area as it can be an extremely active cytokine involved in multiple processes. What controls the basal expression of RANKL by stromal cells in PPs and other organized intestinal lymphoid aggregates has yet to be determined. Still it is apparent that RANKL controls the continual development of M cells and ILFs that must occur throughout adulthood to maintain homeostasis with the changing enteric flora. These novel roles of RANKL outlined in this work show the potential contribution of RANKL to the development and maintenance of oral tolerance. A better appreciation of both M cell and ILF development and their connectedness can lead to the full understanding of the mucosal response and lead to improvements in the formulation of oral vaccines.

References Cited in Introduction and Discussion

1. Iweala OI, Nagler CR. Immune privilege in the gut: the establishment and maintenance of non-responsiveness to dietary antigens and commensal flora. *Immunol Rev.* 2006;213:82-100.
2. Hamada H, Hiroi T, Nishiyama Y, Takahashi H, Masunaga Y, Hachimura S, et al. Identification of multiple isolated lymphoid follicles on the antimesenteric wall of the mouse small intestine. *J Immunol.* 2002;168(1):57-64.
3. Fagarasan S, Honjo T. Regulation of IgA synthesis at mucosal surfaces. *Curr Opin Immunol.* 2004;16(3):277-83.
4. Pabst O, Bernhardt G, Forster R. The impact of cell-bound antigen transport on mucosal tolerance induction. *J Leukoc Biol.* 2007;82(4):795-800.
5. Macpherson AJ, Uhr T. Induction of protective IgA by intestinal dendritic cells carrying commensal bacteria. *Science.* 2004;303(5664):1662-5.
6. Macpherson AJ, McCoy KD, Johansen FE, Brandtzaeg P. The immune geography of IgA induction and function. *Mucosal Immunol.* 2008;1(1):11-22.
7. Kaetzel CS, Robinson JK, Chintalacheruvu KR, Vaerman JP, Lamm ME. The polymeric immunoglobulin receptor (secretory component) mediates transport of immune complexes across epithelial cells: a local defense function for IgA. *Proc Natl Acad Sci U S A.* 1991;88(19):8796-800.
8. Lycke N, Eriksen L, Holmgren J. Protection against Cholera Toxin after Oral Immunization is Thymus-Dependent and Associated with Intestinal Production of Neutralizing IgA Antitoxin. *Scandinavian Journal of Immunology.* 1987;25(4):413-9.
9. Tsuji NM, Kosaka A. Oral tolerance: intestinal homeostasis and antigen-specific regulatory T cells. *Trends in immunology.* 2008;29(11):532-40.

10. Andre C, Heremans J, Vaerman J, Cambiaso C. A mechanism for the induction of immunological tolerance by antigen feeding: antigen-antibody complexes. *Journal of Experimental Medicine*. 1975;142.
11. Mestecky J, Russell MW, Elson CO. Perspectives on Mucosal Vaccines: Is Mucosal Tolerance a Barrier? *The Journal of Immunology*. 2007;179(9):5633-8.
12. Fukuda K, Yoshida H, Sato T, Furumoto T-a, Mizutani-Koseki Y, Suzuki Y, et al. Mesenchymal expression of Foxl1, a winged helix transcriptional factor, regulates generation and maintenance of gut-associated lymphoid organs. *Developmental Biology*. 2003;255(2):278-89.
13. DeTogni P, Goellner J, Ruddle NH, Streeter PR, Fick A, Mariathasan S, et al. Abnormal development of peripheral lymphoid organs in mice deficient in lymphotoxin. *Science*. 1994;264(5159):703-7.
14. Adachi S, Yoshida H, Kataoka H, Nishikawa S. Three distinctive steps in Peyer's patch formation of murine embryo. *Int Immunol*. 1997;9(4):507-14.
15. Lorenz RG, Chaplin DD, McDonald KG, McDonough JS, Newberry RD. Isolated lymphoid follicle formation is inducible and dependent upon lymphotoxin-sufficient B lymphocytes, lymphotoxin b receptor, and TNF receptor I function. *J Immunol*. 2003;170(11):5475-82.
16. Kweon M-N, Yamamoto M, Rennert PD, Park EJ, Lee A-Y, Chang S-Y, et al. Prenatal blockage of lymphotoxin b receptor and TNF receptor p55 signaling cascade resulted in the acceleration of tissue genesis for isolated lymphoid follicles in the large intestine. *J Immunol*. 2005;174(7):4365-72.
17. Hase K, Murakami T, Takatsu H, Shimaoka T, Iimura M, Hamura K, et al. The membrane-bound chemokine CXCL16 expressed on follicle-associated epithelium and M cells mediates lympho-epithelial interaction in GALT. *J Immunol*. 2006;176(1):43-51.

18. Debard N, Sierro F, Kraehenbuhl JP. Development of Peyer's patches, follicle-associated epithelium and M cell: lessons from immunodeficient and knockout mice. *Semin Immunol.* 1999;11(3):183-91.
19. Lorenz RG, Newberry RD. Isolated lymphoid follicles can function as sites for induction of mucosal immune responses. *Ann N Y Acad Sci.* 2004;1029:44-57.
20. Fujihashi K, Kato H, Ginkel Fv, Koga T, Boyaka P, Jackson R, et al. A revisit of mucosal IgA immunity and oral tolerance. *Acta Odontol Scand.* 2001;59(5).
21. Fagarasan S, Muramatsu M, Suzuki K, Nagaoka H, Hiai H, Honjo T. Critical roles of activation-induced cytidine deaminase in the homeostasis of gut flora. *Science.* 2002;298(5597):1424-7.
22. Bouskra D, Brezillon C, Berard M, Werts C, Varona R, Boneca IG, et al. Lymphoid tissue genesis induced by commensals through NOD1 regulates intestinal homeostasis. *Nature.* 2008;456(7221):507-10.
23. Eberl G, Littman DR. Thymic origin of intestinal ab T cells revealed by fate mapping of ROR γ t⁺ cells. *Science.* 2004;305(5681):248-51.
24. Kanamori Y, Ishimaru K, Nanno M, Maki K, Ikuta K, Nariuchi H, et al. Identification of novel lymphoid tissues in murine intestinal mucosa where clusters of c-kit⁺ IL-7R⁺ Thy1⁺ lympho-hemopoietic progenitors develop. *J Exp Med.* 1996;184(4):1449-59.
25. Taylor RT, Williams IR. Lymphoid organogenesis in the intestine. *Immunol Res.* 2005;33(2):167-82.
26. Velaga S, Herbrand H, Friedrichsen M, Jiong T, Dorsch M, Hoffmann MW, et al. Chemokine receptor CXCR5 supports solitary intestinal lymphoid tissue formation, B cell homing, and induction of intestinal IgA responses. *J Immunol.* 2009;182(5):2610-9.
27. Taylor RT, Lugering A, Newell KA, Williams IR. Intestinal cryptopatch formation in mice requires lymphotoxin a and the lymphotoxin b receptor. *J Immunol.* 2004;173(12):7183-9.

28. Pabst O, Herbrand H, Friedrichsen M, Velaga S, Dorsch M, Berhardt G, et al. Adaptation of solitary intestinal lymphoid tissue in response to microbiota and chemokine receptor CCR7 signaling. *J Immunol.* 2006;177(10):6824-32.
29. Owen RL, Jones AL. Epithelial cell specialization within human Peyer's patches: an ultrastructural study of intestinal lymphoid follicles. *Gastroenterology.* 1974;66(2):189-203.
30. Neutra MR, Frey A, Kraehenbuhl JP. Epithelial M cells: gateways for mucosal infection and immunization. *Cell.* 1996;86(3):345-8.
31. Trier JS. Structure and function of intestinal M cells. *Gastroenterol Clin North Am.* 1991;20(3):531-47.
32. Neutra MR, Mantis NJ, Frey A, Giannasca PJ. The composition and function of M cell apical membranes: Implications for microbial pathogenesis. *Semin Immunol.* 1999;11(3):171-81.
33. Bockman D, Cooper M. Pinocytosis by epithelium associated with lymphoid follicles in the bursa of Fabricius, appendix, and Peyer's patches. An electron microscopic study. *Am J Anat.* 1973;136(4).
34. Owen RL. Uptake and transport of intestinal macromolecules and microorganisms by M cells in Peyer's patches-- a personal and historical perspective. *Semin Immunol.* 1999;11(3):157-63.
35. Foxwell AR, Cripps AW, Kyd JM. Optimization of oral immunization through receptor-mediated targeting of M cells. *Hum Vaccin.* 2007;3(5):220-3.
36. Nochi T, Yuki Y, Matsumura A, Mejima M, Terahara K, Kim DY, et al. A novel M cell-specific carbohydrate-targeted mucosal vaccine effectively induces antigen-specific immune responses. *J Exp Med.* 2007;204(12):2789-96.
37. Hase K, Kawano K, Nochi T, Pontes GS, Fukuda S, Ebisawa M, et al. Uptake through glycoprotein 2 of FimH+ bacteria by M cells initiates mucosal immune response. *Nature.* 2009;462(7270):226-30.

38. Helander A, Silvey KJ, Mantis NJ, Hutchings AB, Chandran K, Lucas WT, et al. The Viral s1 Protein and Glycoconjugates Containing α 2-3-Linked Sialic Acid Are Involved in Type 1 Reovirus Adherence to M Cell Apical Surfaces. *J Virol*. 2003;77(14):7964-77.
39. Clark MA, Hirst BH, Jepson MA. M-cell surface β 1 integrin expressing and invasion-mediated targeting of *Yersinia pseudotuberculosis* to mouse Peyer's patch M cells *Infect Immun*. 1998;66(3).
40. Nakato G, Fukuda S, Hase K, Goitsuka R, Cooper MD, Ohno H. New Approach for M-Cell-Specific Molecules Screening by Comprehensive Transcriptome Analysis. *DNA Res*. 2009;16(4):227-35.
41. Foster N, Macpherson GG. Murine Cecal Patch M Cells Transport Infectious Prions In Vivo. *Journal of Infectious Diseases*. 2010;202(12):1916-9.
42. Ermak TH, Giannasca PJ. Microparticle targeting to M cells. *Adv Drug Deliv Rev*. 1998;34(2-3):261-83.
43. Chabot S, Wagner JS, Farrant S, Neutra MR. TLRs regulate the gatekeeping functions of the intestinal follicle-associated epithelium. *J Immunol*. 2006;176(7):4275-83.
44. Tyrer PC, Ruth Foxwell A, Kyd JM, Otczyk DC, Cripps AW. Receptor mediated targeting of M-cells. *Vaccine*. 2007;25(16):3204-9.
45. Kraehenbuhl JP, Neutra MR. Epithelial M cells: differentiation and function. *Annu Rev Cell Dev Biol*. 2000;16:301-32.
46. Keren D. Antigen processing in the mucosal immune system. *Semin Immunol*. 1992;4(4).
47. Snippert HJ, van der Flier LG, Sato T, van Es JH, van den Born M, Kroon-Veenboer C, et al. Intestinal crypt homeostasis results from neutral competition between symmetrically dividing *Lgr5* stem cells. *Cell*. 2010;143(1):134-44.
48. van der Flier LG, Clevers H. Stem Cells, Self-Renewal, and Differentiation in the Intestinal Epithelium. *Annual Review of Physiology*. 2009;71(1):241-60.

49. Gebert A, Fassbender S, Werner K, Weissferdt A. The development of M cells in Peyer's patches is restricted to specialized dome-associated crypts. *Am J Pathol.* 1999;154(5):1573-82.
50. Sierro F, Pringault E, Assman PS, Kraehenbuhl JP, Debard N. Transient expression of M-cell phenotype by enterocyte-like cells of the follicle-associated epithelium of mouse Peyer's patches. *Gastroenterology.* 2000;119(3):734-43.
51. Kerneis S, Bogdanova A, Kraehenbuhl JP, Pringault E. Conversion by Peyer's patch lymphocytes of human enterocytes into M cells that transport bacteria. *Science.* 1997;277(5328):949-52.
52. Lo D, Tynan W, Dickerson J, Scharf M, Cooper J, Byrne D, et al. Cell culture modeling of specialized tissue: identification of genes expressed specifically by follicle-associated epithelium of Peyer's patch by expression profiling of Caco-2/Raji co-cultures. *Int Immunol.* 2004;16(1):91-9.
53. des Rieux A, Fievez V, Theate I, Mast J, Preat V, Schneider YJ. An improved in vitro model of human intestinal follicle-associated epithelium to study nanoparticle transport by M cells. *Eur J Pharm Sci.* 2007;30(5):380-91.
54. Gebert A, Steinmetz I, Fassbender S, Wendlandt KH. Antigen transport into Peyer's patches: increased uptake by constant numbers of M cells. *Am J Pathol.* 2004;164(1).
55. Golovkina TV, Shlomchik M, Hannum L, Chervonsky A. Organogenic role of B lymphocytes in mucosal immunity. *Science.* 1999;286(5446):1965-8.
56. Rumbo M, Sierro F, Debard N, Kraehenbuhl JP, Finke D. Lymphotoxin b receptor signaling induces the chemokine CCL20 in intestinal epithelium. *Gastroenterology.* 2004;127(1):213-23.
57. Mach J, Hsieh T, Hsieh D, Grubbs N, Chervonsky A. Development of intestinal M cells. *Immunol Rev.* 2005;206:177-89.

58. Kanaya T, Miyazawa K, Takakura I, Itani W, Watanabe K, Ohwada S, et al. Differentiation of a murine intestinal epithelial cell line (MIE) toward the M cell lineage. *Am J Physiol Gastrointest Liver Physiol*. 2008;295(2):G273-84.
59. Terahara K, Yoshida M, Igarashi O, Nochi T, Pontes GS, Hase K, et al. Comprehensive gene expression profiling of Peyer's patch M cells, villous M-like cells, and intestinal epithelial cells. *J Immunol*. 2008;180(12):7840-6.
60. Jang MH, Kweon M-N, Iwatani K, Yamamoto M, Terahara K, Sasakawa C, et al. Intestinal villous M cells: An antigen entry site in the mucosal epithelium. *Proceedings of the National Academy of Sciences of the United States of America*. 2004;101(16):6110-5.
61. Schulz O, Jaensson E, Persson EK, Liu X, Worbs T, Agace WW, et al. Intestinal CD103+, but not CX3CR1+, antigen sampling cells migrate in lymph and serve classical dendritic cell functions. *J Exp Med*. 2009;206(13):3101-14.
62. Hadis U, Wahl B, Schulz O, Hardtke-Wolenski M, Schippers A, Wagner N, et al. Intestinal Tolerance Requires Gut Homing and Expansion of FoxP3+ Regulatory T Cells in the Lamina Propria. *Immunity*. 2011;34(2):237-46.
63. Miller H, Zhang J, Kuolee R, Patel GB, Chen W. Intestinal M cells: the fallible sentinels? *World J Gastroenterol*. 2007;13(10):1477-86.
64. Halle S, Bumann D, Herbrand H, Willer Y, Dahne S, Forster R, et al. Solitary intestinal lymphoid tissue provides a productive port of entry for *Salmonella enterica* serovar Typhimurium. *Infect Immun*. 2007;75(4):1577-85.
65. Muehlhoefer A, Saubermann LJ, Gu X, Luedtke-Heckenkamp K, Xavier R, Blumberg RS, et al. Fractalkine Is an Epithelial and Endothelial Cell-Derived Chemoattractant for Intraepithelial Lymphocytes in the Small Intestinal Mucosa. *The Journal of Immunology*. 2000;164(6):3368-76.

66. Niess JH, Adler G. Enteric Flora Expands Gut Lamina Propria CX3CR1+ Dendritic Cells Supporting Inflammatory Immune Responses under Normal and Inflammatory Conditions. *The Journal of Immunology*. 2010;184(4):2026-37.
67. Voedisch S, Koenecke C, David S, Herbrand H, Forster R, Rhen M, et al. Mesenteric Lymph Nodes Confine Dendritic Cell-Mediated Dissemination of Salmonella enterica Serovar Typhimurium and Limit Systemic Disease in Mice. *Infect Immun*. 2009;77(8):3170-80.
68. Manocha M, Pal PC, Chitralkha KT, Thomas BE, Tripathi V, Gupta SD, et al. Enhanced mucosal and systemic immune response with intranasal immunization of mice with HIV peptides entrapped in PLG microparticles in combination with Ulex Europaeus-I lectin as M cell target. *Vaccine*. 2005;23(48-49):5599-617.
69. Chionh Y-T, Wee JLK, Every AL, Ng GZ, Sutton P. M-cell targeting of whole killed bacteria induces protective immunity against gastrointestinal pathogens. *Infect Immun*. 2009;IAI.01522-08.
70. Gupta PN, Khatri K, Goyal AK, Mishra N, Vyas SP. M-cell targeted biodegradable PLGA nanoparticles for oral immunization against hepatitis B. *Journal of Drug Targeting*. 2007;15(10):701-13.
71. Misumi S, Masuyama M, Takamune N, Nakayama D, Mitsumata R, Matsumoto H, et al. Targeted Delivery of Immunogen to Primate M Cells with Tetragalloyl Lysine Dendrimer. *The Journal of Immunology*. 2009;182(10):6061-70.
72. Mohamadzadeh M, Duong T, Sandwick SJ, Hoover T, Klaenhammer TR. Dendritic cell targeting of Bacillus anthracis protective antigen expressed by Lactobacillus acidophilus protects mice from lethal challenge. *Proceedings of the National Academy of Sciences*. 2009;106(11):4331-6.
73. Smith DW, Nagler-Anderson C. Preventing Intolerance: The Induction of Nonresponsiveness to Dietary and Microbial Antigens in the Intestinal Mucosa. *The Journal of Immunology*. 2005;174(7):3851-7.

74. Branum AM LS. Food allergy among U.S. children: trends in prevalence and hospitalizations. *NCHS Data Brief*. 2008(10):1-8.
75. Suzuki H, Sekine S, Kataoka K, Pascual DW, Maddaloni M, Kobayashi R, et al. Ovalbumin-protein sigma 1 M-cell targeting facilitates oral tolerance with reduction of antigen-specific CD4+ T cells. *Gastroenterology*. 2008;135(3):917-25.
76. Roth-Walter F, Schöll I, Untersmayr E, Ellinger A, Boltz-Nitulescu G, Scheiner O, et al. Mucosal targeting of allergen-loaded microspheres by *Aleuria aurantia* lectin. *Vaccine*. 2005;23(21):2703-10.
77. Schöll I, Kopp T, Bohle B, Jensen-Jarolim E. Biodegradable PLGA Particles for Improved Systemic and Mucosal Treatment of Type I Allergy. *Immunology and Allergy Clinics of North America*. 2006;26(2):349-64.
78. Nagatake T, Fukuyama S, Kim D-Y, Goda K, Igarashi O, Sato S, et al. Id2-, RORgt-, and LTbR-independent initiation of lymphoid organogenesis in ocular immunity. *J Exp Med*. 2009;206(11):2351-64.
79. Liu H, Meagher CK, Moore CP, Phillips TE. M Cells in the Follicle-Associated Epithelium of the Rabbit Conjunctiva Preferentially Bind and Translocate Latex Beads. *Investigative Ophthalmology & Visual Science*. 2005;46(11):4217-23.
80. Spit BJ, Hendriksen EGJ, Bruijntjes JP, Kuper CF. Nasal lymphoid tissue in the rat. *Cell and Tissue Research*. 1989;255(1):193-8.
81. Nair PNR, Schroeder HE. Duct-associated lymphoid tissue (DALT) of minor salivary glands and mucosal immunity. *Immunology*. 1986;57(2):171-80.
82. Pabst R, Tschernig T. Bronchus-Associated Lymphoid Tissue: An Entry Site for Antigens for Successful Mucosal Vaccinations? *Am J Respir Cell Mol Biol*. 2010;43(2):137-41.
83. Takata S, Ohtani O, Watanabe Y. Lectin Binding Patterns in Rat Nasal-Associated Lymphoid Tissue (NALT) and the Influence of Various Types of Lectin on Particle Uptake in NALT. *Archives of Histology and Cytology*. 2000;63(4):305-12.

84. Ronan EO, Lee LN, Tchilian EZ, Beverley PCL. Nasal associated lymphoid tissue (NALT) contributes little to protection against aerosol challenge with *Mycobacterium tuberculosis* after immunisation with a recombinant adenoviral vaccine. *Vaccine*. 2010;28(32):5179-84.
85. Bachmann MF, Wong BR, Josien R, Steinman RM, Oxenius A, Choi Y. TRANCE, a tumor necrosis factor family member critical for CD40 ligand-independent T helper cell activation. *J Exp Med*. 1999;189(7):1025-31.
86. Lum L, Wong BR, Josien R, Becherer JD, Erdjument-Bromage H, Schlondorff J, et al. Evidence for a role of a tumor necrosis factor- α (TNF- α)-converting enzyme-like protease in shedding of TRANCE, a TNF family member involved in osteoclastogenesis and dendritic cell survival. *J Biol Chem*. 1999;274(19):13613-8.
87. Hikita A, Yana I, Wakeyama H, Nakamura M, Kadono Y, Oshima Y, et al. Negative regulation of osteoclastogenesis by ectodomain shedding of receptor activator of NF- κ B ligand. *J Biol Chem*. 2006;281(48):36846-55.
88. Wong BR, Josien R, Lee SY, Vologodskaia M, Steinman RM, Choi Y. The TRAF family of signal transducers mediates NF- κ B activation by the TRANCE receptor. *J Biol Chem*. 1998;273(43):28355-9.
89. Galibert L, Tometsko ME, Anderson DM, Cosman D, Dougall WC. The involvement of multiple tumor necrosis factor receptor (TNFR)-associated factors in the signaling mechanisms of receptor activator of NF- κ B, a member of the TNFR superfamily. *J Biol Chem*. 1998;273(51):34120-7.
90. Kim N, Odgren PR, Kim DK, Marks SC, Jr., Choi Y. Diverse roles of the tumor necrosis factor family member TRANCE in skeletal physiology revealed by TRANCE deficiency and partial rescue by a lymphocyte-expressed TRANCE transgene. *Proc Natl Acad Sci USA*. 2000;97(20):10905-10.

91. Kong YY, Yoshida H, Sarosi I, Tan HL, Timms E, Capparelli C, et al. OPGL is a key regulator of osteoclastogenesis, lymphocyte development and lymph-node organogenesis. *Nature*. 1999;397(6717):315-23.
92. Kim D, Mebius RE, MacMicking JD, Jung S, Cupedo T, Castellanos Y, et al. Regulation of peripheral lymph node genesis by the tumor necrosis factor family member TRANCE. *J Exp Med*. 2000;192(10):1467-78.
93. Akiyama T, Shimo Y, Yanai H, Qin J, Ohshima D, Maruyama Y, et al. The tumor necrosis factor family receptors RANK and CD40 cooperatively establish the thymic medullary microenvironment and self-tolerance. *Immunity*. 2008;29(3):423-37.
94. Hikosaka Y, Nitta T, Ohigashi I, Yano K, Ishimaru N, Hayashi Y, et al. The cytokine RANKL produced by positively selected thymocytes fosters medullary thymic epithelial cells that express autoimmune regulator. *Immunity*. 2008;29(3):438-50.
95. Wong BR, Josien R, Lee SY, Sauter B, Li HL, Steinman RM, et al. TRANCE (tumor necrosis factor [TNF]-related activation-induced cytokine), a new TNF family member predominantly expressed in T cells, is a dendritic cell-specific survival factor. *J Exp Med*. 1997;186(12):2075-80.
96. Fata JE, Kong YY, Li J, Sasaki T, Irie-Sasaki J, Moorehead RA, et al. The osteoclast differentiation factor osteoprotegerin-ligand is essential for mammary gland development. *Cell*. 2000;103(1):41-50.
97. Taylor RT, Patel SR, Lin E, Butler BR, Lake JG, Newberry RD, et al. Lymphotoxin-independent expression of TNF-related activation-induced cytokine by stromal cells in cryptopatches, isolated lymphoid follicles, and Peyer's patches. *J Immunol*. 2007;178(9):5659-67.
98. Schramek D, Leibbrandt A, Sigl V, Kenner L, Pospisilik JA, Lee HJ, et al. Osteoclast differentiation factor RANKL controls development of progestin-driven mammary cancer. *Nature*. 2010;468(7320):98-102.

99. Savidge T, Smith M, James P, Aldred P. Salmonella-induced M-cell formation in germ-free mouse Peyer's patch tissue. *Am J Pathol.* 1991;139(1).
100. Barker N, van de Wetering M, Clevers H. The intestinal stem cell. *Genes Dev.* 2008;22(14):1856-64.
101. Hondo T, Kanaya T, Takakura I, Watanabe H, Takahashi Y, Nagasawa Y, et al. Cytokeratin 18 is a specific marker of bovine intestinal microfold (M) cell. *American Journal of Physiology - Gastrointestinal and Liver Physiology.*
102. Suzuki K, Meek B, Doi Y, Muramatsu M, Chiba T, Honjo T, et al. Aberrant expansion of segmented filamentous bacteria in IgA-deficient gut. *Proc Natl Acad Sci U S A.* 2004;101(7):1981-6.
103. Pfeffer K. Biological functions of tumor necrosis factor cytokines and their receptors. *Cytokine & growth factor reviews.* 2003;14(3-4):185-91.
104. Hsieh E, Fernandez X, Wang J, Hamer M, Calvilli S, Croft M, et al. CD137 is required for M cell functional maturation but not lineage commitment. *Am J Pathol.* 2010;177(2).

LIST OF PUBLICATIONS AND PRESENTATIONS

Publications

Kathryn A. Knoop, Nachiket Kumar, Betsy R. Butler, Senthil Sakthivel, Rebekah T. Taylor, Tomonori Nochi, Hisaya Akiba, Hideo Yagita, Hiroshi Kiyono, and Ifor R. Williams “RANKL is necessary and sufficient to initiate development of antigen-sampling M cells in the intestinal epithelium,” *The Journal of Immunology*, 2009 183:5738-47. Cover picture for the November 1 2009 issue of the Journal taken from this article.

Kathryn A. Knoop, Betsy R. Butler, Nachiket Kumar, Rodney Newberry, and Ifor R. Williams, “Distinct Developmental Requirements for Isolated Lymphoid Follicle Formation in the Small and Large Intestine: RANKL is Essential Only in the Small Intestine” Submitted to American Journal of Pathology, February 1st, 2011.

Kathryn A. Knoop, Betsy R. Butler, Nachiket Kumar, Hideo Yagita, and Ifor R. Williams, “Differentiation of Peyer’s Patch M Cells Does Not Require Signals from B Cells” In progress

Kathryn A. Knoop, Daniel C. Rios, Betsy R. Butler, Nachiket Kumar, and Ifor R. Williams, “In the absence of secretory IgA, altered enteric microflora can contribute to the development of villous M cells” In progress

Presentations

2008 American Association of Immunologists, San Diego, CA
“M Cell Development Preferentially Occurs in Distal Small Intestinal Peyer’s Patches in Mice Lacking B Cells (μ MT), CCR6, or TRANCE/RANKL”, Oral presentation

2008 American Society for Investigative Pathology, San Diego, CA
“Development of M Cells Within the Follicle-Associated Epithelium of Peyer’s Patches Depends on Expression of TRANCE/RANKL by Stromal Cells”, Oral presentation

2009 American Association of Immunologists, Seattle, WA
“RANKL is Essential for Normal Differentiation of M Cells in the Follicle-Associated

Epithelium of Peyer's Patches", Oral presentation

2009 International Congress of Mucosal Immunology, Boston, MA

"Absence of RANKL in Mice Causes Perturbed Development of Cryptopatches and a Complete Block in Formation of Isolated Lymphoid Follicles", Oral presentation

2009 Microanatomy of Immune Responses in Health and Disease, Birmingham, UK

"Absence of RANKL in Mice Causes Perturbed Development of Cryptopatches and a Complete Block in Formation of Isolated Lymphoid Follicles", Poster presentation

2009 Graduate Division of Biomedical and Biological Sciences Student Symposium, Emory University

"Absence of RANKL in Mice Causes Perturbed Development of Cryptopatches and a Complete Block in Formation of Isolated Lymphoid Follicles", Oral presentation

2010 American Association of Immunologists, Baltimore, MA

"Differentiation of Peyer's Patch M Cells Does Not Require Signals from B Cells: Evidence from a Mouse Model of Acute Antibody-Mediated Depletion of B Cells", Oral presentation

2010 International Congress of Immunology, Kobe, Japan

"RANKL is a critical factor for the differentiation, maintenance, and survival of antigen-sampling M cells in the intestine", Oral presentation

2010 European Mucosal Immunology Group, Amsterdam, Netherlands

"Differentiation of Peyer's Patch M Cells Does Not Require Signals from B Cells: Evidence from a Mouse Model of Acute Antibody-Mediated Depletion of B Cells", Poster presentation